

**Identification and characterisation of a novel gene, DWNN, isolated
from promoter-trapped Chinese hamster ovary cells.**

Amanda Skepu



A thesis submitted in partial fulfilment of the requirements for the degree
of Doctor Philosophiae in the Faculty of Science, University of the
Western Cape.

Supervisor: Prof DJG Rees

January 2005

ABSTRACT.

Identification and characterisation of a novel gene, DWNN, isolated from promoter-trapped CHO cell lines.

A. Skepu

PhD thesis, Department of Biotechnology, Faculty of Science, University of the Western Cape.



The process of cytotoxic T lymphocyte (CTL) killing involves the recognition and destruction of foreign antigens by cytotoxic T cells and is of crucial importance to the defence of the organism against viral infections. Defects in this process can lead to various autoimmune diseases and cancer. The aim of this study was to identify more genes involved in the cell death pathway and to link CTL killing, apoptosis and cancer.

A number of CTL resistant cell lines have been generated in a previous study, using a retroviral promoter trap mutagenesis system, in order to identify novel components involved in the CTL killing pathway. Four of these cell lines were used in this study in order to identify genes mutated in them. The sites of the insertion of the retrovirus into the genome of these cell lines were analysed using inverse PCR. This method

yields two products, one from the 3' end, which is of constant size in all the cell lines and a variable 5' end fragment, containing the insertion site into the unknown gene sequence, which is characterised by sequencing the PCR products. A novel gene, named DWNN, has been identified in two of the four promoter-trapped cell lines and the remaining two cell lines failed to identify any significant genes.

This thesis describes the characterisation of the DWNN gene, in order to identify its function. The sequence analysis of this gene revealed that it constitutes a highly conserved domain found in all eukaryotes. The human DWNN gene encodes two overlapping proteins, which were termed DWNN-13 and DWNN-200, encoding the predicted 13 kD and 200 kD proteins respectively. In different phyla, including humans, it has been shown that the DWNN domain is attached to a number of other conserved domains, including CCHC Zinc finger, C3HC4 RING finger, SR RNA binding domain, Rb binding domain and p53 binding domains found previously in the RBBP6 gene (which is a partial cDNA from the DWNN-200 transcript).

The cDNA constructs encoding the two proteins have been isolated and completely sequenced. A number of mutations within this gene in human cancers and transformed cell lines have been characterised.

Immunofluorescence and GFP studies have been undertaken in order to determine the localisation of this protein. Fusion proteins of GFP linked to DWNN-13 and DWNN-

200 were expressed in CHO cells, and were found to localize to the nucleus. Immunostaining with anti-DWNN antibodies have shown that the endogenous DWNN protein localizes in the nucleus CHO cells and several human cell lines. However, in DWNN-mutant cell lines, anti-DWNN antibodies did not stain the nucleus, but only stained the cytoplasm.

Stable mutant cell lines complemented with both transcripts of DWNN have been generated. These cell lines, as well as DWNN-mutant cell lines, were characterised further in order to clarify the role played by DWNN in mammalian cells and its involvement in CTL killing and apoptosis. Both the DWNN-mutant cell lines and the mutant cell lines complemented by DWNN expression were shown to be totally resistant to CTL killing, compared to the parental cell line, Y10. It was also discovered that some of the DWNN-complemented mutant cell lines were less susceptible to staurosporine-induced apoptosis than the DWNN-mutant cell lines.

KEYWORDS:

Cytotoxic T lymphocyte

Apoptosis

Promoter-trap mutagenesis

Microscopy

Transfection

Inverse PCR

Immunofluorescence staining

Localisation

Western blots

Sequencing

January 2005



UNIVERSITY *of the*
WESTERN CAPE

DECLARATION.

I declare that *“Identification and characterisation of a novel gene, DWNN, isolated from promoter-trapped CHO cell lines”* is my own work that has not been submitted for any degree or examination in any other university and that all the sources I have used or quoted have been indicated and acknowledged by complete references.

Amanda Skepu



January 2005

Signed:.....

TABLE OF CONTENTS.

ABSTRACT.....|

DECLARATION.....	V
TABLE OF CONTENTS.....	VI
LIST OF TABLES.....	XII
LIST OF FIGURES.....	XV
ABBREVIATIONS.....	XXII
ACKNOWLEDGEMENTS.....	XXVI
CHAPTER 1: INTRODUCTION.....	1
1.1 The immune system.....	1
1.1.1 Overview of the immune system.....	1
1.1.2 Types of immunity.....	1
1.1.3 Cells of the immune system.....	3
1.2 T lymphocytes.....	5
1.2.1 T lymphocyte receptor (TcR).....	5
1.2.2 T lymphocyte development.....	6
1.2.3 Types of T lymphocytes.....	7
1.2.4 The MHC class I antigen presentation pathway.....	9
1.2.5 CTL mediated killing.....	11
1.3 Natural killer cells.....	15
1.3.1 How NK cells kill?.....	17
1.3.2 Killer-activating receptors.....	18
1.3.3 Killer-inhibitory receptors.....	19
1.4 Apoptosis.....	19
1.4.1 Introduction.....	19
1.4.2 Apoptosis versus Necrosis.....	20
1.4.3 Molecules controlling apoptosis.....	23
1.4.4 The Apoptotic pathways.....	30
1.5 Tumor suppressor genes.....	32
1.5.1 The p53 gene.....	33
1.5.2 Retinoblastoma (Rb) gene.....	41
1.6 The ubiquitin-proteasome pathway.....	48
1.6.1 Ubiquitin.....	48
1.6.2 The ubiquitin pathway.....	48
1.6.3 The ubiquitin-conjugating machinery.....	50

1.7 The DWNN gene family	52
1.7.1 Identification of DWNN domain	52
1.7.2 DWNN/RBBP6 homologues	56
1.8 Promoter-trap mutagenesis	64
1.9 Objectives	65
CHAPTER 2: MATERIALS AND METHODS.....	66
2.1 Materials and suppliers	66
2.2 Solutions	68
2.3 Bacterial culture	71
2.3.1 Strains	71
2.3.2 Selection	72
2.3.3 Storage of bacterial strains	72
2.4 Cloning vectors	72
2.4.1 pGEM-T Easy vector	72
2.4.2 pBluescript II	73
2.4.3 pEGFP-C1	74
2.4.4 pDsRed1-C1	75
2.4.5 pcDNA3.1/Zeo(+)	76
2.5 Preparation of competent <i>E. coli</i> cells for transformation	77
2.6 Transformation of <i>E. coli</i> cells	78
2.7 Preparation of plasmid DNA.....	78
2.7.1 Large-scale preparation	78
2.7.2 Double CsCl/ethidium bromide fractionation.....	79
2.7.3 Small-scale preparation (minipreps)	80
2.8 Manipulation of plasmid DNA	81
2.8.1 Ethanol precipitation	81
2.8.2 Ammonium acetate precipitation.....	81
2.8.3 Phenol/chloroform extraction	81
2.8.4 Restriction enzyme digests	82
2.8.5 Ligation of DNA.....	82
2.9 Agarose gel electrophoresis of DNA.....	83
2.9.1 DNA molecular weight markers	83
2.9.2 Purification of DNA fragments from agarose gels.....	84
2.10 Polymerase Chain Reaction (PCR) amplification	85
2.10.1 Standard PCR	85
2.10.2 Inverse PCR	85

2.11 Sequencing of double stranded DNA	86
2.12 Preparation of Genomic DNA from mammalian cell lines	87
2.13 Cell culture	88
2.13.1 Cell lines.....	88
2.13.2 Tissue culture media	88
2.13.3 Propagation and storage of cell lines	89
2.13.4 Transfection of cell lines.....	89
2.14 Immunofluorescent microscopy	90
2.14.1 Fixation and permeabilisation of cells	90
2.14.2 Immunostaining of cells.....	90
2.15 FACS Analysis	91
2.16 CTL killing assay	92
2.16.1 Stimulation of CTL.....	92
2.16.2 Harvesting of CTL	92
2.16.3 Harvesting of target cells.....	93
2.17 APOPercentage™ Apoptosis Assay	94
2.18 Proteins	94
2.18.1 Isolation of protein from cell monolayers.....	94
2.18.2 SDS-polyacrylamide gel electrophoresis (SDS-PAGE) of proteins.....	95
2.18.3 Staining and destaining of PAGE gels	95
2.18.4 Western Blotting.....	95
2.19 RNA Extraction	97
2.20 Agarose gel electrophoresis of RNA	97
2.21 cDNA synthesis	98
2.22 Real –Time quantitative RT-PCR	98
CHAPTER 3: IDENTIFICATION OF THE DWNN GENE IN PROMOTER TRAPPED CELL LINES.	100
3.1 Introduction	100
3.2 Analysis of the retroviral promoter-trapped cell lines by Inverse PCR ...	102
3.2.1 Isolation and restriction digestion of genomic DNA	102
3.2.2 Amplification of the hygromycin resistant gene.....	103
3.2.3 Amplification of the 3' end of unknown genomic sequence	103
3.2.4 Sequencing of the 3' end inverse PCR products	104
3.2.5 Amplification of the 5' end of the unknown genomic sequence	105
3.2.6 Sequencing of the 5' end inverse PCR products	106

3.3 Screening for other DWNN knock-out cell lines.....	107
3.4 DWNN sequence analysis	109
3.5 Discussion	109
CHAPTER 4: GENERATION OF THE HUMAN DWNN-13 CONSTRUCT.	113
4.1 Introduction	113
4.2 Amplification of DWNN-13 cDNA	113
4.2.1 Primer design.....	113
4.2.2 Amplification and sequencing of DWNN-13 clone	114
4.3 Subcloning of the DWNN-13 cDNA.....	115
4.3.1 Construction of the pEGFC1-DWNN-13 fusion protein.....	115
4.3.2 Subcloning of DWNN-13 cDNA into pcDNA3.1/Zeo vector	116
4.4 Discussion	116
CHAPTER 5: CONSTRUCTION OF THE HUMAN DWNN-200 CDNA.....	117
5.1 Introduction	118
5.2 Generation of DWNN-200 cDNA by RT-PCR	118
5.2.1 Designing of primers	118
5.2.2 Amplification of DWNN-200 cDNA.....	119
5.3 Sequencing of DWNN-200 cDNA	120
5.3.1 Sequencing of DWNN-200 clones from cancer cell lines	120
5.3.2 Sequencing of DWNN-200 clones from NHF cell line.....	121
5.4 Assembly of the full-length DWNN-200 cDNA.....	122
5.5 Discussion	125
CHAPTER 6: LOCALISATION OF DWNN PROTEIN.....	127
6.1 Introduction	127
6.2 Subcloning of DWNN-13 cDNA into pEGFP-C1 vector	128
6.3 Subcloning of DWNN-200 cDNA into pDsRed1-C1 vector	128
6.4 Transient expression of fusion proteins in cultured cells	129
6.4.1 Transient expression of pEGFPC1-DWNN-13 construct	129
6.4.2 Transient expression of pDsRed1-C1-DWNN-200 fusion proteins.....	130

6.5 Discussion	131
CHAPTER 7: GENERATION OF STABLE DWNN-COMPLEMENTED MUTANT CELL LINES.	132
7.1 Introduction	132
7.2 Subcloning of DWNN-13 cDNA into pcDNA3.1/Zeo vector	133
7.3 Subcloning of DWNN-200 cDNA into pcDNA3.1/Zeo vector	133
7.4 Determination of the optimal concentration of Zeocin for selection of CHO-Y10 cells.....	134
7.5 Stable transfection of pcDNA3.1/Zeo-DWNN-13 and pcDNA3.1/Zeo-DWNN-200 constructs into mammalian cells.....	135
7.6 Discussion	136
CHAPTER 8: ANALYSIS OF THE DWNN-MUTANT AND DWNN-COMPLEMENTED MUTANT CELL LINES.....	137
8.1 Introduction	137
8.2 Analysis of the DWNN expression.....	138
8.2.1 Immunofluorescent microscopy	138
8.2.2 Western blot analysis	140
8.3 CTL killing analysis.....	141
8.3.1 Target cell lines used	141
8.3.2 CTL killing assay.....	142
8.4 Analysis of the expression of the transfected MHC class I H-2K^K and Haemagglutinin transgenes	143
8.4.1 FACS analysis for the expression of the MHC class I H-2K ^K	143
8.4.2 Analysis of the influenza haemagglutinin (HA) expression	145
8.4.3 PCR amplification and sequencing of HA mRNA	146
8.4.5 Real-Time Quantitative PCR analysis of the HA mRNA amplification	148
8.5 Apoptosis killing assay	152
8.6 Discussion	154
CHAPTER 9: GENERAL DISCUSSION.....	157
9.1 Identification of the DWNN gene in promoter-trapped cell lines	158
9.2 Generation of the human DWNN-13 construct	159

9.4 Localisation of DWNN protein.....	160
9.5 Generation of stable DWNN-complemented mutant cell lines.....	161
9.6 Analysis of the DWNN-mutant and DWNN-complemented mutant cell lines	162
9.7 Conclusion.....	165
9.8 Future Work	166
REFERENCES.....	168



LIST OF TABLES.

Table 1.1	Functions of the cells of the immune system
Table 1.2	Morphological and biochemical differences between apoptosis and necrosis
Table 1.3	Types of caspases and their function
Table 1.4	Tumor suppressor genes and associated human cancers
Table 1.5	p53-binding proteins and their function
Table 1.6	First group of Rb-binding proteins

Table 1.7.1	Factors repressing transcription
Table 1.7.2	Factors activating transcription
Table 1.7.3	Factors affecting transcription in unknown ways
Table 1.8	Third group of Rb-binding proteins
Table 1.9	Protein similarities of the RBBP6 homologues to humans
Table 2.1	Bacterial strains used
Table 2.2	The sequencing reaction protocol
Table 2.3	PCR cycles for sequencing
Table 2.4	Cell lines used for tissue culture
Table 2.5	Tissue culture media used
Table 2.6	Reactions used for the first strand cDNA synthesis
Table 2.7	PCR conditions used for the Real-Time quantitative PCR
Table 3.1	Summary of the BLAST search results for the 3' inverse PCR products
Table 3.2	Summary of the BLAST search results for the 5' inverse PCR products
Table 4.1	Design of primers used for the amplification of DWNN-13 cDNA
Table 5.1	Primers used for the amplification of DWNN-200 cDNA
Table 5.2	Cell lines used for the amplification and sequencing of DWNN-200 cDNA.
Table 5.3	DWNN sequencing primers

Table 5.4	Summary of the cell lines used in the construction of the DWNN-200 cDNA.
Table 7.1	Summary of DNA constructs used for transfecting CHO-Mut 8 (3x8)3.5 and CHO-Mut 16 (3x8)3.5 cells
Table 8.1	Description of the cell lines used for Immunostaining
Table 8.2	Cell lines used for Western blot analysis
Table 8.3	Cell lines used for the CTL killing assay
Table 8.4	Cell lines used for the analysis of MHC class I H-2K ^K expression
Table 8.5	Cell lines used in the staining of the endogenous MHC class I H-2K ^K
Table 8.6	Sequence of the primers used for the amplification of HA
Table 8.7	Cell lines used for the analysis of HA expression
Table 8.8	CP values, ΔCP and the calculated ratios of the relative HA expression of CHO-Mut8 (3x8)3.5 and CHO-Mut16 (3x8)3.5 versus CHO-Y10.
Table 8.9	Cell used in the APOPercentage TM apoptosis assay



LIST OF FIGURES.

- Figure 1.1** Representation of the two types of adaptive immune response
- Figure 1.2** An illustrative representation of T lymphocyte development
- Figure 1.3** The MHC class I presentation pathway
- Figure 1.4** Diagrammatic representation of the two pathways by which CTLs kill their target cells
- Figure 1.5** Diagrammatic representation of the Fas-FasL pathway
- Figure 1.6** Electron micrograph showing a Natural killer cell
- Figure 1.7** Killing of the target cell by NK cell using ADCC mechanism
- Figure 1.8** The dual receptor system of NK cells for killing of target cell

- Figure 1.9a** Illustration of the morphological features of necrosis
- Figure 1.9b** Illustration of the morphological features of apoptosis
- Figure 1.10** General structure of procaspase
- Figure 1.11** The Bcl-2 family members
- Figure 1.12** Diagrammatic representation of the two mechanisms by which apoptosis occurs
- Figure 1.13** Structure of p53 showing the functional and regulatory domains
- Figure 1.14** The p53-Mdm2 negative feedback loop
- Figure 1.15** The structure of the retinoblastoma (Rb) pocket domain protein
- Figure 1.16** The ubiquitin pathway
- Figure 1.17** Protein translation of the DWNN-13 gene
- Figure 1.18** Sequence alignment of the DWNN gene
- Figure 1.19** 3D structures of Ubiquitin protein and DWNN domain
- Figure 1.20** Representation of the human DWNN gene structure showing the two transcripts, the exons and the location of the domains within the gene
- Figure 1.21** Schematic representation of the domain structure of the DWNN-200 protein from different species
- Figure 1.22** Diagrammatic representation of the RBBP6 partial cDNAs, including the full length RBBP6
- Figure 2.1** Circular map of pGEM-T Easy vector and the multiple cloning site

- Figure 2.2** pBluescript II SK (+) circular map with its MCS
- Figure 2.3** The map and MCS of pEGFP-C1 vector
- Figure 2.4** Circular map of pDsRed1 vector map and its MCS
- Figure 2.5** Circular map of pcDNA3.1/Zeo vector
- Figure 2.6** Agarose gel showing the sizes of the DNA molecular weight markers
- Figure 3.1** Schematic representation of the 3' inverse PCR
- Figure 3.2** Isolation and restriction digestion of genomic DNA
- Figure 3.3** Amplification of the hygromycin resistant fragment
- Figure 3.4** The hygromycin sequence showing the position of the primers used in the analysis of the 3' genomic DNA sequence
- Figure 3.5** Agarose gel electrophoresis of the 3' Inverse PCR
- Figure 3.6** DNA sequences generated for the CHO-Mut8 (3x8)3.5, CHO-J363 and CHO-Mut16 (3x8)3.5 3' inverse PCR products
- Figure 3.7** BLAST search results for the genomic sequence generated from CHO-Mut8 (3x8)3.5 (top fragment)
- Figure 3.8** BLAST results generated for the sequence from CHO-Mut8 (3x8)3.5 (bottom fragment)
- Figure 3.9** BLAST results generated for the sequence from CHO-J363 inverse PCR product
- Figure 3.10** BLAST results generated for the sequence from CHO-Mut16 (3x8)3.5 inverse PCR product
- Figure 3.11** Schematic representation of the 5' inverse PCR

- Figure 3.12** The first 300 bases of the hygromycin sequence showing the position of the primers used in the analysis of the 5' genomic DNA sequence
- Figure 3.13** Agarose gel electrophoresis of the 5' Inverse PCR
- Figure 3.14** DNA sequences generated for the CHO-Mut8 (3x8)3.5, CHO-Mut16 (3x8)3.5 and CHO-Mut10 (3x8)3.5 5' inverse PCR products
- Figure 3.15** BLAST results generated for the sequence from CHO-Mut8 (3x8)3.5 inverse PCR product
- Figure 3.16** BLAST results generated for the sequence from CHO-Mut16 (3x8)3.5 inverse PCR product
- Figure 3.17** Sequence analysis of 5' inverse PCR on CHO-J363
- Figure 3.18** DWNN gene sequence showing the position of 7.3 primer
- Figure 3.19** Screening for other DWNN knocked-out cell lines
- Figure 3.20** Screening for other DWNN knocked-out cell lines
- Figure 3.21** Sequencing analysis of the retroviral integration site in DWNN mutated cell lines
- Figure 4.1** Amplification of DWNN-13 cDNA
- Figure 4.2** Amplification of DWNN-13 cDNA
- Figure 4.3** Sequencing of the amplified DWNN-13 cDNA
- Figure 4.4** Blast search analysis of DWNN-13 sequence with (a) DWNNF and (b) DWNNR primers
- Figure 4.5** Sequencing analysis of DWNN-13 PCR product

- Figure 4.6** Construction of the pEGFC1-DWNN-118 fusion protein
- Figure 4.7** Subcloning of DWNN-13 cDNA into pcDNA3.1/Zeo vector
- Figure 5.1** Amplification of DWNN-200 cDNA
- Figure 5.2** Restriction digestions of the plasmid DNA isolated from the positive pGEM T Easy transformants
- Figure 5.3** Restriction digestions of the plasmid DNA isolated from the positive pGEM T Easy transformants
- Figure 5.4** Sequence analysis of fragment 1 of DWNN-200 from HeLa cell line
- Figure 5.5** Sequence analysis of fragment 1 of DWNN-200 from HeLa cell line
- Figure 5.6** Sequence analysis of fragment 3 of DWNN-200
- Figure 5.7** Sequence analysis of fragment 1 (residue 1275) of DWNN-200 from NHF cell line
- Figure 5.8** Sequence analysis of fragment 1 (residue 1496) of DWNN-200 from NHF cell line
- Figure 5.9** Sequence analysis of fragment 3 of DWNN-200 from NHF cell line
- Figure 5.10** Analysis of exon 16
- Figure 5.11** Assembly of the full length DWNN-200 cDNA
- Figure 5.12** Cloning of fragments 3 and 4 into pBC SK+
- Figure 5.13** Construction of the full length DWNN-200 cDNA
- Figure 6.1** Subcloning of DWNN-13 cDNA into pEGFP-C1

- Figure 6.2** Subcloning of DWNN-200 cDNA into pDsRed1-C1 vector
- Figure 6.3** Subcloning of DWNN-200 cDNA into pDsRed1-C1 vector
- Figure 6.4** Analysis of the pDsRed1-C1-DWNN-200 fusion constructs
- Figure 6.5** Transient transfections of CHO-Y10 cells with pEGFPC-1 only and pDsRed1-C1 only
- Figure 6.6** Fluorescent microscopy showing the localisation of EGFP-tagged DWNN-13
- Figure 6.7** Fluorescent microscopy showing the localisation of EGFP-tagged 'wild type' DWNN-200
- Figure 6.8** Fluorescent microscopy showing the localisation of 'L289Q:S363P DWNN-200
- Figure 7.1** Subcloning of DWNN-200 cDNA into pcDNA3.1/Zeo vector
- Figure 7.2** Subcloning of the wild type DWNN-200 cDNA into pcDNA3.1/Zeo vector
- Figure 7.3** The effects of using various Zeocin concentrations on CHO Y10 cells after 48 hours
- Figure 7.4** Stable clones on exposure to 300 µg/ml of Zeocin after 4 weeks
- Figure 8.1** Localisation of endogenous DWNN protein in mammalian cells
- Figure 8.2** Western blot analysis of DWNN-mutant and DWNN-complemented mutant cell lines

- Figure 8.3** CTL killing analysis of the DWNN-mutant and DWNN-complemented mutant cell lines
- Figure 8.4** FACS analysis of the expression of the MHC K^K
- Figure 8.5** Immunostaining of cells for MHC K^K expression
- Figure 8.6** Nucleotide and encoded amino acid sequence of the full length L-HA gene from the influenza virus
- Figure 8.7** 1 % agarose gel of the total RNA isolated from cultured cells
- Figure 8.8** Relative positions of the primers
- Figure 8.9** Relative positions of the HA primers
- Figure 8.10** Non-quantitative amplification of the HA fragment
- Figure 8.11** Real-Time Quantitative PCR amplification curves and their respective standard curves of HPRT gene
- Figure 8.12** Real-Time Quantitative PCR amplification curves and their respective standard curves of HA gene
- Figure 8.13** Standard curve of the HPRT and HA genes of CHO-Y10, CHO-Mut8 (3x8)3.5 and CHO-Mut16 (3x8)3.5 cell lines.
- Figure 8.14** Flow cytometric analysis of apoptotic cells with the APOPercentage™ assay

ABBREVIATIONS.

ADCC	Antibody-dependent cellular cytotoxicity
AIDS	Acquired immune deficiency syndrome
AMPS	Ammonium persulphate
Apaf-1	Apoptotic protease-activating factor-1
APC	Antigen presenting cell
ARF	Alternative reading frame
ATM	Ataxia telangiectasia mutated
ATR	Ataxia telangiectasia related
Bad	Bcl-x _L /Bcl-2-associated death protein
Bax	Bcl-2-associated x protein
Bcl-2	B cell leukaemia-2
Bid	BH3 interacting domain
BLAST	Basic local alignment search tool
bp	Base pair
BSA	Bovine serum albumin
CAD	Caspase-activated deoxyribonuclease
CARD	Caspase recruitment domain
Caspases	Cysteine aspartic-specific proteases

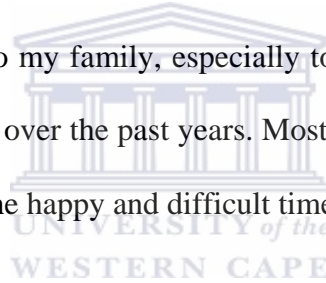
CD	Cluster of differentiation
cDNA	complementary deoxyribonucleotide acid
CED	Cell death defective
Chk2	Checkpoint kinase 2
CHO	Chinese hamster ovary
CMV	Cytomegalo virus
CTL	Cytotoxic T lymphocyte
DAPI	4', 6'-Diamidino-2-phenylindole
DEPC	Diethyl pyrocarbonate
DD	Death domain
DED	Death effector domain
DISC	Death-inducing signalling complex
DWNN	Domain With No Name
DMEM	Dulbecco's modified medium
DMSO	Dimethyl sulphoxide
DNA	Deoxyribonucleic acid
dNTPs	Deoxyribonucleotides
DTT	Dithiothreitol
EDTA	Ethylene diamine tetra acetic acid
EGFP	Enhanced Green fluorescent protein
ER	Endoplasmic reticulum
FACS	Fluorescence activated cell sorter
FADD	Fas associated death domain

Fas	Fibroblast-associated
FasL	Fas ligand
FCS	Foetal calf serum
FITC	Fluorescein isothiocyanate
hrs	hours
ICE	Interleukin-1-B-converting caspase enzyme
IFN γ ,	Interferon gamma
IgG	Immunoglobulin G
IL-2	Interleukin-2
IPTG	Isopropyl β -D-thiogalactopyranoside
ITAMs	Immunoreceptor tyrosine-based activation motifs
ITIMs	Immunoreceptor tyrosine-based inhibitory motifs
JNK	Jun-N-terminal kinase
kb	Kilo base
kD	Kilo dalton
LAK	Lymphokine activated killer
LTR	Long terminal repeat
MCS	Multiple cloning site
Mdm2	Murine double minute clone 2
MHC	Major histocompatibility complex
min	minute
MoMLV	Moloney murine leukaemia virus

MOPS	4-Morpholine propanesulphonic acid
mRNA	messenger RNA
mV	Millivolts
NHF	Normal human fibroblast
NK	Natural killer cells
PAGE	Polyacrylamide gel electrophoresis
PBS	Phosphate buffer saline
PCR	Polymerase chain reaction
PMSF	Phenylmethanesulphonyl fluoride
PVDF	Polyvinylidene difluoride
Rb	Retinoblastoma
RFP	Red Fluorescent Protein
RING	Really Interesting New Gene
RNA	Ribonucleic acid
rRNA	ribosomal RNA
SDS	Sodium dodecyl sulphate
sec	second
SV-40	Simian virus 40
TcR	T cell receptor
TEMED	<i>N, N, N', N'</i> -Tetra methylethylenediamine
Th cells	Helper T cells
TNF	Tumour necrosis factor
UV	Ultraviolet

ACKNOWLEDGEMENTS.

I would like to express my heartfelt gratitude to my supervisor Prof Jasper Rees for all his help, support and encouragement during the course of this project. I am sincerely grateful to Dr Keith Gould for his assistance with the CTL work. Thanks to the National Research Fund and the Cancer Association of South Africa for the financial support. I also wish to extend many thanks to all the members of the Rees lab and all my friends for their support and encouragement. Above all, I wish to express my appreciation to my family, especially to my mother, for all their endless love, support and patience over the past years. Most importantly, I wish to thank God for carrying me through the happy and difficult times.



CHAPTER 1: INTRODUCTION.

1.1 The immune system

1.1.1 Overview of the immune system

The immune system is responsible for protecting our bodies against any life-threatening diseases. It has the ability to recognise anything that is 'non-self' and destroys it. It does this by eliciting an immune response. The immune response can be defined as the ability of the immune system to respond to the presence of infectious organisms in the tissues of the host (Elgert, 1996). It should be stated that the immune system for animals works in a similar way as that for humans.

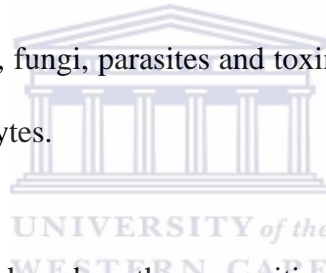
1.1.2 Types of immunity

The human immune system defends the body against invading organisms through two types of immunity: the innate and the adaptive immunity.

Innate immunity is the first generalised defence against all kinds of pathogens. It provides an immediate, non-specific and rapid protection against the invading pathogen (Abbas *et al.*, 1997). It however, does not provide protection against the same pathogen when encountered for the second time. The innate immune system is made up of dendritic cells, macrophages, neutrophils and natural killer cells.

Adaptive immunity provides a specific defence against pathogens. This type of immunity can recognise previously encountered pathogens and reacts faster and more efficiently (Abbas *et al.*, 1997). The adaptive immune cells include B and T lymphocytes. There are two types of adaptive immune responses: humoral and cell mediated responses.

The humoral response is based on the production of antibodies by the immune system for the recognition and destruction of the extracellular antigen. This provides protection against bacteria, fungi, parasites and toxins. This type of immune response is mediated by B lymphocytes.



Cell mediated response is based on the recognition of an intracellular antigen by T lymphocytes. This immune response destroys cells that are infected with viruses or mutating cells. Figure 1.1 shows a diagrammatic representation of the two types of adaptive immunity.

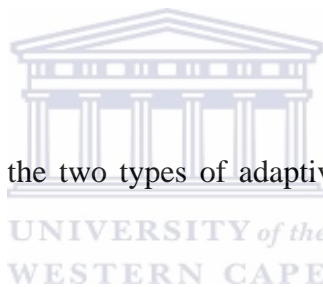


Fig 1.1 Representation of the two types of adaptive immune response (taken from Clancy, 1998).

1.1.3 Cells of the immune system

The immune system is composed of interdependent cell types that collectively protect the body from bacteria, parasites, fungi, viruses and tumor cells (Clancy, 1998). These cells develop from stem cells starting at a gestational age of 5 weeks. They are distributed through various organs in the lymphatic system as the fetus develops. Many of these cell types have specialised functions. They can engulf bacteria; kill parasites, tumor cells and viral infected cells. The cells include T and B lymphocytes, Natural killer cells, granulocytes, dendritic cells and macrophages. A comprehensive description of T lymphocytes and natural killer cells is presented below.

TYPE OF CELL	DESCRIPTION	CD MARKERS
T lymphocytes	Mature in the thymus gland and are divided into two subsets. The cytotoxic T lymphocytes destroy infected cells, while the helper T lymphocytes regulate the immune system by controlling the quality of all immune responses. More details about this type of lymphocyte are discussed in section 1.2.	CD2, CD3, CD4, CD28, CD45R, CD8, TcR
B lymphocytes	Mature in the bone marrow. The major function of B lymphocytes is to produce antibodies in response to foreign proteins of bacteria, viruses and tumour cells. The antibodies bind to and mediated the destruction of the foreign proteins.	CD19-22, CD35, CD40, CD45, CD32
Natural killers (NK) cells	Similar to cytotoxic T lymphocytes, but they mature in the bone marrow. They function as effector cells that directly kill certain tumours. More on NK cells is discussed in section 1.3.	NK1, CD16
Granulocytes	Are a group of white blood cells composed of three cell types: neutrophils, eosinophils and basophils. These cells are important in the removal of bacteria and parasites from the body. They engulf these foreign bodies and degrade them using their powerful enzymes.	CD13, CD15, CD16, CD30
Macrophages-	Are important in the regulation of immune responses. They are often referred to as antigen-presenting cells (APC) because they phagocytose foreign antigens and present these antigens to T and B lymphocytes.	CD26
Dendritic cells	Originate in the bone marrow. They are usually found in the structural compartment of the lymphoid organs. However, they are also found in the bloodstream and other tissues of the body. It is believed that they capture the antigen and bring it to the lymphoid organs, where an immune response is initiated. Dendritic cells are believed to function as APC.	CD21, CD23

Table 1.1 Functions of the cells of the immune system.

1.2 T lymphocytes

1.2.1 T lymphocyte receptor (TcR)

T lymphocytes have antigen receptor molecules on their surface, which are composed of two different polypeptide chains: alpha (α) and beta (β) chains. A minor population of T lymphocytes have two other chains, a gamma (γ) and delta (δ) chain (Davis and Bjorkman, 1988). Little is understood about the activities of the γ - δ T lymphocytes. The TcR has a constant and a variable region. The variable region is created by gene rearrangement and selection of minigenes in a random order to create diversity of antigen recognition sites in the population of TcR (Clancy, 1998).

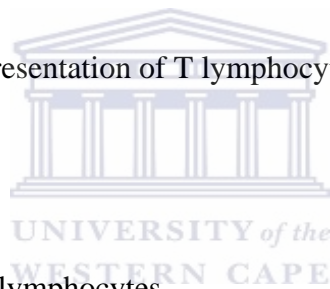
The α and β chains are associated with a group of five proteins called CD3. The TcR complex includes the α , β and the associated CD3 proteins. The recognition of the antigen-MHC complex by the TcR-CD3 complex does not require any other molecules. TcR recognise antigens in a different manner than antibodies. Antibodies recognise antigens in their native form, while the T cell antigen recognition by the TcR requires the antigen to be digested into short peptides and presented on the surface of another cell (e.g. APC) in context with the MHC class I or class II molecules (section 1.2.4).

1.2.2 T lymphocyte development

T lymphocyte development occurs in the thymus. Immature lymphocytes develop from stem cells in the bone marrow, from where they migrate into the thymus (Benoist and Mathis, 1998). In the thymus, they mature and are positively or negatively selected depending on the affinity of their TcRs for self major histocompatibility (MHC) antigens (Krammer, 2000). The MHC antigens are molecules that bind with peptide fragments from foreign and self protein and present them to the T cells. Every cell produces thousands of MHC molecules. T cells with high affinity for self MHC molecules and peptides are eliminated to ensure tolerance to normal tissues and to prevent autoimmunity. T cells develop their specific T cell markers, including TcR, CD3, CD4 or CD8 and CD2, during development and maturation (Fig 1.2).

There are two types of MHC molecules: the MHC class I and MHC class II. T cells that interact with MHC class II molecules develop into cells expressing CD4 molecules on their surface (Pieters, 1997), and those interacting with MHC class I molecules turn into T lymphocytes that express CD8 antigens (Benoist and Mathis, 1999). Only mature T cells that produce a functional TcR leave the thymus and enter the secondary lymphoid organs. Mature CD4⁺ T cells function as helper T cells and secrete cytokines that regulate either cellular immune responses or antibody responses. Mature CD8⁺ T cells function as cytokine effector (killer) cells.

Fig 1.2 An illustrative representation of T lymphocyte development (from Krammer, 2000).



1.2.3 Types of T lymphocytes

There are two subpopulations of T cells that develop and surface markers can trace their development in the thymus. The least mature T cells have a TcR associated with CD3. In the thymus, the cells express both the CD4 and CD8 markers. These cells are referred to as double positive ($CD4^+CD8^+$). Eventually the cells lose either CD4 or CD8 to become one of the functional subsets. The $CD4^+CD8^-$ cells are called helper T cells (Th cells) and the $CD4^-CD8^+$ cells are the cytotoxic T lymphocytes (CTL). Th cells and CTL both have a TcR, but they perform different functions in the immune system (Clancy, 1998).

1.2.3.1 Helper T cells (Th cells)

The generation of an immune response, both humoral (by B lymphocytes) and cell-mediated by (CTLs), depends on the activation of Th cells. The importance of Th cells has become apparent because of their involvement in AIDS (Clancy, 1998). There are two subsets of Th cells, Th1 and Th2. Th1 and Th2 look the same and have the same T cell markers and receptors. However, they differ in the cytokines that they secrete upon activation. In addition, the Th1 subset produces the cytokines IL-2 and IFN γ , which are important in cell mediated immunity. The Th2 subset helps B cells by secreting IL-4, -5 and 6. The cytokines produced by the two subsets are said to have a cross-regulatory role, meaning that Th1 cytokines down regulate the Th2 responses, and vice versa.

1.2.3.2 Cytotoxic T lymphocytes (CTLs)

CTLs are derived from a lymphocyte stem cell matured in the thymus. These cells are characterised by the presence of a CD8 marker on their surface, and an antigen-specific TcR, which recognises antigens in the context of MHC class I.

The major role of CTL is to kill other cells, especially virus-infected and tumor cells. The cytotoxic T cells must be activated in order to be able to kill. The activation of CTL requires firstly, that the TcR on the CD8+ cell interact with an antigen-MHC class I on the surface of a target cell. Secondly, the CD8+ T cell must be stimulated

by cytokines. Once activated, the CTLs are effective in killing target cells. The killing happens in three steps: (1) conjugate formation between the CTL and the target cell, (2) membrane attack on the target cell, and (3) dissociation of the two cells and the target cell death.

1.2.4 The MHC class I antigen presentation pathway

The MHC class I antigen presentation pathway plays a crucial role in the detection of virally infected cells. CD8⁺ T cells recognise peptides in association with MHC class I molecules. The principle pathway of antigen processing in association with MHC class I involves three major steps: cytosolic peptide generation, peptide transport into the endoplasmic reticulum (ER) and peptide assembly with class I molecules. Both the MHC class I and class II molecules present peptides rather than intact proteins to T cells.

Following synthesis of antigenic proteins, peptides may be generated following the action of ubiquitin and proteosomes. The newly processed peptides are transported into the ER by the transporter associated with antigen processing (TAP), an ABC transporter, in order to access the class I molecules (Koopmann *et al.*, 1997). The class I molecules do not leave the ER unless they have bound a peptide with sufficient affinity. Newly synthesised class I peptides first associate with calnexin. After binding with β 2 microglobulin, human class I molecules bind to the

calreticulin, while murine ones remain associated with calnexin. In the presence of tapasin, empty MHC class I molecules complex with calreticulin/calnexin and the reductase Erp57 can associate with TAP transporters (Sadasivan *et al.*, 1996). Once a peptide has bound to them, class I molecules are exported to the cell surface for recognition by CTL. Calnexin is thought to assist in the folding of class I heavy chains and to promote their assembly with β 2-microglobulin light chain. Tapasin plays an essential role in efficient peptide assembly with class I molecule, while the Erp57 is a cysteine protease and a chaperone for other proteins. There is still much remaining to be learned about the mechanism of peptide translocation by TAP (van Endert, 1999).

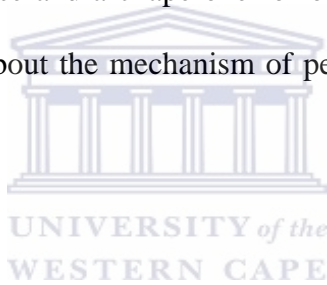


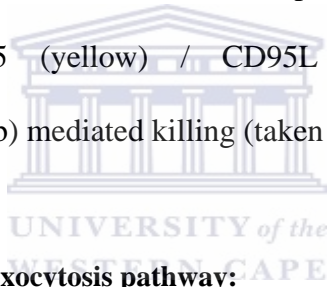


Fig 1.3 The MHC class I presentation pathway (taken from Lehner *et al.*, 2000).

1.2.5 CTL mediated killing

CTLs are able to recognise and kill virus-infected and malignant cells (Berke, 1995). There are two mechanisms by which CTLs destroy their target cells and both are caspase-dependent mechanisms. These mechanisms trigger apoptotic signals either through a Fas receptor or by granule-mediated exocytosis (Fig 1.4).

Fig 1.4 Diagrammatic representation of the two pathways by which CTLs kill their target cells: the CD95 (yellow) / CD95L (red) mediated killing and perforin/Granzyme B (GRb) mediated killing (taken from Krammer, 2000).

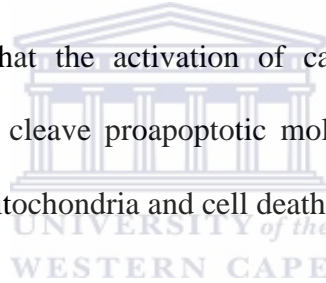


1.2.5.1 Granule-mediated exocytosis pathway:

The granule-mediated exocytosis involves the release of the lytic granules from CTLs after the adhesion of CTLs and target cells. The granules migrate towards the site of contact, where they release their contents. The granules consist of proteins necessary for inducing target cells, including a pore-forming protein, perforin, other granule-containing proteins and a family of serine proteases known as granzymes. Perforin is thought to facilitate the entry of other granule components into the cytoplasm of the target cell (Krahenbuhl and Tschopp).

Granzyme B is a member of a family of serine proteases that reside in the cytolytic granules of CTL, Natural killer (NK) and Lymphokine- activated killer (LAK) cells

(Masson and Tshopp, 1987). The first substrate to be identified for granzyme B was caspase 3, which is a member of a family of cysteine proteases involved in inducing apoptosis (Darmon *et al.*, 1995). Multiple caspases have been identified as substrates for granzyme B *in vitro* (Darmon *et al.*, 1995) and this suggests that granzyme B induces apoptosis by triggering the activation of multiple caspases within intact cells. Perforin alone has been shown to cause necrosis by osmolysis, while apoptosis is mediated by the actions of both perforin and granzymes. Granzyme B and perforin have been shown to cause DNA fragmentation in target cells (Darmon *et al.*, 1995). It has been demonstrated that the activation of caspases 8, another substrate for granzyme B, can directly cleave proapoptotic molecule, Bid, resulting in caspase-independent collapse of mitochondria and cell death (Barry *et al.*, 2000).

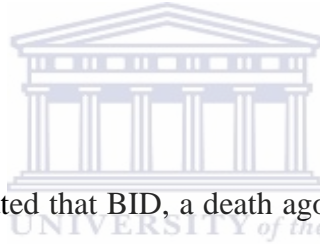


1.2.5.2 Fas-FasL pathway (Fig 1.5)

The second pathway by which CTLs destroy target cells is through a Fas pathway. Fas and FasL play an important role in three types of physiological apoptosis: (i) peripheral deletion of activated mature T cells at the end of an immune response; (ii) killing of targets such as virus-infected cells or cancer cells by CTLs and by NK cells; and (iii) killing of inflammatory cells (Krammer, 2000).

Like other TNF family members, FasL is a homotrimeric molecule. The crystal structure of lymphotoxin in complex with TNFR1 suggests that each FasL trimer binds three Fas molecules (Smith *et al.*, 1994). Because death domains have a

tendency to associate with one another, Fas ligation leads to clustering of the receptor's death domains. An adapter protein called FADD (Fas-associated death domain; also called Mort 1) (Chinnaiyan *et al.*, 1995) then binds through its own death domain to the clustered receptor death domains. FADD also contains a death effector domain (DED) that binds to an analogous domain repeated in tandem within the zymogen form of caspase-8 (Boldin *et al.*, 1996). Upon recruitment by FADD, caspase-8 oligomerisation drives its activation through self-cleavage. Caspase-8 then activates downstream effector caspases such as caspase-9, 3, 6 and 7 and initiates mitochondrial damage.



It has also been demonstrated that BID, a death agonist member of the Bcl-2 family, is a specific proximal substrate of caspase-8 in the Fas signalling pathway (Li *et al.*, 1998). Cleavage of BID by caspase-8 leads to the release of cytochrome c from the mitochondria, which will result in the inactivation of the electron transfer chain and triggers caspase-3 activation through Apaf 1 (Krippner *et al.*, 1996), which will induce mitochondrial damage. Expression of Bcl_{xL} inhibits all the apoptotic phenotypes induced by truncated BID, whereas caspase inhibitors inhibit the loss of mitochondrial membrane potential, cell shrinkage, and nuclear condensation, but not cytochrome c release.

A family of viral proteins called vFLIPs and a related cellular protein called cFLIP (also called Casper, I-FLICE or CASH) (Thorne *et al.*, 1997) contain a death effector domain that is similar to the corresponding segment in FADD and caspase-8.

Overexpression of FLIP either inhibits or activates apoptosis (Thorne *et al.*, 1997). Several other cytoplasmic proteins besides FADD can bind to CD95, including Daxx, which recognises the CD95 death domain (Yang, 1997). Daxx can activate a FADD-independent death pathway that involves the stress-activated c-Jun NH₂-terminal kinase (JNK).



Fig 1.5 Diagrammatic representation of the Fas-FasL pathway (from Yang, 1997).

1.3 Natural killer cells

Natural Killer (NK) cells were discovered in the 1970's and are a subset of large granular lymphocytes that are cytotoxic. They are derived from the bone marrow and lack most markers for T and B cells. They are called “natural” killers because, unlike cytotoxic T cells, they do not need to recognize a specific antigen before killing (Stone *et al.*, 1997). They can spontaneously kill tumor or virus-infected cells (Trinchieri, 1989) and attack cells that lack the expression of MHC class I antigens. They are said to be the first line of defence against malignant cells and cells infected with viruses, bacteria and protozoa. They account for about 15 % of the human white blood cells.



Fig 1.6 Electron micrograph showing a Natural killer cell.

NK cells share several similarities with CTLs. They both kill certain tumor cells and virus-infected cells. NK cells have similar mechanisms for killing with CTLs, including the secretion of pore-forming proteins, serine proteases and other proteins.

However, NK cells can be distinguished from T lymphocytes in that they do not express the TCR and bind antigen through a different set of receptors. Unlike CTLs, NK killing is non-specific, they do not recognize antigen/MHC on the target cell and they do not have T cell receptors.

1.3.1 How NK cells kill?

There are two ways in which NK cells kill certain mutant and virus-infected cells. The first mechanism involves the killing of cells to which antibody molecules have attached. This process is called antibody-dependent cellular cytotoxicity (ADCC) (Fig 1.7). NK cells bind and kill targets coated with IgG antibodies via their receptors for IgG (CD16). The NK cell is then able to contact the cell and release perforins, granzymes and chemokines. The granzymes pass through the pores and activate the enzymes that lead to apoptosis of the target cell.

Fig 1.7 Killing of the target cell by NK cell using ADCC mechanism.

The second mechanism involves the killing of cells lacking the MHC class I molecules on their surface. NK cells use a dual receptor system in determining whether to kill human cells or not (Fig 1.8). NK cells express two families of membrane receptors: the killer-activating receptor and the killer-inhibitory receptor.



Fig 1.8 The dual receptor system of NK cells for killing of target cell.

1.3.2 Killer-activating receptors

Killer-activating receptors belong to the immunoglobulin (Ig), integrin and C-type lectin families. These receptors activate NK cells in response to MHC class I molecules (Lanier and Bakker, 2000). They have charged amino acid residues in their

transmembrane domain, allowing them to interact with other signaling proteins containing immunoreceptor tyrosine-based activation motifs (ITAMs). When the NK stimulatory receptors bind to their ligands, ITAM recruit downstream molecules, resulting in the stimulation of NK cells and the killing of the target cell.

1.3.3 Killer-inhibitory receptors

This type of receptor recognizes class I MHC molecules and prevents the lysis of the cells that express class I molecules and allow destruction of the cells not expressing class I molecules (Long, 1999). There are two types of inhibitory receptors of NK cells: the Ig-like and lectin-like receptors. They have short amino acid sequences in their cytoplasmic domains called immunoreceptor tyrosine-based inhibitory motifs (ITIMs), which contribute to the activation of certain tyrosine phosphatases. When these receptors bind to the MHC class I ligands, the ITIMs are phosphorylated and recruit phosphatases, preventing killing by NK cells (Janeway-Travers, 1996).

1.4 Apoptosis

1.4.1 Introduction

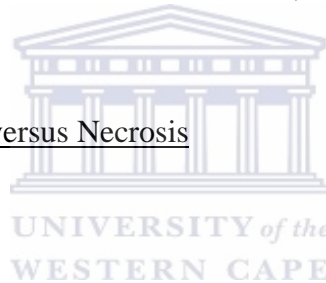
The word apoptosis has been derived from a Greek word meaning ‘a falling away’, which is used in the context of leaf fall, as opposed to necrosis, meaning ‘to make dead’ (Kerr *et al.*, 1972). Apoptosis is a physiological process, which plays a central

role in the development of multicellular eukaryotes and in maintaining homeostasis. Apoptosis is the mode of death by which cells reactive to T cells in the thymus are eliminated. NK cells also utilise the apoptotic mechanism to kill virally infected cells.

The physiological role of apoptosis is crucial; malfunctions of this process can be detrimental. Too little apoptosis may result in cancers and autoimmune diseases. Whereas, too much apoptosis can be associated with the damage observed in stroke or the neurodegeneration of Alzheimer's disease (Thompson, 1995).

1.4.2 Apoptosis versus Necrosis

1.4.2.1 Definitions



There are two ways in which cells die: they are either killed by injurious agents (necrosis) or induced to commit suicide (apoptosis). Necrosis is an accidental death, which occurs when cells are exposed to a serious physical or chemical insult, while apoptosis is a programmed cell death by which unwanted cells are eliminated during development and other normal biological processes.

1.4.2.2 Morphological changes between necrosis and apoptosis

There are many morphological and biochemical differences between necrosis and apoptosis. Some of the changes are listed in Table 1.2 and illustrated in Figure 1.9.

NECROSIS	APOPTOSIS
----------	-----------

Loss of membrane integrity	Membrane blebbing, no loss of integrity
Swelling of cytoplasm and mitochondria	Shrinkage of cytoplasm and condensation of the nucleus
Total cell lysis	Fragmentation of cell into smaller bodies
No vesicle formation	Formation of membrane bound vesicles (apoptotic bodies)
Disintegration of organelles	Mitochondria leakage
Random digestion of DNA	Non-random mono- and oligonucleosomal length fragmentation of DNA
Significant inflammatory response	No inflammatory response

Table 1.2: Morphological and biochemical differences between apoptosis and necrosis.

Exposure to extreme variance from physiological conditions (e.g. hypothermia and hypoxia) may lead cells to undergo necrosis, resulting in plasma membrane damage. Under physiological conditions, agents like complement and lytic viruses cause direct damage to the plasma membrane. Necrosis begins when there is impairment in the cell's ability to maintain homeostasis, leading to an influx of water and extracellular ions. Intracellular organelles, including the mitochondria, and the entire cell swell and rupture (Kroemer *et al.*, 1995). Ultimately, the plasma membrane breaks down and the cytoplasmic contents are released into the extracellular fluid (Fig 1.9a). *In vivo*, necrosis is associated with tissue damage resulting in an inflammatory response.

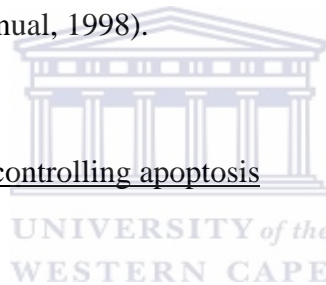
Fig 1.9a Illustration of the morphological features of necrosis (taken from Boehringer Mannheim manual, 1998).



Apoptosis, however, occurs under physiological conditions and the cell is responsible for its own demise. It is mostly found during tissue homeostasis, embryogenesis, induction and maintenance of immune tolerance and development of the nervous system. Morphological and biochemical features of cells undergoing apoptosis include chromatin aggregation, nuclear and cytoplasmic condensation, and the division of cytoplasm and nucleus into membrane-bound vesicles known as apoptotic bodies (Kerr *et al.*, 1972). *In vivo*, the apoptotic bodies are recognised and phagocytosed by macrophages. Due to this efficient removal of apoptotic bodies *in vivo*, no inflammation is induced. However, *in vitro*, the apoptotic bodies swell up and lyse, and this phase is called 'secondary necrosis' (Fig 1.9b).

Fig 1.9b Illustration of the morphological features of apoptosis (taken from Boehringer Mannheim manual, 1998).

1.4.3 Molecules controlling apoptosis



The process of apoptosis must be carefully controlled. There are two groups of molecules which are responsible for this: caspases and the Bcl-2 family.

1.4.3.1 The Caspase Family

Most of the morphological and cellular changes of apoptosis are caused by a well-conserved, highly specific set of cysteine proteases known as caspases. The term caspases is a short form for Cysteine Aspartate-specific Proteases, because of the substrate specificity of the caspases (Alnemri *et al.*, 1996). Caspases specifically cleave their substrates after Asp residues (Wolf and Green, 1999). All caspases exist within the cell as inactive zymogens. These zymogens can be cleaved to form active

enzymes following the induction of apoptosis (Wilson *et al.*, 1994). The initial cleavage of a procaspase into its active form is accomplished either by self-catalysis or cleavage by another caspase. Since a single caspase molecule can trigger the activation of many procaspases, a propagation of active caspases, termed a caspase cascade, can occur (Feleiro *et al.*, 1997).

Caspases share a number of common structural motifs (Wolf and Green, 1999, Cohen, 1997). There is an N-terminal pro-domain, which varies in length amongst the caspases, a large subunit containing cysteine active site, a C-terminal small subunit, an Aspartate between pro-domain and large subunit and an interdomain containing 1 or 2 aspartate residues between the large and small subunit (Fig1.10).

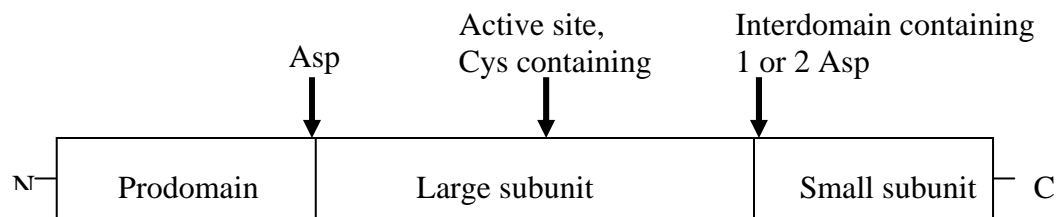


Fig 1.10 General structure of procaspase.

Activation of the pro-caspase is accompanied by proteolysis of the interdomain and results in the removal of the prodomain. The active site is composed of residues from both small and large domains.

1.4.3.1.1 Types of caspases

Although members of the caspase family share a common structure (Fig 1.10), there are subfamily differences that reflect their slightly different roles in apoptosis (Lincz, 1998). So far, fourteen different members of the caspase family have been identified in mammals. Caspases can be divided into three classes based on their roles in cellular processes (Talanian *et al.*, 2000).

Initiator caspases (2, 8, 9 and 10)

This group of caspases contain functional pro-domains, which allow association with receptor complexes for receptor-stimulated apoptosis. Caspases 2 and 10 contain CARDs and caspases 8 and 9 contain DEDs. The initiator caspases act upstream of the execution caspases.

Execution caspases (3, 6 and 7)

This group of caspases contain short (23 amino acid) non-functional pro-domains. They are responsible for interacting with other caspases and non-caspase molecules to induce apoptosis.

Cytokine processor caspases (1, 4, 5, 12, 13, and 14)

Not much is known about the members of this group. Caspases 1, 4, 5 and 11 may play a role in inflammation (Cohen, 2000). Caspase 11 acts as a cofactor for caspase 1 activation.

1.4.3.1.2 Activation of Caspases

Induction of apoptosis via cell death receptors results in the activation of initiator caspases, such as caspase 8 or 10. These caspases can then activate other caspases in a cascade. This cascade eventually leads to the activation of the effector caspases, such as caspase 3 and 6. These caspases are responsible for the cleavage of the key cellular proteins that leads to the typical morphological changes observed in cells undergoing apoptosis (section 1.4.2.2).

There are other mechanisms through which caspases can be activated. For example, granzyme B can be delivered into cells by CTLs and is able to directly activate caspases 3, 7, 8 and 10 (section 1.2.3.2.2).

The mitochondria are also the key regulators of the caspase cascade and apoptosis. The release of cytochrome c from the mitochondria can lead to the activation of caspase 9 and then caspase 3 (section 1.4.4.2).

The following table lists the main caspases and some of their substrates and functions:

CASPASE	ALTERNATE NAME	SUBSTRATES	FUNCTION
Caspase-1	ICE	Pre-Interleukin-1b Lamins	Processing of interleukins. Can also induce apoptosis.
Caspase-2	Ich-1 (human) Nedd2 (rat, mouse)	Golgin-160	Apoptosis
Caspase-3	CPP32, YAMA, apopain	PARP Caspases-6, 7, 9 DNA-PK MDM2 Fodrin Lamins Topoisomerase I ICAD	Apoptosis
Caspase-4	Ich-2, ICE (rel)II	Caspase-1	Inflammation/Apoptosis
Caspase-5	ICE(rel)III	?	Inflammation/Apoptosis
Caspase-6	Mch2	PARP Lamins NuMA FAK Caspase-3	Apoptosis
Caspase-7	Mch3, ICE-LAP3, CMH-1	PARP Gas2 SREB1 EMAP II FAK Calpastatin	Apoptosis
Caspase-8	FLICE, MACH, Mch5	Caspases-3, 4, 6, 7, 9, 10, 13 PARP Bid	Apoptosis (death receptors)
Caspase-9	Apaf-3, ICE-LAP6, Mch6	Caspase-3, 7 Pro-caspase-9 PARP	Apoptosis
Caspase-10	FLICE-2, Mch4	Caspases-3, 4, 6, 7, 8, 9	Apoptosis (death receptors)
Caspase-11	Ich-3, ICE-B	?	Inflammation and apoptosis
Caspase-12	ICE-C	?	Apoptosis
Caspase-13	ERICE	?	Inflammation

Table 1.3 Types of caspases and their function.

1.4.3.2 The Bcl-2 Family

The gene *bcl-2* (B-cell lymphoma-2) was first identified on human chromosome 18 (Friend *et al.*, 1986). It encodes a membrane-associated protein, Bcl-2, present in ER, nuclear and outer mitochondrial membranes. Bcl-2 proteins are the mammalian homologues to the *C. elegans* protein *ced-9* and pro-apoptotic protein, *egl-1*. At least 15 Bcl-2 family members have been identified in mammalian cells and several others in viruses. The members of the Bcl-2 family are classified into three functional groups (Fig 1.11). Group I members, such as Bcl-2 and Bcl-X_L, are characterised by four short, conserved Bcl-2 homology (BH) domains (BH1-4) (White *et al.*, 1994). They also contain a C-terminal hydrophobic tail, which localises the proteins to the outer surface of mitochondria. Members of group I all possess an anti-apoptotic activity and protect cells from death. Group II consists of Bcl-2 family members with pro-apoptotic activity. Members include Bax and Bak, and they have a similar overall structure to group I proteins, except for the absence of the N-terminal BH4 domain (Adams and Cory, 1998). Group III consists of a large and diverse proteins, whose common feature is the presence of a 12-16 amino acid BH3 domain (Adams and Cory, 1998).

Fig 1.11 The Bcl-2 family members (taken from Hengartner, 2000).

Some of the members of the Bcl-2 family known to date include:

Bcl-2: B cell lymphoma 2. It codes for 2 proteins, α and β . Bcl-2 refers to Bcl-2 α , which is anti-apoptotic.

Bcl-X: It codes for two proteins: Bcl-X_L, which is anti-apoptotic and Bcl-X_S, is pro-apoptotic.

Bad: Bcl-XL/Bcl-2-associated death promoter homologue. It is pro-apoptotic.

Bid: Bcl-2 Interacting Protein. It is pro-apoptotic.

Bak: Bcl-2 homologous antagonist killer.

A1: a novel haemopoietic specific early response gene.

Mcl-1: myeloblastic leukaemia cell line gene.

Bax: It is pro-apoptotic and is seen as the most fundamental member of the Bcl-2 family as the other members act (directly or indirectly) to control the actions of Bax.

1.4.4 The Apoptotic pathways

There are two different mechanisms involved in apoptosis: the death receptor or extrinsic pathway and the mitochondrial or intrinsic pathway (Fig 1.13).

1.4.4.1 Death receptor or extrinsic pathway

Death receptors belong to the tumour necrosis factor receptor (TNFR) gene superfamily, with cysteine-rich extracellular domains (Smith *et al.*, 1994). The death receptors also contain a homologous cytoplasmic domain known as the "death domain" (Tartaglia *et al.*, 1993). Death domains enable death receptors to engage the cell's apoptotic machinery. The best-characterised death receptors are CD95 (also called Fas or Apo1) and TNFR1 (also called p55 or CD120a) (Smith *et al.*, 1994). Additional death receptors are avian CAR1; death receptor 3 (DR3; also called Apo3, WSL-1, TRAMP, or LARD) (Chinnaiyan *et al.*, 1997); DR4 (Pan *et al.*, 1997); and DR5 (also called Apo2, TRAIL-R2, TRICK2 or KILLER). The ligands that activate these receptors are structurally related molecules that belong to the TNF gene superfamily (Smith *et al.*, 1994). Fas ligand (FasL) binds Fas; TNF and lymphotoxin bind to TNFR1; Apo3L (also called TWEAK) binds to DR3; and Apo2L (also called TRAIL) binds to DR4 (Pan *et al.*, 1997) and DR5. The ligand for CAR1 is unknown.

Receptors such as TNFR1 and Fas (section 1.2.3.2.2) interact with their respective ligands at the surface of the cell, which then induces the formation of a death-

inducing signalling complex (DISC). This complex recruits several procaspase-8 molecules through an adaptor molecule such as Fas-associating death domain (FADD) or MORT1 (Mediator of receptor-induced toxicity). This results in caspase-8 activation, which initiates a cascade of caspase activation leading to the destruction of the cell.

1.4.4.2 Mitochondrial or intrinsic pathway

In a healthy cell, the outer mitochondrial membranes express Bcl-2 on their cytoplasmic surface. Bcl-2 is bound to a protein called Apaf-1 (apoptotic protease activating factor-1). Internal damage to the cell, such as DNA damage, causes Bcl-2 to release Apaf-1 and the release of cytochrome c. Apaf-1, cytochrome c and ATP activate caspase-9. The activated caspase-9, in turn, activates caspase-3, which is responsible for the execution of the cell.

Although the two pathways operated independently of each other under most conditions, each of them involves the activation of specific initiator caspases, such as caspase-8 and 9. Both pathways eventually converge at the level of caspase-3 activation.



Fig 1.12 Diagrammatic representation of the two mechanisms by which apoptosis occurs: the death receptor and the mitochondrial pathways (from Hengartner, 2000).

1.5 Tumor suppressor genes

Tumour suppressor genes are negative regulators of the cell cycle growth, DNA replication and division (Vogelstein *et al.*, 2000). Tumour suppressor genes are needed to keep cell division under control. Many tumour suppressor proteins function by inducing apoptosis in response to DNA damage, hypoxia and other stresses (Macleod, 2000). It has been shown that a loss of function of the tumour suppressor gene results in reduced apoptosis and increased tumour growth. There are at least 24

tumor suppressor genes that have been described (Table 1.4). The two best understood tumor suppressor genes are the retinoblastoma (Rb) and the p53 genes.

Tumor suppressor gene	Location on human chromosomal	Human tumors
RB1	13q14	Retinoblastoma, osteosarcoma
Wt1	11p13	Nephroblastoma
P53	17q11	Sarcomas, breast/brain tumors
NF1	17q11	Neurofibromas, sarcomas, gliomas
NF2	22q12	Schwannomas, meningiomas
VHL	3p25	Hemangiomas, renal, pheochromocytoma
APC	5q21	Colon cancer
INK4a	9p21	Melanoma, pancreatic
PTC	9q22.3	Basal cell carcinoma, medulloblastoma
BRCA1	17q21	Breast/ ovarian tumors
BRCA2	13q12	Breast/ ovarian tumors
DPC4	18q21.1	Pancreatic, colon, hamartomas
FHIT	3p14.2	Lung, stomach, kidney, cervical carcinoma
PTEN	10q23	Glioblastoma, prostate, breast
TSC2	16	Renal, brain tumors
NKX3.1	8p21	Prostate
LKB1	19p13	Hamartomas, colorectal, breast
E-Cadherin	16q21.1	Breast, colon, skin, lung carcinoma
MSH2	2p22	Colorectal cancer
MLH1	3p21	Colorectal cancer
PMS1	2q31	Colorectal cancer
PMS2	7p22	Colorectal cancer
MSH6	2p16	Colorectal cancer

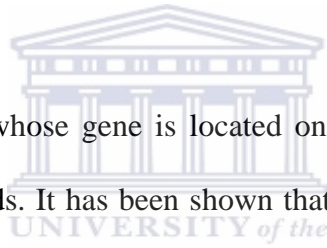
Table 1.4 Tumor suppressor genes and associated human cancers (from Macleod, 2000).

1.5.1 The p53 gene

p53 was the second tumour suppressor gene to be identified in 1979 after the Rb gene, and it was found to be associated with the transforming protein of SV40 tumour

virus (Linzer and Levine, 1979). p53 was named in reference to its molecular weight of 53 kD. It has been discovered that in most human cancers, p53 was inactivated due to mutations in the gene (Rodrigues *et al.*, 1990). About 50 % of human cancers can be associated with a p53 mutation including cancers of the bladder, breast, cervix, colon, lung, liver, prostate and skin. It has been shown that p53 related cancers are more aggressive and have a higher degree of fatalities (Rodrigues *et al.*, 1990).

1.5.1.1 The structure of p53 protein



p53 is a nuclear protein whose gene is located on human chromosome 17p13 and consists of 393 amino acids. It has been shown that a single amino acid substitution can lead to a loss of function of the p53 protein (Hupp *et al.*, 2000). p53 protein is divided into four domains (Fig 1.13): (1) the N terminal transactivation domain, which is a highly charged, acidic region of 75- 80 residues. This domain contains binding sites for transactivating factors, MDM2 and regulatory phosphorylation sites; (2) the core sequence-specific DNA binding domain, containing most of the p53 mutations found in human cancers (Hollstein *et al.*, 1991). It is a hydrophobic, proline-rich domain; (3) the tetramerisation domain which ensures the assembly of p53 into conformationally active tetramers (Jeffrey *et al.*, 1995); and (4) a negative regulatory, basic C terminal domain containing a heat-shock cognate 70 stress protein (hsc70)-binding site (Hansen *et al.*, 1996), a cyclin A docking site (Luciani *et al.*, 2000) and multiple sites for phosphorylation (Hupp and Lane, 1994), SUMOlation (Rodriguez *et al.*, 1990) and acetylation (Gu and Roeder, 1997).

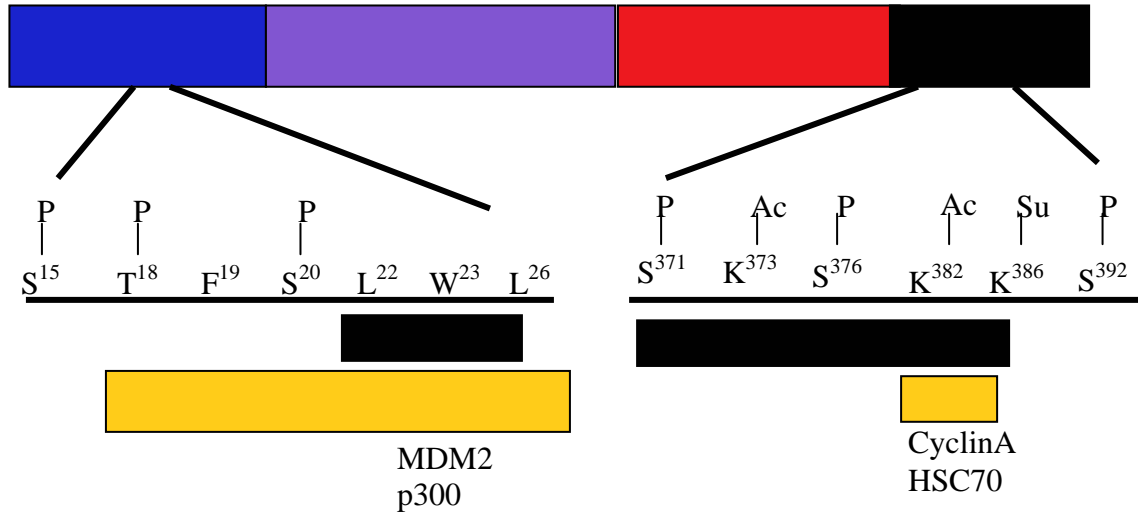


Fig 1.13 Structure of p53 showing the functional and regulatory domains (taken from Hupp *et al.*, 2000).

1.5.1.2 Functions of the p53 gene

The p53 tumor suppressor gene plays an important role in the prevention of tumor development. It suppresses progression through the cell cycle in response to DNA damage in order to allow DNA repair to occur. If the damage to the cell is severe, p53 will initiate apoptosis. These responses prevent replication of or eliminate cells with damaged DNA. Defective p53 can allow abnormal cells to grow, resulting in cancer.

p53 functions as a transcription factor and binds to DNA as a tetramer, thereby regulating the transcription of a large number of genes (el-Deiry *et al.*, 1992). These genes include those that are involved in cell cycle arrest (e.g. the cyclin-dependent kinase inhibitor, p21^{Waf1/Cip1}); DNA repair (e.g. p53R2) and those involved in

apoptosis (e.g. Bax, and Apaf-1 (Vousden, 2000). p53 also represses the transcription of other genes, such as those involved in stimulating cell growth.

Other functions of p53 include the ability of p53 to relocalise death receptors like Fas from the Golgi to the cell surface (Bennett *et al.*, 1998), and the direct involvement of p53 in the mitochondria (Marchenko *et al.*, 2000).

1.5.1.3 p53-activating pathways

There are three independent pathways that play a role in activating the p53 network. One pathway is triggered by DNA damage, e.g. ionising radiation. This pathway depends on two protein kinases: ATM (ataxia telangiectasia mutated) and Chk2 (checkpoint kinase 2) (Carr, 2000). ATM is activated by double stranded breaks in DNA, and in turn stimulates Chk2.

The second pathway is stimulated by aberrant growth signals, resulting from the expression of the oncogenes Ras and Myc. In humans, the activation of p53 network depends on p14^{ARF} tumor suppressor protein (Lowe and Lin, 2000).

The third pathway is triggered by a wide of range of chemotherapeutic drugs, UV light and protein kinase inhibitors. It involves kinases called ataxia telangiectasia related (ATR) and casein kinase II (Meek, 1999).

All three pathways inhibit the degradation of p53 protein and therefore stabilize p53 at high concentrations. Increased p53 concentrations allow p53 to bind to particular DNA sequences and activate transcription of adjacent genes. It is these genes that ultimately lead to cell death or the inhibition of cell division.

1.5.1.4 Regulation of p53 activity

Signals that activate the p53 response lead to rapid increase in p53 protein concentration through stabilization of the protein and activation of the DNA binding function of p53 (Ashcroft and Vousden, 1999). p53 levels must be tightly regulated. Although p53 suppresses tumors, high levels of p53 may increase the aging process by excessive apoptosis. The major regulator of p53 is Mdm2 (murine double minute clone 2) (section 1.5.1.2). The p53 protein binds specifically to Mdm2 promoter and activates its transcription (Barak *et al.*, 1993). The resultant Mdm2 protein binds directly to p53 and targets it for degradation through an ubiquitin-dependent pathway (section 1.6.1) (Kubbutat *et al.*, 1997). This defines a negative feedback loop (Fig 1.14), which keeps p53 in check. The importance of the p53-Mdm2 feedback loop was illustrated in Mdm2 knockout mice. These experiments showed that the inactivation of Mdm2 resulted in excess p53 activity, which lead to embryonic death (Jones *et al.*, 1995 and Montes de Oca Luna *et al.*, 1995).

Fig 1.14 The p53-Mdm2 negative feedback loop (taken from Oren, 1999).

It has been reported that stabilisation and activation of p53 protein upon stress also involves covalent modifications of p53, including phosphorylation, acetylation and glycosylation. Phosphorylation within the p53-Mdm2 binding interface blocks the binding, and thereby preventing p53 from degradation (Shieh *et al.*, 1997). Mdm2 may also become phosphorylated, blocking p53 degradation. Other types of modification of both p53 and Mdm2 have also been reported. Acetylation and glycosylation of p53 have been reported to result in increased DNA binding (Gu and Roeder, 1997 and Shaw *et al.*, 1996).

Protein-protein interactions also play a role in regulating cellular p53 levels and activity. An example is provided by the ARF (alternative reading frame) protein. ARF is a small protein, which arises through the translation of an alternative reading frame derived from the INK4A tumor suppressor gene (Kamijo *et al.*, 1998). ARF binds to Mdm2 and p53, thus preventing p53 degradation (Zhang *et al.*, 1998).

1.5.1.5 p53-binding proteins

Wild-type p53 binds to specific genomic sites with a consensus binding site 5'-PuPuPuC (A/T)(T/A)GpyPyPy-3' (el-Deiry *et al.*, 1992). A number of targets for p53 have been identified (reviewed by Tokino and Nakamura, 2000). Table 1.5 lists the p53 target genes and their function.

TARGET GENES	FUNCTION
Mdm2	Involvement in p53 control
P21 WAF1/CIP1, GADD45, WIP1, Mdm2, EGFR, PCNA, CyclinD1, Cyclin G, TGF α	Involvement in cell cycle control
GADD45, PCNA, p21 WAF1/CIP1	Involvement in DNA repair
BAX, Bcl-L, FAS1, FASL, DR5	Involvement in apoptosis
TSP-1, BAI1	Involvement in angiogenesis
TP53TG1, CSR, PIG3	Involvement in cellular stress response

Table 1.5 p53-binding proteins and their function.

1.5.1.6 MDM2 protein

MDM2 (murine double minute-2) was first identified as an amplified gene in a spontaneously transformed mouse 3T3 cell line (reviewed in Gu *et al.*, 2003). It is overexpressed in many human tumours and cancers (Oliner *et al.*, 1992). It functions as an E3 ligase for p53 and itself through its RING finger domain at the C-terminus (Honda *et al.*, 1997). MDM2 binds to p53 and targets p53 protein degradation via the ubiquitin-mediated pathway (Haupt *et al.*, 1997). It interferes with p53's ability to transactivate target genes. It binds to the N terminus of p53 at its transactivation domain (Fig 1.13) and inhibits its ability to function as a transcription factor. It

delocalises p53 from the nucleus to cytoplasm where it undergoes proteosomal degradation (Tao and Levine, 1999). p53 binds to the promoter region of MDM2 and activates its transcription. The MDM2 protein then binds to p53 and stimulates p53 degradation. MDM2 can ubiquitinate p53 and itself (Lohrum and Vousden, 2000).

Another member of MDM2 family, MDMX, has been shown to bind to p53 and MDM2 and both these interactions can stabilize p53 (Ashcroft and Vousden 1999). The MDMX protein is structurally homologous to MDM2. The interaction of MDMX with MDM2 is mediated through the RING-finger domains of the two proteins and results in the inhibition of MDM2-mediated degradation (Ashcroft and Vousden, 1999). MDMX binding therefore stabilizes MDM2 as well as p53.

MDM2 has also been shown to interact with the Rb tumor suppressor protein and regulates the transcription factor E2F1 to promote cell cycle S-phase entry (Xiao *et al.*, 1995). It inhibits the growth suppression at G1 imposed by p53 and Rb. Rb has been shown to regulate the apoptotic function of p53 through binding to MDM2, thus preventing MDM2 from targeting p53 for degradation (Hsieh *et al.*, 1999). Rb does this by forming a trimeric complex with p53 via binding to MDM2. However, Rb cannot prevent MDM2 from inhibiting p53-mediated transactivation (Hsieh *et al.*, 1999). This, therefore, directly links the function of the two tumour suppressor proteins and demonstrates a new role of Rb in regulating the apoptotic function of p53.

Another interesting protein that has been shown to interact with MDM2 is the ARF tumour suppressor protein. ARF activates p53 by binding directly to MDM2, thereby inhibiting the E3-ligase activity of MDM2 and interfering with nucleocytoplasmic cycling of MDM2 that is necessary for p53 degradation (Tao and Levine, 1999).

1.5.2 Retinoblastoma (Rb) gene

Retinoblastoma is a tumour of the retina. It occurs in two forms: the familial retinoblastoma in which multiple tumours occur in the retinas of both eyes in the first week of infancy; while in sporadic retinoblastoma a single tumour occurs in one eye early in childhood before the retina is fully developed. Both forms are caused by a mutation in the Retinoblastoma (Rb) gene, located on human chromosome 13.

The Rb gene was the first tumor suppressor gene to be identified and was isolated from retinoblastoma tumors (Lee *et al.*, 1987). It is a member of a family of proteins, which includes p107 and p130. The protein product of the retinoblastoma gene, Rb, is a nuclear phosphoprotein that arrests cells during the G1 phase of the cell cycle by repressing transcription of genes required for the G1-to-S-phase transition (Weinberg, 1995). The retinoblastoma protein is a master regulator of the cell cycle, cell differentiation and apoptosis (Williams and Grafi, 2000). Rb is frequently mutated in tumours such as retinoblastoma, osteosarcoma and small-cell lung carcinoma (reviewed in Hsieh *et al.*, 1999).

1.5.2.1 Structure of Rb protein

The human Rb protein contains 928 amino acids, with a relatively long half-life (>8 hours) (Morris and Dyson, 2001). The Rb protein is made up of three type of pocket domains: A, B and C and they are situated at residues 379-928 (Hsieh *et al.*, 1999) (Fig 1.15). The A and B domains are separated by a spacer region and are important in the binding of viral oncoproteins. The C domain binds to the tyrosine kinase c-Abl (Welch and Wang, 1993) and can also interact with Mdm2 (Xiao *et al.*, 1998).



Fig 1.15 The structure of the retinoblastoma (Rb) pocket domain protein (from Morris and Dyson, 2001).

1.5.2.2 The role of Rb protein

Rb is known to regulate the progression from G1 to S phase of the cell cycle (Weinberg, 1995) and has been implicated in the differentiation of muscle cells (Gu *et al.*, 1993) and adipocytes (Chen *et al.*, 1996).

The regulation of the G1 phase of the cell cycle requires the binding of Rb to a number of cellular proteins, many of which are transcription factors. The best-studied transcription factor is the E2F family. Rb binds to E2F through its large pocket domain and negatively regulates its activity (Weinberg, 1995). Progression of a cell through the G1 and S phase requires inactivation of Rb by phosphorylation. Phosphorylation of Rb by cyclin D-dependent kinases (CDKs) and their cyclin partners (such as cyclin D, Cdk4 or Cdk6 and cyclin E) results in the release of Rb from E2F, leading to progression through the cell cycle (Lundberg and Weinberg, 1998). It has been shown that the phosphorylation of Rb leads to its loss of function as cells progress through the G1 and S phase (Harbour *et al.*, 1999). Loss of Rb function creates a selective pressure for the tumor to inactivate p53, which serves to eliminate cells with mutations in the Rb pathway (Harbour and Dean, 2000). Therefore, many tumors have mutations that inactivate both Rb and p53.

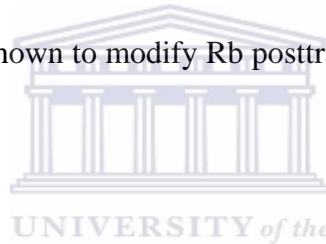
1.5.2.3 Function of Rb in apoptosis

Rb is inactivated either by a mutation in the gene or by the phosphorylation of the protein in almost all tumors. Loss of Rb function triggers the p53 apoptotic pathway (Morgenbesser *et al.*, 1994). This link between Rb and p53 pathways can be explained by the fact that loss of Rb function leads to the release of E2F, which in turn triggers apoptosis by activating the tumour suppressor protein ARF (alternative reading frame) expression, which is encoded by the INK4A locus (Pomerantz *et al.*, 1998).

Loss of Rb function can also induce p53-independent apoptosis and this may not be triggered by E2F.

1.5.2.4 Rb-binding proteins

Currently, there are at least 110 Rb-binding proteins reported. They are divided into three groups based on certain characteristics (Morris and Dyson, 2001). The first group consists of 15 kinases, phosphatases and kinase-regulators (Table 1.6). Most of these proteins have been shown to modify Rb posttranslationally in order to affect the function of Rb.



Rb-binding protein	Region of Rb binding
Cyclin A	Not mapped
Cyclin A1	Large pocket
Cyclin D1	Small pocket
Cyclin D2	Small pocket
Cyclin D3	Small pocket
Cyclin E	Not mapped
p25 ^{NCK5a}	Large pocket
Cdc2	Not mapped
Cdk2	C-domain
Cdk4	Not mapped
JNK 1	C-domain
Raf	Small pocket
pRb kinase	N-domain
PP1 α	C-domain
PP1 δ	Not mapped

Table 1.6 The first group of Rb-binding proteins (i.e. kinases, phosphatases and their regulators).

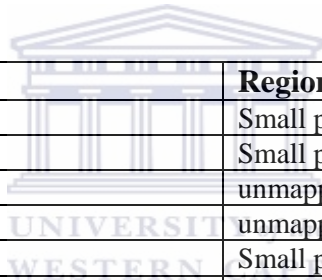
The second group contains 72 transcriptional regulators, which in turn are grouped into three functional categories (Table 1.7): (1) factors repressing transcription, (2) factors activating transcription, and (3) factors affecting transcription in unknown ways.

Rb-binding protein	Region of Rb binding
E2F-1	Large pocket
E2F-2	Large pocket
E2F-3a	Large pocket
E2F-3b	Not mapped
E2F-4	Large pocket
DP-1	Not mapped
DP-2	Not mapped
RBP60	Large pocket
RbAp46	Small pocket
RbAp48	Small pocket
HDAC1	Small pocket
HDAC2	Small pocket
HDAC3	Small pocket
c-Ski	B-domain
Sno	Not mapped
Sin3a	Not mapped
RBP1	Small pocket
RBP2	A-domain and spacer
Bdp	C-domain
Elf-1	Large pocket
CtIP	Small pocket
TFIIIB	Large pocket
TBP	Not mapped
BRF/TFIIIB	Not mapped
UBF	C-domain
HBP1	Small pocket
DNMT1	Small pocket
NFκB p50	Not mapped
RBak	Not mapped
P120 ^{E4F}	B and C-domain

Table 1.7.1 A group of Rb-binding proteins that function by repressing transcription.

Rb-binding protein	Region of Rb binding
MyoD	B and C-domain (605-792)
Myogenin	B and C-domain (605-792)
Myf-5	B and C-domain (605-792)
MRF4	B and C-domain (605-792)
NF-IL6	Small pocket
C/EBP	B and C-domain (612-767)
c-Jun	Small pocket
JunB	Not mapped
JunD	Not mapped
Sp1	Not mapped

Table 1.7.2 A group of Rb-binding proteins that function by activating transcription.



Rb-binding protein	Region of Rb binding
BRG1	Small pocket
HBRm1	Small pocket
ATF-1	unmapped
ATF-2	unmapped
c-myc	Small pocket
N-myc	Small pocket
PU.1	Large pocket
AP-2	Large pocket
Id-2	Small pocket
Pur α	Not mapped
Cream-1/Rbap2	Not mapped
Che-1	Not mapped
TAF _{II} 250	All regions
TAF _{II} 150	Large pocket
TAF _{II} 80	Large pocket
RIZ	Not mapped
Rim	Not mapped
Estrogen receptor	Not mapped
PML	Small pocket
Mdm2	C-domain
p202	N (1-254) and large pocket
Mi	Not mapped
pRb	N (1-300) to C-domain

Table 1.7.3 A group of Rb-binding proteins that affect transcription in unknown ways.

The third group of Rb-binding proteins consists of 23 proteins that have a variety of functions, including regulating DNA replication, cell cycle and various nuclear processes (Table 1.7.3).

Rb-binding protein	Function	Region of Rb binding
c-Abl	Tyrosine kinase	C-domain
Rak	Tyrosine kinase	Small pocket
Bog	Oncogene	Not mapped
Prohibitin	Tumor suppressor gene	Not mapped
BRAC1	Tumor suppressor gene	Large pocket
p21 ^{CIP1/WAF1}	Cdk inhibitor	Small pocket
p57 ^{KIP2}	Cdk inhibitor	Not mapped
H-nuc	Metaphase spindle control	Small pocket
Mitotin	Centromeres regulation	Not mapped
Nuclear lamin A	Nuclear matrix	B and C-domain
Nuclear lamin C	Nuclear matrix	B and C-domain
NRP/B	Nuclear matrix	Not mapped
*P2P-R	RNA processing	Small pocket
P84N5	RNA processing/ apoptosis	N-domain (1-300)
*RBQ-1/PACT	Pre-RNA splicing	unmapped
RBQ-3	unknown	B and C-domain
Topo-II α	Relax DNA supercoiling	Small pocket
DNA pol α	Replicative DNA polymerase	Not mapped
REC2	Recombinase	Large pocket
MCM7	Pre-replication complex	N-domain (1-400)
hsHec1p	Chromosomal segregation	Large pocket
hsc73	Heat-shock protein	N-domain
hsp75	Heat -shock protein	Small pocket

*These are truncated homologues of the RBBP6 protein.

Table 1.8 Rb binding proteins involved in regulating DNA replication, cell cycle and various nuclear processes.

1.6 The ubiquitin-proteasome pathway

1.6.1 Ubiquitin

Ubiquitin is a highly conserved 76 residue protein found in all eukaryotes either free or covalently attached to cellular proteins (reviewed by Liakopoulos *et al.*, 1998). The process by which ubiquitin is covalently linked to other proteins, is called ubiquitination. It involves the formation of an isopeptide bond between the C-terminal glycine residue of ubiquitin and the amino group of a lysine residue of the target protein. Ubiquitination can target proteins for degradation by the 26S proteasome, a major protease of the cytosol and the nucleus of eukaryotes, which degrades proteins to small peptides, whereas ubiquitin is recycled. Ubiquitination can also target certain cell surface proteins to lysosomal degradation via the endocytic route (Jentsch and Pyrowolakis, 2000). Conjugated ubiquitin can act as a substrate for further ubiquitination reactions to form polyubiquitin.

1.6.2 The ubiquitin pathway

The ubiquitin pathway occurs via two steps: (1) the covalent attachment of multiple ubiquitin molecules to the target protein and (2) the degradation of the tagged protein by the 26S proteasome (Fig 1.16). Conjugation of ubiquitin to the target protein occurs via three steps involving ubiquitin activating enzyme (E1), ubiquitin-conjugating enzyme (E2) and ubiquitin-protein ligases (E3) (Scheffner *et al.*, 1995). E1 activates ubiquitin in an ATP-dependent manner, forming a thiol ester linkage

(Haas, 1997). E2 then transfers the activated ubiquitin from E1 to a target protein that is specifically bound to E3 via a thiol ester linkage. There are different classes of E3 enzymes. For the HECT (homologous to the E6-AP COOH terminus) domain E3s, the activated ubiquitin is transferred to E3, generating a third thiol ester intermediate, before being transferred to an E3-bound substrate. RING finger-containing E3s catalyse the direct transfer of the activated ubiquitin to the E3-bound substrate. E3 is then responsible for the covalent attachment of ubiquitin to the substrate. The ubiquitin molecule is generally transferred an amino group of an internal lysine residue in the substrate to generate an isopeptide bond. This resultant monoubiquitin substrate is usually not targeted for degradation by the 26S proteasome. However, in other cases, ubiquitin is conjugated to the N-terminal residue of the substrate (Breitschopf *et al.*, 1998). In successive reactions, the polyubiquitin chain is synthesised by the transfer of additional ubiquitin to the Lys 48 of the previously conjugated molecule. The polyubiquitin chain serves as a recognition marker for the 26S proteasome complex. The proteasome degrades the ubiquitin-tagged substrate into short peptides, which are released, as well as ubiquitin, which is recycled (Fig 1.16).

Fig 1.16 The ubiquitin pathway (taken from Glickman and Ciechanover, 2002).

1.6.3 The ubiquitin-conjugating machinery

1.6.3.1 Ubiquitin-Activating enzyme (E1)

E1 exists as two isoforms of 110 and 117 kD, which are derived from a single gene and are found in both the nucleus and cytosol (Haas and Siepmann, 1997). This enzyme generates a high –energy thiolester intermediate with ubiquitin. In mammals there is only one E1 (Herschko and Ciechanover, 1998; Pickart, 2001).

1.6.3.2 Ubiquitin-conjugating enzymes (E2)

E2s are a superfamily of related proteins with a molecular weight of 14 to 35 kD. There are 11 E2 genes in yeast (Pickart, 2001) and 20 to 30 E2 genes in mammals (Scheffner *et al.*, 1998). E2 genes are structurally similar, but have different

biological functions. Only 3 E2 genes in yeast are involved in the formation of the polyubiquitin degradation signal. The other yeast E2 genes are involved in the formation of mono-, di-, and tri-ubiquitin conjugates that are not targeted for degradation.

1.6.3.3 Ubiquitin-protein ligases (E3)

Ubiquitin-protein ligases play an important role in the ubiquitin pathway. They are responsible for the selective recognition of target proteins. E3 can bind both E2 and the target protein. They are classified into two major groups: HECT domain- and RING finger-containing E3s.

The HECT (Homologous to E6-AP C-terminus) domain contains 350 amino acids. It mediates E2 binding and ubiquitination of the target protein via a thiolester linkage formation with ubiquitin. E6-AP (E6-Associated Protein) forms a complex with the papilloma virus E6 oncoprotein to ubiquitinate the p53 protein.

The RING (Really Interesting New Gene) finger structure is defined by 8 cysteine and histidine residues that coordinate two zinc ions (Freemont, 2000). The RING finger E3s are either monomeric proteins or multiple subunit complexes (Pickart, 2001). Some of the members of the monomeric RING finger E3 family are Mdm2, Ubr1 and Parkin, and they contain both the RING finger domain and the substrate-recognition site. Members of the multiple subunit complex include the APC

(Anaphase Promoting Complex), which is involved in the degradation of cell cycle regulators.

1.7 The DWNN gene family

1.7.1 Identification of DWNN domain

DWNN (Domain With No Name) gene was first identified in a study to identify new genes involved in the CTL killing pathway (George, 1995) by RACE and inverse PCR methods. It was given this name because its sequence matched only one entry in the non-redundant NCBI database, a human EST 587 (from 21C4 clone, accession number T25012), which in turn did not match any known sequence in the database. Sequence analysis of the 21C4 clone showed that the mRNA is 1.1 kb long and contains 118 amino acids, encoding a 13 kD protein and hence this protein was named DWNN-13 in this study. Further sequence analysis showed that the sequence encodes a highly conserved region of 80 amino acids and a hydrophobic tail (Fig 1.17).



```

1/1                               31/11
ATG TCC TGT GTg CAT TAT AAA tTT TCC tCT AAA CTC AAC TAt GAT ACC GTC ACC TTT Gat
M  S  C  V  H  Y  K  F  S  S  K  L  N  Y  D  T  V  T  F  D

61/21                              91/31
GGG CTC CAC ATC TCC CTC tGC GAC TTA aAG AAG CAG ATT ATG GgG AGA GAG AAG CTG aAA
G  L  H  I  S  L  C  D  L  K  K  Q  I  M  G  R  E  K  L  K

121/41                             151/51
GCT GCC GAC TGC GAC CTG CAG ATC ACC AAT GCG CAG ACg Aaa gAA gAa TAT ACT GAT GAT
A  A  D  C  D  L  Q  I  T  N  A  Q  T  K  E  E  Y  T  D  D

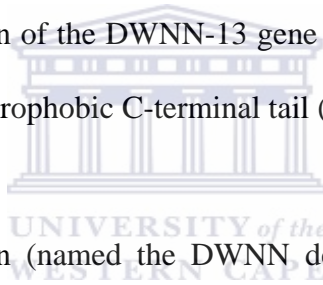
181/61                             211/71
AAT GCT CTG ATT CcT AAG AAT TCT Tct GTA ATT GTT agA aga ATt cCT ATT GGA GGT GTT
N  A  L  I  P  K  N  S  S  V  I  V  R  R  I  P  I  G  G  V

241/81                             271/91
AAA TCT ACA AGC AAG ACa TAT GTT aTA AGT CGA ACT GAA CCa GCg ATG Gca ACT Aca AAA
K  S  T  S  K  T  Y  V  I  S  R  T  E  P  A  M  A  T  T  K

301/101                             331/111
Gca gTA TGT AAA AAC ACa ATC Tca caC TTT TTC TAc ACA TTG CTT TTA CCT TTA
A  V  C  K  N  T  I  S  H  F  F  Y  T  L  L  L  P  L

```

Fig 1.17 Protein translation of the DWNN-13 gene showing the highly conserved 80 aa region (red) and the hydrophobic C-terminal tail (blue).



The 80 amino acid region (named the DWNN domain) was shown to be highly conserved throughout species, including humans, worms, flies, plants, algae and yeast (Fig 1.18) and has not been characterised previously.

Fig 1.18 Sequence alignment of the DWNN gene, showing the conserved amino acids within the DWNN domain in various species.

The secondary structure of the conserved 80 amino acid DWNN domain has been recently solved and shown to consist of α -helices and β -sheets (Faro, 2004). The 3D structure of the DWNN domain has been found to be similar to that of ubiquitin (Fig 1.19). There is no evidence that has been presented to date on the functional similarities between these two proteins.

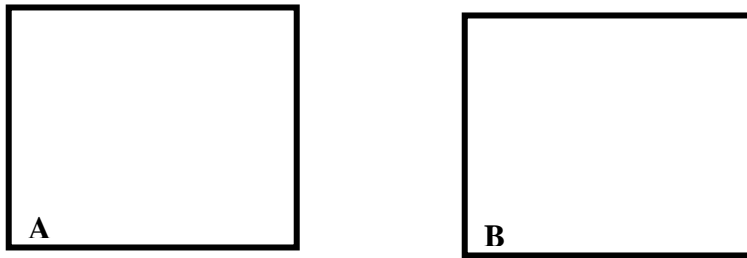
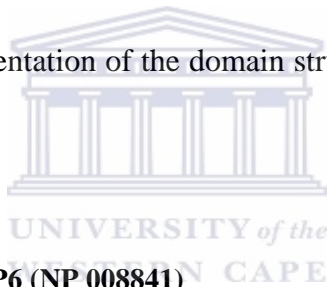


Fig 1.19 3D structures of (A) Ubiquitin and (B) DWNN domain (Faro, 2004).

The human DWNN gene has been mapped on chromosome 16p11.1. Previous EST data showed that the human DWNN and RBBP 6 genes (previously identified gene which binds Rb and p53) lie separate, but adjacent on chromosome 16 (Rees, unpublished data). RT-PCR data, however, showed that DWNN and RBBP6 gene are part of the same transcript (Dlamini, unpublished data). Further analysis of this transcript revealed that its mRNA is 6.1 kb long that encodes a 200 kD protein (and hence this protein was named DWNN-200 in this study). Sequence analysis illustrated that this gene contains 18 exons and consists of several domains (Fig 1.20). These domains include the conserved DWNN domain (situated in exons 1 to 3), a CCHC zinc finger domain (situated in exon 5 and exon 6) and a C3HC4 type of RING finger domain, located in exons 7 to 10 (Fig 1.20). CCHC zinc finger domains are known to interact with single stranded RNA or DNA, while the C3HC4 RING finger domain has been shown to have ubiquitin-ligase activity. They are often found in E3 ubiquitin ligases (see section 1.6.3.3). Also, on the C terminal end of the gene, an alternatively spliced region has been identified in certain human cell lines (Chapter 5) and has been mapped to exon 16. There is also an SR domain and an Rb-binding

Fig 1.21 Schematic representation of the domain structure of the DWNN-200 protein from different species.



1.7.2.1 *Homo sapiens* RBBP6 (NP 008841)

The human sequence of this gene has been sequenced to completion recently. The human RBBP6 encodes a protein that binds the underphosphorylated Rb protein (Sakai *et al.*, 1995). The sequence analysis of this gene according to AceView revealed that it contains 13 alternatively spliced transcript variants that encode 13 different isoforms. The gene is expressed highly in the placenta and various tissues, as well as in human cancer tissues. This data is consistent with the previous data showing the high levels of DWNN domain expression in human esophageal cancer tissues (Dlamini, unpublished). Sakai and colleagues first described the human RBBP6 gene in 1995. However, the full length sequence of this gene was not known then and they described the partial sequence of the gene, which they named RBQ-1.

RBQ-1 (RBBP6) protein

RBQ-1 (also known as RBBP6) was cloned from a human small cell lung carcinoma library as a novel protein of 140 kD in size and has been shown to bind to the Rb gene product (Sakai *et al.*, 1995). Two other proteins; RBQ-2 and RBQ-3, which bind the Rb gene were also cloned in that study (Sakai, *et al.*, 1995)). All three proteins bind to the underphosphorylated pRb. RBQ-1 and RBQ-3 showed no significant homology to each other (Saijo *et al.*, 1995).

The RBQ-1 sequence showed that this protein is homologous but shorter to that of the mouse PACT protein, (948 amino acids compared to 1583 amino acids of mouse PACT) but continues 182 bp upstream of the PACT protein. The overall amino acid homology between mouse PACT and human RBQ1 is 94 %, suggesting that the two proteins are highly conserved (Simons *et al.*, 1997).

The nucleotide sequence of RBQ-1 cDNA was shown to be 3011 bp in length and contains an open reading frame (ORF) that encodes 948 amino acids, with multiple repetitive motifs, one (the SRS) of which was previously described in the DNA-binding protein Son3 (Berdichevskii *et al.*, 1988). A putative alternatively spliced 34 amino acid region was also found in the middle of this protein. RBQ-1 is a 140-kD protein that consists of 12 exons. Sakai *et al.*, 1995, detected a ubiquitous 8.5 kb

transcript in adult and fetal tissues by Northern blot analysis. They mapped the gene to chromosome 16p12.2.

1.7.2.2 *Mus musculus* Rbbp6 (NM 011247)

Recent data from Ensembl Gene however, reveals that the mouse contains two transcripts of the Rbbp6 gene. The first transcript (Stable ID: ENSMUST00000033043) contains 12 exons and encodes 1556 residue protein. The second transcript (Stable ID: ENSMUST00000052135) also contains 12 exons but encodes a 1590 residue protein. BLAST analysis has mapped the gene on chromosome 7. According to Mouse Genome Database (MGD), February 2004, the nucleic acid sequence of the mouse Rbbp6 shows 82.6 % identity to that of humans.

Two research groups have previously identified the partial cDNAs of the mouse RBBP6 and have named them PACT (Simons *et al.*, 1997) and P2P-R (Witte and Scott, 1997).

p53 associated cellular protein-testes derived (PACT)

PACT was isolated from the mouse testes expression library using p53 as a probe, in a study to identify cellular proteins interacting with p53 (Simons *et al.*, 1997). The sequence analysis of PACT showed that the cDNA is 5177 bp long coding for 1583 amino acids and contains 437 bp 3' non-coding region with a polyA signal and tail.

The amino acid sequence of the 250 kD PACT showed interesting regions within the protein, including the 34 amino acid alternatively spliced region, a serine/arginine (SR) region and a 54 amino acid Lysine-rich region at the C-terminus. The SR domain has been shown to be a site in which serines are phosphorylated by a specific kinase (reviewed by Gui *et al.*, 1994) and the lysine-rich domain has been suggested to play a role in *in vivo* modification. The protein is highly charged, containing 22.5 % basic residues and 14.3 % acidic residues.

PACT has been shown to localize to the nuclear speckles by three different anti-PACT antibodies (Simons *et al.*, 1997), which is where several pre-mRNA splicing components are found (Spector, 1993). This observation suggests that PACT might be connected to cellular pre-mRNA splicing mechanism.

Proliferation potential protein related (P2P-R) protein

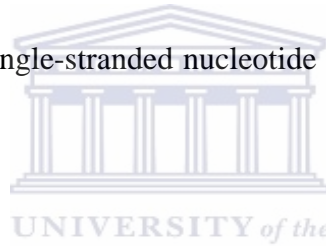
P2P-R is a nuclear protein that binds both p53 and Rb proteins. It was cloned from a mouse cDNA library (Witte and Scott, 1997). It is expressed in a variety of murine tissues and cells. P2P-R cDNA is 5173 bp in length, containing a 4214 bp ORF encoding a highly basic 156.9 kD protein. It is an alternatively spliced product of the mouse PACT gene because it lacks one exon containing 102 nucleotides encoding 34 amino acids (Scott *et al.*, 2003). Analysis of the P2P-R cDNA revealed that the cDNA contains multiple domains including an N-terminal RING type zinc finger, a heterogenous nuclear ribonucleoprotein (hnRNP)-associated domain, an Rb1- and

p53-binding domain, a proline rich domain, an SR region, a single stranded nucleotide binding domain and a C- terminal lysine rich domain. A cell division sequence motif near the amino terminus and a potential nuclear localisation signal were identified within the P2P-R cDNA (Witte and Scott, 1997). The 5' region of P2P-R cDNA shows significant homology to RBQ1 cDNA (Sakai *et al.*, 1995).

P2P-R has been shown to play a role in the control of RNA metabolism (Simons, *et al.*, 1997), apoptosis and p53-dependent transcription. It localizes in the nucleolus during interphase of murine and human cells and therefore is compatible with its role in RNA metabolism (Gao *et al.*, 2002). Its ability to bind p53 correlates with the fact that p53 also localizes to the nucleoli in the interphase cells. P2P-R has been reported to localize in the periphery of chromosomes in the mitotic cells (Gao *et al.*, 2002). P2P-R binds to proline-rich and C-terminal regulatory domains of p53 (Gao *et al.*, 2002). The proline-rich domain of p53 regulates the expression of both pro-apoptotic and anti-apoptotic genes. Western blot experiments have shown that P2P-R protein is expressed at higher levels in mitotic cells compared to other cells cycle states (Gao *et al.*, 2002). Studies showing overexpression of near full length P2P-R resulted in slow cell cycle progression at metaphase and promotion of mitotic apoptosis. This is contrary to the overexpression of a smaller P2P-R domain that showed no significant detectable effect on cell cycle progression or apoptosis (Gao *et al.*, 2002).

Studies have shown that P2P-R is phosphorylated by cdc2 and SRPK1a protein kinases. It also interacts with scaffold attachment factor-B, a MARs (matrix

attachment regions) binding factor, and may interact with nucleolin as well (Gao and Scott, 2002). P2P-R can also bind single stranded RNA. It is suggested that P2P-R may form complexes with Rb1 and /or p53 tumor suppressors and MARs-related factors, in a cell cycle and cell differentiation-dependent manner, to influence gene transcription/ expression and nuclear organization (Gao and Scott, 2002). Recent studies have shown that expression of the near full-length P2P-R promotes camptothecin-induced apoptosis in MCF 7 cells (Gao and Scott, 2003). The region responsible for this effect was identified and it has been shown that it overlaps with the p53-binding and the single-stranded nucleotide binding regions (Witte and Scott, 1997).



1.7.2.3 *Saccharomyces cerevisiae* RBBP6 (NP 012864)

Mpe-1 protein

Mpe1 is a *Saccharomyces cerevisiae* novel gene, identified by Vo and colleagues and is highly homologous to the human RBBP6 protein. It has been shown to interact with the PCF11 protein, encoding a protein of 441 amino acids, with a molecular weight of 49.5 kD (Vo *et al.*, 2001). Mpe-1 is essential for cell viability and contains a zinc knuckle motif, which is implicated in protein-nucleic acid interactions (Breg and Shi, 1996; Laity *et al.*, 2001). The zinc knuckle motif found in Mpe-1 is homologous to the zinc knuckle found in the human RBBP6 protein.

Mpe-1 is required for the specific cleavage and polyadenylation of pre-mRNA. Mpe1 has been shown to be a component of the cleavage and polyadenylation factor complex (CPF) but it is not essential for the stability of the CPF (Vo *et al.*, 2001). It is a conserved protein, with homologies found in *S. pombe*, *A. thaliana*, *D. melanogaster* and humans. The protein sequence of Mpe1 contains the conserved zinc and RING finger motifs, as well as the DWNN domain.

Figure 1.22 shows the schematic representation of the some of the RBBP6 homologues, discussed above.



1.7.2.4 Other RBBP6 homologues

The UniGene and GeneCard databases show evidence for the presence of other RBBP6 homologues, including *Arabidopsis thaliana* (accession number NM124114), *Drosophila melanogaster* (accession number CG3231), *Danio rerio* (BG 737479), *Xenopus laevis* (BJ614254) and *Rattus norvegicus* (XP219296). Table 1.8 shows the comparison of the RBBP6 protein sequences from different species homologues to the human RBBP6 sequence. No work has been undertaken in these organisms, as compared to the human, mouse and yeast RBBP6 genes.

Organism	% identity to humans	Database
<i>Rattus norvegicus</i> (rat)	85.1	HomoloGene
<i>Xenopus laevis</i> (African clawed frog)	82.14	HomoloGene

<i>Drosophila melanogaster</i> (fruit fly)	73.42	HomoloGene
<i>Mus musculus</i> (mouse)	82.66	Mouse Genome Database (MGD)
<i>Danio rerio</i> (zebrafish)	77.14	HomoloGene
<i>Ciona intestinalis</i> (sea squirt)	73.93	HomoloGene
<i>Arabidopsis thaliana</i> (thale cress)	73.3	HomoloGene

Table 1.9 Protein similarities of the RBBP6 homologues to humans.

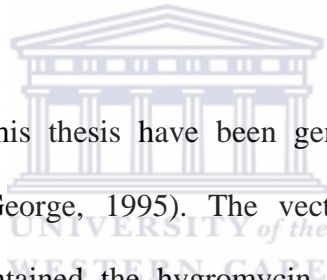
1.8 Retrovirus promoter-trap insertional mutagenesis

Retrovirus insertional mutagenesis has been used to isolate genes responsible for recessive phenotypes (Goff, 1987). However, this approach is inefficient due to the large number (5×10^6 - 1×10^8) of integration events it requires to disrupt a single copy cellular gene (Varmus *et al.*, 1981). Promoter-trap retroviral vectors have therefore been designed in order to increase the efficiency of insertional mutagenesis (von Melchner and Ruley, 1989). One such vector involved the positioning of a promoter-less selectable marker gene downstream of the splice acceptor site so that when the retrovirus inserts into an intron of an expressed gene, the selectable marker gene is expressed (Brenner *et al.*, 1989).

Another type of promoter-trap retrovirus vector involved the insertion of a promoter-less selectable marker gene into the U3 region of the 3' long terminal repeat (LTR) of an enhancer-less MoMLV (von Melchner and Ruley, 1989). Upon duplication of the LTR prior integration, the selectable marker is situated in the 5' LTR such that it is located 30 nucleotides from the host genomic DNA. The selectable marker is only

expressed when the retroviral vector integrates within a few hundred base pair of an active cellular promoter.

The latter vector has been used to isolate cellular promoters by using the retrovirus as a promoter trap (von Melchner *et al.*, 1990). This vector has also been used to isolate genes involved in the processing and presentation of antigens to cytotoxic T cells (CTL) (George, 1995) and in a study to identify genes involved in ceramide-induced apoptosis (Meyer, 2003).



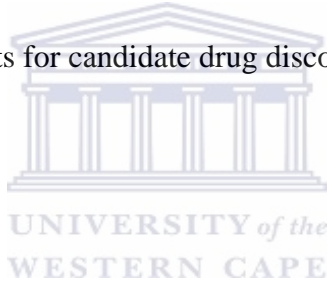
Cell lines described in this thesis have been generated using the promoter-trap mutagenesis approach (George, 1995). The vector used in this case was the tkneoU3hygro, which contained the hygromycin phosphotransferase gene, which confers resistance to hygromycin B. Chinese hamster ovary (CHO) cells were used as targets due to their functionally haploid nature (Siminovitch, 1985), implying that an integration event may lead to a loss of gene function. The CHO cells were initially modified by transfection of L-HA and MHC class I K^k, conferring sensitivity to lysis by HA-specific K^k restricted CTL, the selection agent. Hence, more than 100 CTL resistant cell lines were generated this way (George, 1995).

1.9 Objectives

The aim of this study was to characterise previously generated promoter-trapped CHO cell lines from a study to identify genes involved in the CTL killing pathway

(George, 1995). It is expected that the identified genes would play a role in the expression, processing or presentation of antigens by MHC class I molecules or in the recognition, adhesion or lytic mechanism of CTL. It is predicted that not only novel genes will be identified from this study, but also previously identified genes.

The identified gene(s) would have to be characterized in order to identify their function. Identification of more genes involved in the processing, presentation and killing of antigens by CTLs would lead to a broader understanding of this process and hence, opening more targets for candidate drug discovery.



CHAPTER 2: MATERIALS AND METHODS.

2.1 Materials and suppliers

40 % 37.5:1 acrylamide: bisacrylamide mix

Promega

Agarose	Whitehead Scientific
Alexa Fluor 488 goat anti-rabbit IgG antibody	Molecular Probes
Alexa Fluor 594 goat anti-rabbit IgG antibody	Molecular Probes
Alexa Fluor 488 chicken anti-mouse IgG antibody	Molecular Probes
Ampicillin	Roche Diagnostics
AMPS (Ammonium persulphate)	Merck
APOPercentage Assay kit	Biocolor Ltd
BSA (Bovine serum albumin)	Roche Diagnostics
Boric acid	Merck
Cell culture media and reagents	Gibco Life Technologies
Cesium chloride	Roche Diagnostics
Chloroform	Merck
Chloramphenicol	Sigma
Coomassie Brilliant Blue R-250	Sigma
DAPI (4,6-Diaminidine-2-phenylindole-dihydrochloride)	Roche Diagnostics
DEPC (Diethyl Pyrocarbonate)	Sigma
DMSO (Dimethyl sulphoxide)	Roche Diagnostics
Ethidium bromide	Sigma
EDTA (Ethylenediamine tetraacetic acid)	Merck
Hydrochloric acid	Merck
Kanamycin monophosphate	Roche Diagnostics
LightCycler FastStart DNA Master ^{PLUS} SYBR Green I	Roche Applied Science
Lipofectamine 2000 transfection reagent	Invitrogen

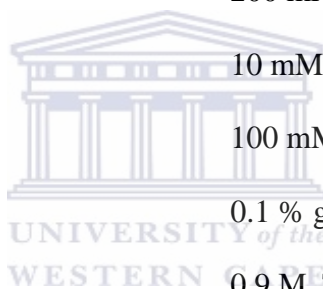


MOPS	Roche Diagnostics
Mouse-anti-mouse MHC I 2q K ^K antibody	Serotec
Phenol	Invitrogen
PMSF (Phenylmethylsulphonyl fluoride)	Roche Diagnostics
Proteinase K	Roche Diagnostics
PVDF (Polyvinylidene difluoride) membrane	Amersham
	Biotechnologies
Restriction enzymes	Roche Diagnostics
SDS (Sodium dodecyl sulphate)	Merck
Staurosporine	Roche Diagnostics
T4 DNA ligase	Promega
TEMED	Promega
Tris (hydroxymethyl) aminomethane	Merck
Triton X-100	Merck
TRIzol reagent	Gibco Life Technologies
Tween-20	Merck
Vectorshield Hard Set mounting medium	Vectorshield
Yeast extract	Merck
Zeocin	Invitrogen

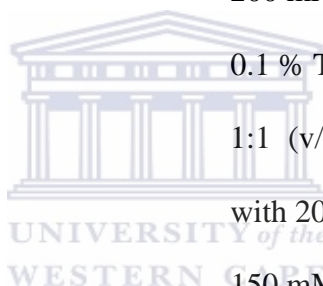


2.2 Solutions

2x TY broth	1.6 % Tryptone, 1 % yeast extract, 5 g/l NaCl
3:5M KOAc	3 M KOAc, 5 M glacial acetic acid pH 5.0
10x Ligase Buffer	660 mM Tris.Cl, 50 mM MgCl ₂ , 10 mM DTT, 10 mM ATP and 10 % polyethylene glycol, pH 7.5
10x MOPS	200 mM MOPS, 50 mM sodium acetate, 10 mM EDTA, pH 8.0
10x PCR Buffer	100 mM Tris.Cl, 500 mM KCl and 0.1 % gelatin, pH 8.3
10x TBE	0.9 M Tris, 0.89 M boric acid, 25 mM EDTA, pH 8.3
AMPS	10 % ammonium persulphate
Coomassie Blue destaining solution	40 % methanol, 10 % acetic acid and 10 % (w/v) glycerol
Coomassie Blue staining solution	40 % methanol, 10 % acetic acid and 0.1 % Coomassie Brilliant Blue R-250 stain
Digestion buffer	100 mM NaCl, 10 mM Tris.Cl, 25 mM EDTA, 0.5 % SDS and 0.1 mg/ml proteinase K, pH 8.0

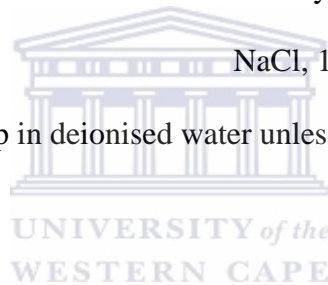


DNA loading buffer	30 % (w/v) glycerol, 15 mM EDTA pH 8.0, 0.5 % (w/v) bromophenol blue
FACS buffer	1 % foetal calf serum in PBS
GTE	10 mM EDTA, 1 % glucose 50 mM Tris.Cl, pH 7.4
L-agar	1 % tryptone, 0.5 % yeast extract, 10 g/l NaCl, 1.2 % agar, antibiotic as required
NaOH/SDS	200 mM NaOH, 1 % SDS
Permeabilising buffer	0.1 % Triton X-100 in PBS
Phenol/Chloroform	1:1 (v/v) phenol: chloroform saturated with 20 mM Tris.Cl, pH 8.0
Protein lysis buffer	150 mM NaCl, 10 mM Tris.Cl, 1 mM MgCl ₂ , 0.1 mM ZnCl ₂ , 1 % (w/v) Triton X-100, 10 mM DTT, 0.5 mM PMSF, pH 7.4
SDS-PAGE running buffer	25 mM Tris, 192 mM Glycine, 0.1 % SDS, pH 7.5
Separating gel	10 % acrylamide mix, 0.375 M Tris.Cl 0.1 % SDS, 0.1 % AMPS and 0.1 % TEMED, pH 8.8
Stacking gel	4 % acrylamide mix, 0.25 M Tris.Cl, 0.1 % SDS, 0.1 % AMPS and 0.1 % TEMED, pH 6.6



TE	10 mM Tris.Cl, 1 mM EDTA, pH 7.4
Transformation buffer 1 (Tfb 1)	30 mM KOAc, 50 mM MnCl ₂ , 100 mM KCl, 10 mM CaCl ₂ , 15 % (w/v) glycerol
Transformation buffer 2 (Tfb 2)	10 mM Na-MOPS 10 mM KCl, 75 mM CaCl ₂ , 15 % (w/v) glycerol, pH 7.0
Transfer Buffer	25 mM Tris, 192 mM Glycine, 10 % Methanol
TYM broth	2 % tryptone, 0.5 % yeast extract, 0.1 M NaCl, 10 mM MgCl ₂

All solutions were made up in deionised water unless stated otherwise.



2.3 Bacterial culture

2.3.1 Strains

Name	Genotype
<i>E. coli</i> MC1061	F ⁻ , araD139, (ara leu)7697, ΔlacX74, galU ⁻ , galK ⁻ , hsr ⁻ , hsm ⁺ , strA (Casadabhan and Cohen, 1980)
<i>E. coli</i> NM554	RecA13, araD139 Δ(araleu)7696 Δ(lac)17A galU galK hsdR rpsL (Str ⁺) mcrA mcrB (Casadabhan and Cohen, 1980)
<i>E. coli</i> XL1-Blue	RecA1, endA1, gyrA96, thi-1, hsdR17, supE44, relA1, lac[F' proAB, lacI ^q ΔZM15, Tn10(tet ^r)] (Stratagene)

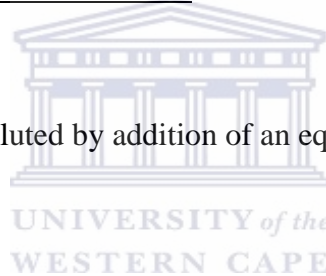
Table 2.1 Bacterial strains used.

2.3.2 Selection

All bacteria were grown in 2xTY broth, and on nutrient agar plates with or without antibiotics. Ampicillin was added to the 2xTY broth at a final concentration of 100 µg/ml, while kanamycin monophosphate was added at a final concentration of 30 µg/ml.

2.3.3 Storage of bacterial strains

Overnight cultures were diluted by addition of an equal volume of sterile glycerol and then frozen at -70°C .



2.4 Cloning vectors

2.4.1 pGEM-T Easy vector (Promega)

pGEM-T Easy vector is used for cloning of PCR products. The vector, which is 3.0 kb in size, is prepared by digestion with the restriction enzyme Eco RV, followed by the addition of a 3' terminal thymidine to both ends. The single 3' -T overhangs at the insertion site improves the efficiency of ligation of a PCR product (which has extra dA residues added to the PCR product by Taq Polymerase) into the plasmid by preventing recircularisation of the vector. The high copy number pGEM-T Easy vector contains T7 and SP6 RNA Polymerase promoters flanking the multiple

cloning site within the α -peptide coding region of the enzyme β -galactosidase. Insertional inactivation of the peptide allows recombinant clones to be directly identified by colour screening on indicator plates. pGEM-T Easy vector also contains the origin of replication of the filamentous phage f1 for the preparation of single-stranded DNA phage.

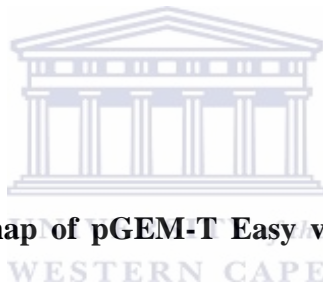


Fig 2.1 Circular map of pGEM-T Easy vector and the multiple cloning site (MCS).

2.4.2 pBluescript II (Stratagene)

pBluescript is a 3.0 kb high copy number ColE1-based phagemid, which has a versatile polylinker in four possible variants of the vector: (SK +/-; KS +/-). It contains the origin of replication from the f1 filamentous phage to allow rescue the single stranded DNA. The (+) and (-) orientations of the f1 intergenic region allow the rescue of either the sense or antisense DNA strand. Single stranded DNA can then be used for sequencing and site-directed mutagenesis. It contains T3 and T7 promoters for *in vitro* transcription of RNA. It contains a gene conferring resistance to ampicillin. The MCS is within the Lac Z α peptide gene.



Fig 2.2 pBluescript II SK (+) circular map with its MCS.

2.4.3 pEGFP-C1 (Clontech)

The green fluorescent protein (GFP) isolated from the jellyfish *Aequorea victoria* as a reporter molecule that can be used to monitor gene expression and protein localisation (Chalfie *et al.*, 1994). GFP fluoresces bright green when exposed to UV light, making it easily detectable by microscopy or flow cytometry. pEGFP-C1 is an optimised GFP variant. It encodes a red-shifted variant of the wild type Green Fluorescent, which has been optimised for brighter fluorescence and higher expression in mammalian cells. It is a 4.7 kb vector and the MCS is situated between the EGFP coding sequences and the SV40 polyadenylation signal. Genes cloned in

the MCS will be expressed as fusions to the C terminus of GFP if they are in the same reading frame as EGFP and there are no intervening stop codons (Clontech, 1999).



Fig 2.3 The map and MCS of pEGFP-C1 vector.

WESTERN CAPE

2.4.4 pDsRed1-C1 (Clontech)

Red Fluorescent Protein (RFP) is the only commercially available red fluorescing protein used for expression studies. pDsRed1-C1, a 4.7 kb vector, encodes a red fluorescent protein, DsRed1. Red fluorescent protein was originally isolated from *Discosoma sp* (Matz *et al.*, 1999). It has a vivid red fluorescence, making it ideal for multiple labelling with other GFP variants, e.g. EGFP. The MCS in pDsRed1-C1 is positioned between the DsRed1 coding sequence and the SV40 polyadenylation signal. Genes cloned in the MCS will be expressed as fusions to the C-terminus of DsRed1 if they are in the same reading frame as DsRed1 and there are no intervening

stop codons. The SV40 poly A signal downstream of the MCS directs proper processing of the 3' end of mRNA transcripts. The vector also contains an SV40 origin for replication in mammalian cells expressing the SV40 T-antigen. A neomycin resistance cassette (Neo^r) allows stably transfected eukaryotic cells to be selected using G418. A bacterial promoter upstream of this cassette expresses kanamycin resistance in *E. coli*. The pDsRed1-C1 backbone also provides a Col E1 origin of replication for propagation in *E. coli* and f1 origin for single-stranded DNA production (Living Colors, 1996).



Fig 2.4 Circular map of pDsRed1 vector map and its MCS.

2.4.5 pcDNA3.1/Zeo(+) (Invitrogen)

pcDNA3.1/Zeo (+) is a 5.0 kb vector designed for high-level stable and transient mammalian expression. It is available with the MCS in the forward (+) and reverse

(-) orientations to facilitate cloning. The CMV promoter provides high-level expression in a wide range of mammalian cells. The Zeocin resistance gene allows selection in both *E. coli* and mammalian cells in the presence of the antibiotic Zeocin. The vector also contains the T7 promoter for *in vitro* transcription in the sense orientation, an ampicillin resistant gene and f1 origin for the rescue of single-stranded DNA.



Fig 2.5 Circular map of pcDNA3.1/Zeo vector.

2.5 Preparation of competent *E. coli* cells for transformation

A single colony of the desired bacterial strain was inoculated into 20 ml TYM broth and grown with vigorous shaking at 37°C to $A_{600} = 0.2$. The culture was added to 100 ml TYM and grown to $A_{600} = 0.2$. The culture was transferred to 400 ml TYM broth and grown under the same conditions to $A_{600} = 0.6$. The cells were rapidly cooled in iced water and were centrifuged at 3000 g for 10 min at 4°C. The bacterial pellet was resuspended on ice in 250 ml of ice cold Tfb1 and incubated for 60 min on ice. The cells were recovered by centrifugation at 3000 g for 10 min at 4°C. The pellet was

gently resuspended in 50 ml of Tfb2, divided into 500µl aliquots and frozen in liquid nitrogen. The aliquots were stored at -70°C .

2.6 Transformation of *E. coli* cells

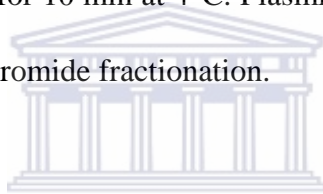
Competent cells were thawed on ice and 100 µl was added to 10 ng of plasmid DNA. The mixture incubated left on ice for 30 min, followed by heat shocking at 37°C for 5 min. 900 µl of 2xTY broth was added to the transformation and the cells incubated for a further 60 min at 37°C , to allow expression of the antibiotic resistance markers. The transformed cells were plated on appropriate antibiotic-containing plates and incubated at 37°C for 16 hrs.

2.7 Preparation of plasmid DNA

2.7.1 Large-scale preparation

10 ml of a saturated culture of plasmid-containing *E. coli* was diluted into 1000 ml 2xTY broth containing the appropriate antibiotic and grown for 16 hrs with shaking at 37°C . The bacteria were pelleted by centrifugation at 4 500 g for 10 min at 4°C . The pellet was resuspended in 4 ml GTE and incubated on ice for 10 min. The cells

were lysed by the addition of 8 ml NaOH/SDS with gentle swirling and incubated on ice for 10 min. 6 ml of 3:5 M KOAc was added and mixed gently to neutralise the alkali, and the mixture incubated on ice for 10 min. The precipitate of cell debris, chromosomal DNA and SDS was removed by centrifugation at 4 500 g for 15 min at 4°C. The supernatant was filtered through glass wool to remove particulate material and the nucleic acids precipitated by the addition of 0.8 volumes propan-2-ol, followed by incubation at -20°C for 20 min. The precipitate was pelleted by centrifugation at 10 000 g for 10 min at 4°C. Plasmid DNA was separated from RNA by double CsCl/ethidium bromide fractionation.



2.7.2 Double CsCl/ethidium bromide fractionation

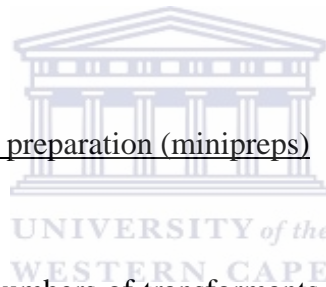
WESTERN CAPE

This method was used to prepare high quality plasmid DNA for transfection of eukaryotic cell lines.

The propan-2-ol pellet (section 2.7.1) was resuspended in 4.5 ml of TE. The solution was mixed with 4 mg ethidium bromide and 5.75 g CsCl to give a final density of 1.61 g/ml. This mixture was centrifuged at 10 000 g for 10 min at 20°C. The pellet was mainly RNA. The supernatant was transferred to Quickseal tubes and centrifuged at 55 000 g for 18 hrs at 20°C in NVi 65 rotor. The plasmid DNA was visualised with a 360 nm UV illumination and recovered using a syringe and made up to 5 ml with TE/CsCl and ethidium bromide to give a final density of 1.61 g/ml. This mixture was

transferred to a clean Quickseal tube and centrifuged at 55 000 g for 18 hrs at 20°C in NVi 65 rotor. The plasmid DNA was again recovered and an equal volume of NaCl-saturated isopropan-2-ol was added to remove the ethidium bromide. This extraction was repeated four times. Two volumes of water and one volume of isopropan-2-ol were added to precipitate the DNA. This mixture was mixed well and incubated on ice for 10 min. The DNA was recovered by centrifugation at 10 000 g for 15 min. The pellet was resuspended in TE at 1 mg/ml and stored at 4°C (short term) or –20°C (long term).

2.7.3 Small-scale preparation (minipreps)



In order to analyse large numbers of transformants, plasmid DNA was isolated from overnight cultures of *E. coli* picked from single colonies. This method yielded DNA of sufficient quantity and purity to perform restriction analyses and DNA sequencing. 4 ml cultures of plasmid-containing *E. coli* were grown in 2xTY broth containing the appropriate antibiotic for 16 hrs. The bacteria were pelleted at 6 000 g for 10 min, and resuspended in 200 µl GTE. The mixture was incubated at 22°C for 5 min. 400 µl NaOH/SDS was added and mixed gently to lyse the cells and incubated at 22°C for another 5 min. The mixture was neutralised by the addition of 300 µl 3:5 M KOAc, mixed gently and centrifuged at 13 200 g for 15 min. 800 µl of the supernatant was added to 600 µl propan-2-ol in a fresh tube and incubated at –20°C for 30 min. The precipitate of nucleic acid was pelleted and washed with 70 % ethanol. The pellet was

dissolved in 500 μ l TE. 100 μ g/ml RNase was added to the DNA and incubated at 37°C for 1 hr. The RNase treated DNA was extracted with phenol/chloroform and the upper aqueous phase was recovered. The DNA from the recovered phase was precipitated with 0.3 M sodium acetate and 2.5 volumes of ethanol and incubated at –20°C for 30 min. The precipitate was centrifuged at 10 000 g for 10 min, washed with 70 % ethanol and redissolved in 100 μ l TE.

2.8 Manipulation of plasmid DNA

2.8.1 Ethanol precipitation

DNA in solution was precipitated by the addition of NaOAc to 0.3 M, followed by 2 volumes ethanol. The solution was mixed well and incubated at –20°C for 30 min. DNA was recovered as a pellet by centrifugation at 10 000 g for 10 min.

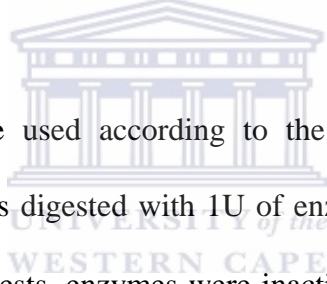
2.8.2 Ammonium acetate precipitation

DNA in solution was separated from dNTPs and short oligonucleotides (18 bases) by precipitating the DNA as above, except that a final concentration of 2 M NH_4OAc was used in place of 0.3 M sodium acetate.

2.8.3 Phenol/chloroform extraction

This is a general method for removing proteins such as restriction enzymes from a solution of DNA. Generally, 100 μ l of the DNA solution was vortexed with an equal volume of phenol/chloroform and centrifuged at 10 000 g for 2 min. The supernatant was recovered and re-extracted with phenol: chloroform. This supernatant was precipitated with ethanol (section 2.8.1) to recover the DNA and remove trace amounts of organic solvents.

2.8.4 Restriction enzyme digests



Restriction enzymes were used according to the manufacturers' instructions. In general, plasmid DNA was digested with 1U of enzyme per 1 μ g DNA for 2 hrs at 37°C. After restriction digests, enzymes were inactivated if necessary by incubation at 65°C for 15 min, or by extraction with phenol/chloroform followed by precipitation with ethanol. Where multiple digests were performed, the buffer conditions were selected to be compatible with both enzymes. When this was not possible the first enzyme was removed by phenol/chloroform extraction and ethanol precipitation, the buffer conditions adjusted accordingly and the second digest performed.

2.8.5 Ligation of DNA

Ligations were carried out in a 10 μ l total reaction, consisting of 1 μ l 10x Ligase buffer, 1 ng of the vector, 10 ng DNA, 1 U T4 DNA ligase at 22°C for at least 3 hrs or at 4°C for 16 hrs.

2.9 Agarose gel electrophoresis of DNA

A variety of DNA fragments used in this project ranged between 0.3 and 6 kb and were resolved on a 0.6 or 2 % agarose gel. Gels were prepared by boiling the appropriate amount of agarose in 1xTBE, cooling to 50°C, adding EtBr to 1 μ g/ml and allowing it to set in a gel tray. The DNA sample to be electrophoresed was mixed with 0.5 volumes of DNA loading buffer before loading into the gel. DNA molecular weight markers (section 2.9.1) were also loaded in order to estimate the size of DNA fragments. Gels were electrophoresed in 1xTBE at 10 V/cm and the DNA was visualised by illuminating the gel under UV light on a transilluminator. When DNA was to be recovered from the gel, a long wavelength 360 nm lamp was used to avoid damage to the DNA.

2.9.1 DNA molecular weight markers

Two DNA molecular weight markers were used: pTZ and pKG 2. pTZ was used to estimate DNA sizes of 1.2 kb and less, while pKG 2 was used to estimate DNA sizes of between 6 kb and 1.6 kb. pTZ marker was made by digesting pTZ 18R vector

with Hinf I and pKG 2 was made by digesting pKG-IX with Bam HI and Hind III at 37°C for 1 hr to produce the indicated sizes.

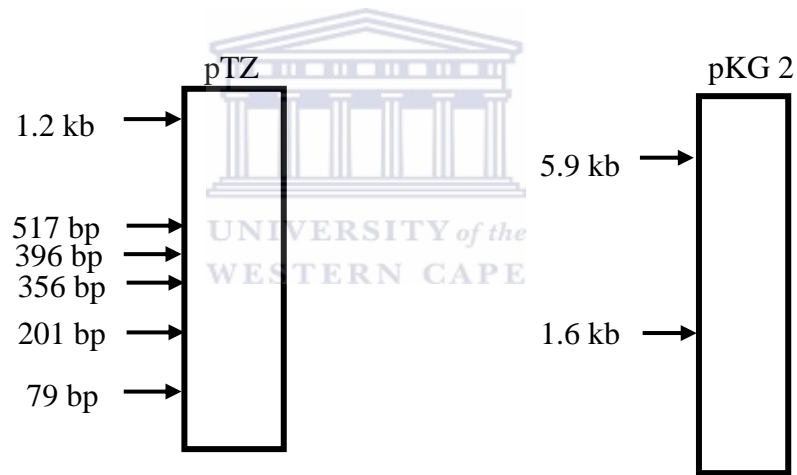


Fig 2.6 Agarose gel showing the sizes of the DNA molecular weight markers.

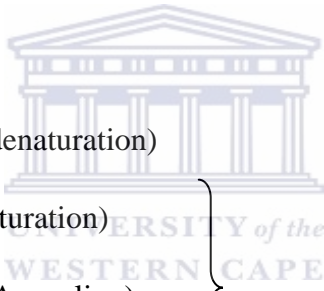
2.9.2 Purification of DNA fragments from agarose gels

After electrophoresis, the DNA of interest was recovered from the gel using the GeneClean kit II (Southern Cross Biotechnology). This kit was used according to the manufacturer's instructions.

2.10 Polymerase Chain Reaction (PCR) amplification

2.10.1 Standard PCR

The PCR was used to amplify regions of the DNA from plasmids. The reaction consisted of template DNA, 1X PCR buffer, 50 μ M dNTPs, 0.2 pmol of each of the two PCR primers, 1 U Taq DNA polymerase and 2 mM $MgCl_2$. The final volume was made up to 25 μ l with sterile water. The reaction was performed using following cycles:



95°C for 2 minute (Initial denaturation)
94°C for 30 seconds (Denaturation)
($T_m-5^\circ C$) for 30 seconds (Annealing)
72°C for 2 minutes (Extension)

} 35 cycles

72°C for 10 minutes (Final extension)

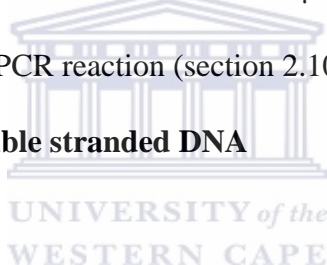
The cycles were followed by incubation at 4°C.

2.10.2 Inverse PCR (Figure 2.7)

This protocol was used to isolate DNA adjacent to known sequence in genomic DNA. Primers were designed to one end of the known sequence (Hygromycin sequence) that prime in opposite directions and have a six base-cutter enzyme site between them. 1 μ g of genomic DNA was digested with a frequent cutting enzyme (e.g. *Nla*

III) and that does not cut between the ends of the two primers. The enzyme was removed from the DNA by heat inactivating at 65°C for 15 minutes or by phenol/chloroform extraction (section 2.8.3). The genomic DNA fragments generated were recircularised by adding 10µl of digested DNA, 1 x ligase buffer and 3U T4 DNA ligase to a final volume of 100 µl. The reaction was incubated at 22°C for 3 hrs. The T4 DNA ligase was inactivated by heating at 70°C for 20 min. The recircularised DNA was digested with Aat II or Eag I in a total volume of 60µl for 2 hrs and the enzyme was heat inactivated at 70°C for 15 min. 2µl of the resultant reaction mix was used in a subsequent 25µl PCR reaction (section 2.10).

2.11 Sequencing of double stranded DNA



DNA sequencing using the ABI 310 DNA Sequencer was employed. The BigDye Terminator Ready Reaction Kit version 3.0 (ABI) was used and this kit includes AmpliTaq DNA Polymerase, FS, the BigDye terminators and all the required components for the sequencing reaction. Sequencing reaction consisted of the following:

REAGENT	QUANTITY
Terminator Ready Reaction Mix	2 µl
Double-stranded DNA	200-500 ng
Primer	3.2 pmol
Deionised water	To a final volume of 10 µl

Table 2.2 The sequencing reaction protocol.

GeneAmp PCR System 9700 was used and the following conditions were used:

STEP	ACTION
------	--------

1	Repeat the following for 25 cycles: 96°C for 10 sec. 60°C for 4 min.
2	Hold at 4°C

Table 2.3 PCR cycles for sequencing.

Precipitation of extension products:

The contents of each extension reaction were transferred into a 1.5 ml tube. 8 µl deionised water and 32 µl of 95 % ethanol were added. The tubes were vortexed briefly and incubated at room temperature for 30 min. Tubes were centrifuged for 20 min at 15 000 g. Supernatants were carefully aspirated. 250 µl of 70 % ethanol was added to the tubes and vortexed briefly. Tubes were centrifuged at 15 000 g for 20 min. This step was repeated twice and the pellets were dried and either stored at –20°C or loaded immediately onto the ABI 310 Genetic Analyser. 12.5 µl of Template Suppressor Reagent (TSR) was added and tubes were vortexed briefly. The samples were denatured at 95°C for 2 min and tubes were placed on ice immediately. The samples were loaded onto the ABI 310 PRISM™ Genetic Analyser (Applied Biosystem) and the data was collected using the ABI 310 PRISM™ Collection Software and analysed using the Sequencing Analysis 3.4.1 Software.

2.12 Preparation of Genomic DNA from mammalian cell lines

Cells cultured in 25cm² tissue culture flasks were washed with 10 ml ice-cold PBS. 1 ml of digestion buffer was added to the cells, which were then scraped off from the

flasks. The sample was incubated for 12-18 hrs with gentle shaking at 37°C in tightly capped tubes. The samples were thoroughly extracted with an equal volume of phenol/chloroform/isoamyl alcohol and centrifuged at 15 000 g for 10 min. The aqueous (top) layer was transferred to a new tube and 0.5 volumes of 7.5 M ammonium acetate and 2 volumes 100 % ethanol was added. The DNA was recovered by centrifugation at 15 000 g for 2 min and rinsed with 70 % ethanol. The pellet was resuspended in TE buffer.

2.13 Cell culture

2.13.1 Cell lines



CELL LINES	SPECIES	CELL TYPE	MEDIA
CHO-Y10	Chinese Hamster	Ovary, epithelial	Complete Hams F12
CHO-Mut8 (3x8)3.5	Chinese Hamster	Ovary, epithelial	Complete Hams F12
CHO-Mut10 (3x8)3.5	Chinese Hamster	Ovary, epithelial	Complete Hams F12
CHO-Mut16 (3x8)3.5	Chinese Hamster	Ovary, epithelial	Complete Hams F12
CHO-J363	Chinese Hamster	Ovary, epithelial	Complete Hams F12
NHF	Human	Normal Fibroblast	Complete DMEM
HeLa	Human	Cervix, carcinoma, epitheloid	Complete DMEM
MG-63	Human	Bone, osteosarcoma	Complete DMEM
MEL-2	Human	Melanoma	Complete DMEM
Hep G2	Human	Liver carcinoma	Complete DMEM

Table 2.4 Cell lines used for tissue culture.

2.13.2 Tissue culture media

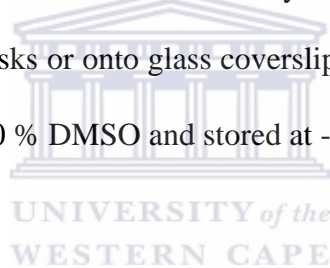
MEDIA	COMPONENTS
Complete Hams F12	Hams F12 + 5 % FCS + 1 µg/ml Penicillin Streptomycin

Complete DMEM	DMEM + 10 % FCS + 1 µg/ml Penicillin Streptomycin
CTL assay medium	RMPI-1640 + 10 % FCS + Glutamine + 10 mM HEPES+1 µg/ml Penicillin Streptomycin

Table 2.5 Tissue culture media used.

2.13.3 Propagation and storage of cell lines

Cells were maintained in an incubator at 37°C in 5 % CO₂. Cells were passaged when confluent by trypsinisation of the cell monolayer (0.125 % trypsin in PBS), and seeded into cell culture flasks or onto glass coverslips at a density of 1:10. Cells were frozen in 90 % FCS and 10 % DMSO and stored at -150°C.



2.13.4 Transfection of cell lines

2.13.4.1 Transient transfection of cell lines

DNA prepared by double caesium chloride/ethidium bromide fractionation was used for all transfection procedures (section 2.7.2). Cells were transfected using Lipofectamine 2000 transfection reagent (Invitrogen) in 6 well plates (1 µg DNA per well) according to the manufacturer's instructions. After 24-48 hours, cells were fixed with 4 % paraformaldehyde, stained with DAPI and mounted on slides for evaluation by fluorescent microscopy.

2.13.4.2 Stable transfection of cell lines

Stable transfections were performed using the lipofectamine method used for transient transfections (section 2.13.3.1). After 24 hours, the cells were passaged at a 1:10 dilution into a fresh growth medium. Cells were grown in the selective medium, containing 300 µg/ml Zeocin, for 3 to 8 weeks until colonies of resistant cells grew. The individual colonies were cloned using cloning rings and propagated for subsequent assays.

2.14 Immunofluorescent microscopy

2.14.1 Fixation and permeabilisation of cells

Cells were grown on coverslips until confluent. Cells were washed twice with warm PBS and incubated with 4 % paraformaldehyde in PBS at 22°C for 15 min and were rinsed three times with PBS. This was followed by permeabilisation in permeabilisation buffer for 5 min. The cells were washed twice in PBS and incubated for 30 min PBS/0.5 % BSA.

2.14.2 Immunostaining of cells

Fixed and permeabilised cells on cover slips were incubated at 22°C for 1 hr in primary antibody diluted in PBS/0.05 % BSA. The cells were washed in PBS/0.5 %

BSA and then incubated in a diluted dye-conjugated secondary antibody for 1 hr and washed again. The cells were then counterstained with DAPI, which stains the DNA, for 5 min, washed with PBS/0.5 % BSA and mounted onto a microscope slide using the Vectorshield hard set mounting medium. Staining was visualised with a Zeiss Axiophot immunofluorescence microscope/camera system.

2.15 FACS Analysis



UNIVERSITY of the
WESTERN CAPE

Approximately 3×10^6 cells were harvested from confluent flasks and resuspended in 100 μ l of a 1:100 dilution of the primary antibody (mouse monoclonal anti-mouse MHC-I 2qK^K) in FACS buffer. Cells were incubated on ice with occasional shaking for 1 hour, washed twice with FACS buffer and resuspended in 100 μ l of a 1:100 dilution of FITC conjugated chicken anti-mouse IgG monoclonal antibody. Cells were incubated on ice for 1 hour with occasional shaking, washed twice with FACS buffer and resuspended in 400 μ l FACS buffer. Cells were analysed using the Cell Quest Pro Software.

2.16 CTL killing assay

2.16.1 Stimulation of CTL

Spleens from 3-month old female CBA/Ca mice were provided by Dr Keith Gould (Imperial College London, UK). Each spleen was placed into 10 ml RPMI-1640 medium and crushed in a tissue culture plate using forceps. The cells were further disaggregated by drawing the suspension up five times through a 19 gauge needle and syringe. The spleenocytes were harvested by centrifugation at 2600 rpm and washed twice with RPMI-1640 medium. The final pellet was resuspended in 3 ml of filter sterilised RPMI-1640 containing 10 % FCS and 5 μ M synthetic peptide epitope (IEGGWTGMI for HA8 CTL clone) and incubated at 37°C in an atmosphere of 5 % CO₂ for 90 min. The feeder cells were then irradiated with 2500 rads for 5 min using Gammacell 40 irradiation apparatus to prevent cell division and incubated for 1 hr at 37°C in an atmosphere of 5 % CO₂. The feeder cells were then washed three times with RPMI-1640 medium to prevent carry over of the peptide. 10⁷ feeder cells were then resuspended in RPMI medium and added to 2x10⁶ CTL in 25 cm² flasks.

2.16.2 Harvesting of CTL

The effector CTL cells were harvested by centrifugation and were resuspended in CTL assay medium at a concentration of 2x10⁶ cells/ml. Successive two fold dilution of the effector CTL were made representing 10, 5, 2.5 and 1.25 effector: 1 target

ratio. The CTL were plated in round-bottomed 96 well microtitre plates in triplicates in a final volume of 100 μ l. The experimental wells contained 100 μ l of CTL and 50 μ l of the target cells. The control wells were prepared in quadruplicates containing 50 μ l target cells and 100 μ l CTL assay medium for spontaneous release or 100 μ l 5 % Triton X 100 for maximum release. The plates were incubated for 6 hrs at 37°C in an atmosphere of 5 % CO₂. After the incubation of the plates for 6 hrs, the plates were centrifuged at 1000 rpm for 5 min and removed 40 ml of the supernatant into a Luma plate and the plate was left to dry in a 37°C oven for 16 hrs for counting on a microplate scintillation counter. The amount of target cells killed was calculated by measuring the amount of ⁵¹Cr released. The following formula was used for the calculation of the amount of target cells killed:

$$\% \text{ specific } ^{51}\text{Cr release} = \frac{\text{release from target by CTL} - \text{spontaneous release}}{\text{maximum release} - \text{spontaneous release}} \times 100$$

2.16.3 Harvesting of target cells

The target cells were cultured in 75 cm² flask and were harvested when confluent in PBS containing 0.5 mM EDTA. The cells were then resuspended in CTL assay medium at a concentration of 10⁷ cells/ml. 2x10⁶ cells were labelled with 40 μ Ci of ⁵¹Cr in a total volume of 0.3 ml and were incubated at 37°C in an atmosphere of 5 % CO₂ for 90 min.

The cells were then washed twice with CTL assay medium and were adjusted to be 2×10^5 cells/ml with the CTL assay medium. The cells were then incubated at 37°C in an atmosphere of 5 % CO₂ whilst harvesting the CTL (section 2.16.2).

2.17 APOPercentage™ Apoptosis Assay

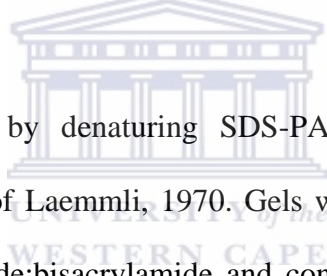
The APOPercentage assay is a detection and measurement system to monitor the occurrence of apoptosis in mammalian cells. Cells were grown in six well plates until confluent. Cells were then induced with at a concentration of 1 μM for 1-3 hrs. The cells were then washed twice with PBS and 1 ml of the APOPercentage dye was added to each well and incubated at 37°C for 1 hr. The Dye was removed and the cells were washed twice with PBS. Photographs were taken using the Nikon inverted light microscopy. The PBS was removed from the cells and 0.5 ml of trypsin was added to each well and cells were allowed to round up (and not detach) before the trypsin was removed. The cells were then gently resuspended in 2 ml of complete Hams F12 median and were analysed by FACS (section 2.15).

2.18 Proteins

2.18.1 Isolation of protein from cell monolayers

Cells were grown to ~80 % confluency in 75 cm² tissues culture flasks and were washed twice with PBS to remove traces of serum and then 150 µl of protein lysis buffer was added per flask. The cells were scraped from the flasks using cell scrapers. The samples were vortexed for 1 min, sonicated for 1 min and boiled for 5 min and stored at -20°C until required. Approximately 30 µl of protein was subjected to SDS-PAGE and analysed by Western blotting.

2.18.2 SDS-polyacrylamide gel electrophoresis (SDS-PAGE) of proteins



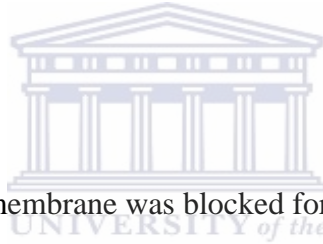
Proteins were separated by denaturing SDS-PAGE under reducing conditions according to the method of Laemmli, 1970. Gels were made from a 40 % stock of premixed 37.5:1 acrylamide:bisacrylamide and consisted of a separating gel and a stacking gel, which was added to the top of the separating gel. Gels were run at 10V/cm for 1 hr, using the Mighty Small apparatus (Hoeffer).

2.18.3 Staining and destaining of PAGE gels

Gels were fixed in SDS-PAGE staining solution for 30 min. De-staining was achieved by multiple washes with SDS-PAGE destaining solution.

2.18.4 Western Blotting

A Bio-Rad MiniProtean Trans Blot system was used to transfer proteins separated by SDS-PAGE onto PVDF membranes. Gels, sponges, Whatman paper were equilibrated in pre-chilled transfer buffer for 30 min. PVDF membrane was immersed in 100 % methanol, rinsed in distilled water before equilibration in transfer buffer and blotting. The gel was then positioned on top of a piece of Whatman 3MM paper. PVDF membrane was placed on top of the gel, taking care to remove bubbles. 3MM paper was placed over the PVDF membrane and then placed inside a blotting cassette. Protein was electroblotted onto the PVDF membrane at 200 mA for 2-3 hrs at 4°C.



After blotting, the PVDF membrane was blocked for 1 hr at 22°C in PBS, 5 % non-fat dried milk, 0.1 % (v/v) Tween-20. The filter was rinsed three times for 10 minutes in wash buffer. The membrane was incubated in 1:5000 dilution of the primary antibody for 1 hr at 22°C in a shaker. The membrane was rinsed three times for 10 min in wash buffer. The membrane was incubated in 1:20000 dilution of the secondary antibody for 1 hr at 22°C in a shaker. Finally the membrane was rinsed three times for 10 minutes with fresh changes of wash buffer at 22°C. The membrane was placed on Saran Wrap. Chemiluminescent detection was carried out according to the manufacturer's instructions (ECL, Amersham) and the blots were exposed to ECL film (Amersham).

2.19 RNA Extraction

Approximately 10^8 cultured cells in 25cm^2 tissue culture flasks were washed with PBS. The cells were homogenised in 3 ml TRIzol reagent (Gibco life technologies) and incubated with shaking at 22°C for 2 hrs. 1.5 ml of chloroform was added to the homogenate and this solution was mixed vigorously and incubated at 22°C for 10 min. After centrifugation at 15 000 g for 1 hr at 4°C , the upper aqueous layer was transferred to a new tube. RNA was precipitated by the addition of 1.5 ml propan-2-ol and incubated at 22°C for 15 min and then incubated at 4°C for 16 hrs. The RNA was pelleted by centrifugation at 3000 g for 30 min at 4°C . The pellet was washed with 70 % ethanol and resuspended in 100 μl of DEPC treated water. The RNA was stored at -70°C in 20 μl aliquots.

2.20 Agarose gel electrophoresis of RNA

1 % (w/v) of agarose melted in 10 ml 10 x MOPS buffer and 85 ml distilled water and was allowed to cool about 50°C , 5.4 ml of 37 % (v/v) formaldehyde was added and the solution was allowed to set in a gel tray. RNA to be electrophoresed was mixed with 10 μl of formaldehyde gel loading buffer. The sample was heated at 65°C for 5 min and loaded on the gel. The gel was run in 1x MOPS running buffer at 50 V/cm for 1 hr.

2.21 cDNA synthesis

First strand cDNA synthesis (AMV) kit for RT (Roche Applied Science) was used.

The reaction for the first strand cDNA synthesis consisted of the following reagents:

REAGENT	VOLUME/ 1 SAMPLE	FINAL CONCENTRATION
10x reaction buffer	2 μ l	1x
25 mM MgCl ₂	4 μ l	5 mM
10 mM dNTPs	2 μ l	1 mM
Primer	Variable	0.75-1.0 μ M
RNAse inhibitor	1 μ l	50 units
AMV reverse transcriptase	0.8 μ l	20 units
Sterile water	To final volume of 20 μ l	
RNA	1 μ g	

Table 2.6 Reactions used for the first strand cDNA synthesis.

The mixture was vortexed and centrifuged briefly. The reaction was incubated at 25°C for 10 minutes and then at 42°C for 60 minutes. Following the 42°C incubation, the AMV reverse transcriptase was denatured by incubating at 99°C for 5 minutes and then cooled to 4°C for 5 minutes and the resultant first strand cDNA preparation was stored at -20°C. The cDNA synthesised was used for amplification using the standard PCR protocol (section 2.10.1).

2.22 Real –Time quantitative RT-PCR

A PCR reaction mix containing 4 μl of LightCycler FastStart DNA Master^{PLUS} SYBR Green Reaction Mix (Roche Applied Science), 140 ng cDNA, 0,5 μM of each primer and water added to a final volume of 20 μl was prepared. A negative control contained the above mix, except that the DNA was replaced with water. The PCR mix was then transferred into capillary tubes in pre-cooled centrifuge adapters and these were centrifuged at 700 x g for 5 sec. The capillaries were placed into the LightCycler Carousel and into the LightCycler instrument. The reaction were performed using the following cycles:



Program	Step	Temp	Time	Temperature Transition Rate	Fluorescence acquisition
Pre-incubation		95°C	10 min	20°C/sec	None
Amplification	Denaturation	95°C	10 sec	20°C/sec	None
Amplification	Annealing	Primer-dependent	10 sec	20°C/sec	None
Amplification	Extension	72°C	5 sec	20°C/sec	Single
Melting curve	Denaturation	95°C	0	20°C/sec	None
Melting curve	Annealing	65°C	15 sec	20°C/sec	None
Melting curve	Melting	95°C	0	0.1°C/sec	Continuous
Cooling		40°C	30 sec	20°C/sec	None

} 45 cycles

Table 2.7 PCR conditions used for the Real-Time quantitative PCR.



CHAPTER 3: IDENTIFICATION OF THE DWNN GENE IN PROMOTER TRAPPED CELL LINES.

3.1 Introduction

Over 100 CTL resistant cell lines were generated in a previous study using promoter trap mutagenesis experiments (George, 1995). The system of retrovirus promoter trap mutagenesis involves the insertion of a promoter-less selectable marker gene, hygromycin, into the U3 region of the Long Terminal Repeat (LTR) of the Moloney murine leukaemia virus (MoMLV). Prior integration, the LTR duplicates and the

hygromycin gene is positioned in the 5' LTR such that it is located 30 nucleotides from the host genomic DNA (von Melchner and Ruley, 1989). Hamster ovary (CHO) cells were used because of their 'functional haploidy' characteristic and therefore integration can lead to the loss of gene function (Hubbard *et al.*, 1994).

In order to identify the DNA sequence adjacent to the site of retroviral integration, inverse PCR has been exploited. Inverse PCR is a specific application of the general PCR technique (Ochman *et al.*, 1988). It amplifies cellular DNA adjacent to an integrated provirus given the sequence information for the provirus (Silver and Keerikatte, 1989). This technique is useful for studies of insertional mutagenesis and other situations in which one wishes to isolate DNA adjacent to a region of known sequence. The protocol consists of five steps (Fig 3.1): isolation of genomic DNA, restriction digestion of the genomic DNA, circularisation of the digested DNA, reopening of the circular DNA and amplification of the inverse DNA fragment (section 2.10.2). The inverse PCR primers are designed such that they are directed away from each other, as opposed to the conventional PCR primers, which are facing towards each other. This allows for the amplification of the unknown sequence either on the 5' or 3' end of the integrated provirus. Analysis of the 5' end of the integrated provirus is referred to as 5' inverse PCR, while the analysis of the 3' end of the integrated provirus is called 3' inverse PCR.

This chapter describes the analysis of both the 5' and 3' end of the retrovirus from four promoter-trapped cell lines using the inverse PCR.

3.2 Analysis of the retroviral promoter-trapped cell lines by Inverse PCR

3.2.1 Isolation and restriction digestion of genomic DNA

Genomic DNA was isolated from four promoter trapped cell lines, CHO-Mut8 (3x8)3.5, CHO-Mut10 (3x8)3.5, CHO-Mut16 (3x8)3.5 and CHO-J363 (section 2.12). Fig 3.2 shows an agarose gel electrophoresis of the undigested and digested genomic DNA samples from three of the promoter-trapped cell lines. The undigested genomic DNA samples show a high molecular weight fragment, which represents the genomic DNA, as well as the low molecular weight fragments, which represent RNA. Upon digestion of the genomic DNA with Eco RI, the low molecular weight RNA fragments disappear due to degradation and the genomic DNA is digested to a low molecular weight smear (Fig 3.2).

The digested DNA was circularised with T4 DNA ligase (Promega) at a dilute DNA concentration that favours the formation of monomeric circles (Collins and Weissman, 1984). In order to increase the efficiency of PCR amplification, the circular DNA molecules were first cleaved with a restriction enzyme that cuts between the inverse PCR primers only, within the hygromycin gene (Fig 3.4). In this case, the restriction enzyme Eag I was used for the 3' IPCR (Fig 3.1) and Aat II was used for amplification of the 5' end (Fig 3.11). The inverse PCR primers were designed within the hygromycin gene (Figure 3.4).

3.2.2 Amplification of the hygromycin resistant gene

In order to confirm that the cell lines that were analysed contained the promoter trap retrovirus, amplification of the hygromycin resistant gene (which is expressed upon integration of the retrovirus) was performed. Primers flanking the hygromycin sequence were designed. These primers would amplify both 5' and 3' of the Long Terminal Repeat (LTR) hygromycin gene and produce the same size fragment (Fig 3.3a). The PCR was performed on the genomic DNA of the four cell lines and yielded a 249 bp fragment in all the cell lines (Fig 3.3c). This means that all four of these cell lines contain the retrovirus and would be suitable for inverse PCR analysis.

3.2.3 Amplification of the 3' end of unknown genomic sequence

Two rounds of amplification were performed in order to obtain the inverse PCR products. The first round was performed using primers 1051 and 1052, while the second round of amplification was carried out using internal primers 1050 and 1053 (Figure 3.4). This kind of amplification is supposed to produce two products: the 5' end hygromycin fragment derived from the 5' LTR end of the provirus and the 3' end of the provirus containing the adjacent genomic sequence (Fig 3.1).

Figure 3.5 shows the inverse PCR products of an Eco RI digested DNA. CHO-Mut8 (3x8)3.5 cell line produced two fragments of approximately 1.2 kb to 1.3 kb. These fragments should correspond to the 5' hygromycin “control” fragment and part of the hygromycin gene plus the genomic DNA in which the retrovirus has integrated into.

CHO-Mut10 (3x8)3.5 cell showed no amplification at all. This could be due to the low concentration of the genomic DNA (Fig 3.2). CHO-Mut16 (3x8)3.5 cell lines gave a single fragment of >1.2 kb, while CHO-J363 also produced a single fragment of about 1.0 kb.

3.2.4 Sequencing of the 3' end inverse PCR products

All the inverse PCR fragments were purified from the agarose gel and sequenced directly (section 2.11). The fragments were sequenced with primer 1053. The sequences of the entire inverse PCR products obtained are shown in figure 3.6. The DNA sequence of the tkneoU3hygro hygromycin gene is indicated in red, while that of the hamster genomic DNA is indicated in blue (Fig 3.6).

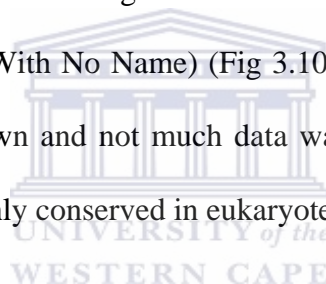
The sequences obtained were analyzed using the BLAST (Basic Local Alignment Search Tool) (Altschul *et al.*, 1990). BLAST was performed using the non-redundant database, which included all GenBank, RefSeq, Nucleotide, EMB, DDB and PDB sequences.

The 1.3 kb fragment (top fragment) from CHO-Mut8 (3x8)3.5 produced significant matches against three regions. One was from a mouse DNA sequence from clone RP23-35D7, on chromosome 11 (Fig 3.7). The other two regions matched the human chromosome 17 (CTD-2301B9) and clone RP11-253F9 respectively. Further analysis on these three regions showed no gene sequences have been assigned in these regions

yet. Therefore, no further analysis was undertaken on these fragments. The 1.2 kb fragment (bottom fragment) matched the Moloney murine leukemia virus sequence as expected (Fig 3.8).

The sequence obtained from the inverse PCR product of CHO-J363 cell line matched the hygromycin sequence (Fig 3.9).

The BLAST search analysis of sequence of the inverse PCR product obtained from CHO-Mut16 (3x8)3.5 produced a significant match against a mouse gene, which was named DWNN (Domain With No Name) (Fig 3.10). It was named DWNN since its function was not yet known and not much data was known about it. The sequence data revealed that it is highly conserved in eukaryotes.



CELL LINE	NCBI SEQUENCE MATCHES
CHO-Mut8 (3x8)3.5 (top fragment)	Mouse DNA sequence from clone RP23-35D7, chromosome 11 Homo sapiens chromosome 17 clone CTD-2301B9 Homo sapiens 12 BAC RP11-253F9
CHO-Mut8 (3x8)3.5 (bottom fragment)	Retrovirus sequence
CHO-Mut16 (3x8)3.5	Mouse DWNN
CHO-J363	Retrovirus sequence
CHO-Mut10 (3x8)3.5	No PCR product

Table 3.1 Summary of the BLAST search results for the 3' inverse PCR products.

3.2.5 Amplification of the 5' end of the unknown genomic sequence

5' inverse PCR was performed in order to analyze the 5' end of the genomic sequence and also to compare the 5' and 3' genomic sequences. This PCR was performed the same way as the 3' inverse PCR, except that the ligated genomic DNA was linearised with Aat II (Fig 3.11.). The first round of amplification was performed using primers 884 and C, while the second round of amplification was performed with primers 1034 and G (Fig 3.12).

Figure 3.13 shows an agarose gel of the 5' inverse PCR results. Lane 1 represents the negative control (no DNA added) and lanes 2, 3 and 4 represent the inverse PCR results from CHO-Mut8 (3x8)3.5, CHO-Mut16 (3x8)3.5 and CHO-Mut10 (3x8)3.5 cell lines respectively. The hygromycin 'control' fragment of 428 bp was detected in all the cell lines. Other fragments were cut out of the gel and purified for sequencing.

3.2.6 Sequencing of the 5' end inverse PCR products

Only one fragment from each cell line was sequenced using primer G. All the sequences analyzed showed the presence of the retrovirus (red text) and the genomic sequence (blue). Figure 3.14 shows the DNA sequences CHO-Mut8 (3x8)3.5, CHO-Mut16 (3x8)3.5 and CHO-Mut10 (3x8)3.5.

The genomic DNA sequence was analyzed using the BLAST. The BLAST search results of the genomic sequences from CHO-Mut8 (3x8)3.5 and CHO-Mut16 (3x8)3.5 produced the same match, which is the mouse DWNN (Fig 3.15 and Fig

3.16). This gene was also identified from CHO-Mut16 (3x8)3.5 from the 3' inverse PCR (section 3.2.4).

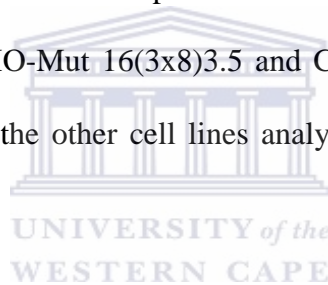
The genomic sequence from CHO-Mut10 (3x8)3.5 was too short (9 bases long) to match anything significant in the database using the BLAST (Fig 3.17). The sequence from CHO-J363 cells did not show any match with the retrovirus sequence (Fig 3.17a). This was of concern because it meant that this fragment was not an inverse PCR product, although the hygromycin resistant gene was amplified from this fragment (section 3.2.2). It was therefore, concluded that this fragment was a contamination picked up during PCR. However, the BLAST search analysis was performed on the whole sequence and the sequence matched a mouse DNA sequence on chromosome 11. Figure 3.17b shows the first 11 hits obtained using BLAST. Table 3.2 summarizes the BLAST search results from the 5' inverse PCR.

CELL LINE	DATABASE SEQUENCE MATCHES
CHO-Mut8 (3x8)3.5	Mouse DWNN gene
CHO-Mut16 (3x8)3.5	Mouse DWNN gene
CHO-Mut10 (3x8)3.5	No significant match
CHO-J363	Mouse DNA sequence from clone RP23-170A23, chromosome 11

Table 3.2 Summary of the BLAST search results for the 5' inverse PCR products.

3.3 Screening for other DWNN knock-out cell lines

Primers have been designed within the DWNN and the hygromycin sequence in order to screen for other cell lines in which the DWNN gene has been knocked-out. A forward primer, designated 7.3, was designed within the 5' region of the DWNN gene (Fig 3.18) and was used in conjunction with the reverse primer from the hygromycin gene of the retrovirus (primer 883) (Fig 3.3). This PCR would produce a fragment of >301 bp in those cell lines that contain the promoter-trapped DWNN gene, and no fragment would be produced in cell lines where the DWNN gene has not been mutagenised by the retrovirus. The presence of the promoter-trapped DWNN in CHO-Mut 8 (3x8)3.5, CHO-Mut 16(3x8)3.5 and CHO-J363 has been confirmed in this way (Fig 3.19b) and the other cell lines analyzed have shown negative results (data not shown).



Another primer (7.3R) was designed on 3' end of the DWNN sequence and this primer was used in conjunction with primer 1041 on the hygromycin gene in a PCR reaction. This PCR reaction would amplify a fragment of 223 bp in length (Fig 3.20a). This PCR was performed as to double check that the PCR fragment being amplified are genuine. The PCR was performed on the four promoter-trapped CH cell lines used in this study, as well as other promoter-trapped cell lines. The results showed that only CHO-Mut8 (3x8)3.5 and CHO-Mut8 (3x8)3.5 produced a fragment of 223 bp and no other cell lines analyzed produced a fragment (Fig 1.20b). These results complement the inverse PCR data and the PCR performed with 7.3 and 883 primers for CHO-Mut8 (3x8)3.5 and CHO-Mut8 (3x8)3.5. However, since the inverse PCR and this PCR failed to identify DWNN in CHO-J363, it was safe to

conclude that the data obtained in the 7.3 and 883 PCR for CHO-J363 was not genuine, it could have been a PCR contamination.

3.4 DWNN sequence analysis

The sequences of the cell lines in which DWNN was identified (i.e. CHO-Mut 8 (3x8)3.5, CHO-Mut 16(3x8)3.5 and CHO-Mut 7 (3x8)3.5 from RACE PCR, George, 1995) were analyzed in order to determine the site of retroviral integration. The ‘trivial’ sequence from CHO-J363 was also included in this analysis (data not shown). The sequence analysis showed that in all these cell lines the site of retroviral integration is the same (Fig 3.21a-c, f). The site of integration on these cell lines was also identical to that of CHO-Mut 7(3x8)3.5 (Fig 3.21e), where DWNN was first isolated using RACE PCR (George, 1995). This could mean that either this particular integration site is the ‘hot spot’ for retroviral integration or that these cell lines originate from the same clone. The former speculation confirms previous reports of the presence of retroviral ‘hot spots’ within the host genome (Shih *et al.*, 1988).

3.5 Discussion

Four promoter-trapped retroviral mutagenesis CHO cell lines have been analyzed in this study. A positive control experiment was performed in order to confirm the

presence of the retrovirus in these cell lines. All four cell lines produced the hygromycin fragment, indicating that the promoter-trap mutagenesis experiment was performed successfully and that these cell lines contained the promoter-trapped retrovirus.

In order to identify genes that have been mutagenised within these cell lines, both 5' and 3' inverse PCR has been employed. This method yields two products, one from the 3' end for the 5' inverse PCR (or from the 5' end in case of the 3' inverse PCR) which is of constant size in all the cell lines and a variable 5' end fragment for the 5' inverse PCR (or a variable 3' end fragment for the 3' inverse PCR), containing the insertion site into the unknown genomic sequence. However, in some cell lines, only one fragment was amplified (Fig 3.5), which either represented the genomic sequence or the control hygromycin sequence. This could be due to the inability of the Taq Polymerase to amplify the big-sized fragments produced from these cell lines. It is expected that PCR products produced by Eco RI digests would result in big-sized fragments. However, the 5' IPCR was able to produce the control hygromycin fragment as well as the genomic fragment.

Sequence analysis of the 5' and 3' inverse PCR products identified an interesting gene, named DWNN, from CHO-Mut 8 (3x8)3.5 and CHO-Mut 16 (3x8)3.5). In other cell lines, the genomic sequences were either too short to show any significant matches from the database or only the retrovirus could be identified. The DWNN gene identified from CHO-Mut 8 (3x8)3.5 and CHO-Mut 16 (3x8)3.5 corresponds to

the previously research done (George, 1995), where the same gene was isolated on CHO-Mut 7 (3x8)3.5 using RACE PCR.

Primers were designed within the DWNN and the hygromycin sequences in order to screen other cell lines for the presence of DWNN. This was used to screen for other cell lines in which has been knocked out. The presence of the knocked-out DWNN in CHO-Mut 8 (3x8)3.5, CHO-Mut 16 (3x8)3.5 and CHO-J363 has been confirmed in this way. It was later determined that product amplified from the CHO-J363 cell line was not authentic and that it was a possible PCR contaminant.

Further analysis of the DWNN sequence in these cell lines showed that they all had the same site of retroviral integration, meaning that the retrovirus inserted in the same position of the DWNN gene. This either meant that this particular site was a hot spot for retroviral integration or that these cell lines all originated from the same clone. The latter might be a possibility since CHO-Mut 8 (3x8)3.5, CHO-Mut 16 (3x8)3.5 and CHO-Mut 17 (3x8)3.5 cell lines were cloned from the same plate (George, 1995). These results also confirmed the suggestion that the DWNN sequence amplified from CHO-J363 was not authentic. There was no possibility that CHO-J363 cell line might have originated from the same clone as CHO-Mut 8 (3x8)3.5, CHO-Mut 16 (3x8)3.5 and CHO-Mut 17 (3x8)3.5 cell lines since CHO-J363 cell line was generated by a different person in a different study (Newton, 1995) from the CHO-Mut 8 (3x8)3.5, CHO-Mut 16 (3x8)3.5 and CHO-Mut 17 (3x8)3.5 cell lines. Therefore, the possibility that CHO-J363 could be a DWNN-knocked cell line was ruled out.

It is unclear why the 3' and 5' IPCR from CHO-Mut 8 (3x8)3.5 cell line amplified two different sequences. However, the DWNN-Hygro PCR (section 3.3) confirmed the presence of the DWNN gene in this cell line.

The research undertaken in this project was designed to evaluate the role of DWNN and to elucidate its involvement in CTL killing.



CHAPTER 4: GENERATION OF THE HUMAN DWNN-13 CONSTRUCT.

4.1 Introduction

The DWNN gene was first isolated from a promoter-trapped CHO cell line, CHO-Mut7 (3x8)3.5 (George, 1995). The sequence of the DWNN gene from CHO-Mut7 (3x8)3.5 matched a human EST 587, from the 21C4 cDNA clone (accession number T25012). The 21c4 cDNA clone was ordered from ATCC (Rockville, USA). The cDNA was then sequenced and the complete consensus sequence showed that it is 1.1 kb in length and codes for a 118-residue protein (Pretorius, 2000). A conserved 80-residue domain was identified within the 118-residue DWNN protein and a hydrophobic C-terminal tail. The 118-residue protein encodes a 13 kD protein and hence was named DWNN-13 (Fig 4.1). This chapter describes the isolation of the 118-residue protein, named DWNN-13 and the cloning of DWNN-13 cDNA into pEGFP-C1 and pcDNA 3.1/Zeo vectors. .

4.2 Amplification of DWNN-13 cDNA

4.2.1 Primer design

Primers amplifying the 118 amino acid DWNN coding sequence were designed such that the forward primer (DWNN F) incorporated a Bam HI restriction site at the 5' end of the coding region (for cloning purposes) and the reverse primer (DWNN R) incorporated an Xho I site at the 3' end of the amplified DWNN gene (for cloning

purposes) and also provided a TAA termination codon for the amplified DWNN gene. Six bases before the Bam HI and Xho I sites were incorporated to allow efficient restriction digest of the PCR product (see Table 4.1).

4.2.2 Amplification and sequencing of DWNN-13 clone

The DWNN-13 gene was amplified from the 21C4 cDNA clone (Fig 4.2a) using the designed DWNNF and DWNNR primers in a PCR reaction (section 2.10.1). A 383 bp PCR product was observed on a 1 % agarose gel electrophoresis (Fig 4.2b).

The PCR products were eluted and sequenced directly with DWNN F and DWNN R primers on the ABI 310 Sequencer (Chapter 2.11). The sequences obtained from both primers showed the presence of the DWNN sequence, the Bam HI and Xho I sites, as well as the TAA stop codon (Fig 4.3). This indicated that the amplified DWNN gene was in the correct reading frame and had all the cloning sites and stop codon. The sequences were analysed using BLAST. The sequences with both DWNNF and DWNNR primers matched the DWNN protein against the non-redundant sequences in the database (Fig 4.4). When comparing the analysed sequences with the 21c4 cDNA (accession number T25012), a 100 % identity was observed (Fig 4.5).

4.3 Subcloning of the DWNN-13 cDNA

4.3.1 Construction of the pEGFPC1-DWNN-13 fusion protein

The pEGFPC1-DWNN-13 fusion protein was constructed by cloning the PCR product (section 4.2.2) into pEGFPC1 vector (section 2.4.3). The resultant PCR product (Fig 4.2) was first digested with Bam HI and Xho I to release a 363 bp fragment. The 363 bp resultant fragment was purified from the agarose gel using the GeneClean Kit II (section 2.9.2). This fragment was then used for cloning into pEGFPC1 vector between the Bgl II and Sal I sites for subsequent experiments (Fig 4.6a). Cloning between Bam HI and Xho I sites of the pEGFPC1 vector was abandoned because this would have allowed cloning of the PCR product in the reverse orientation (Fig 4.6b). Therefore, Bgl II and Sal I sites were instead used for the cloning of the PCR product. The Bam HI/ Bgl II and Xho I/ Sal I sites have the same overhang and therefore cloning was possible but all sites were destroyed during cloning. *E.coli* MC1061 cells were transformed (section 2.6) and the plasmid DNA was isolated and purified using the double cesium chloride gradient centrifugation (section 2.7.2). The plasmid DNA was then digested with Pst I (a site present on the DWNN-13 cDNA) and Bam HI (a site present on the multiple cloning site of pEGFPC1 vector, Fig 4.6b), in order to identify the recombinants that contained the DWNN insert and clone 8 was identified as a positive clone (Fig 4.6c). As a control, pEGFP-C1 vector was also digested with Bam HI and Pst I. Only a 4.7 kb fragment was observed in the control, compared to the 215 bp fragment obtained from the restriction digestion of clone 8 (Fig 4.6c).

4.3.2 Subcloning of DWNN-13 cDNA into pcDNA3.1/Zeo vector

The 21C4 clone (obtained from ATCC, Rockville, USA) containing the 118 amino acid DWNN, was cloned between Not I and Xho I sites of pTd7 vector. This clone was digested with Bam HI and Xho I, in order to release the 929 bp DWNN insert (Fig 4.7a). This insert was purified from an agarose gel using the GeneClean kit (section 2.9.2) and was cloned between Bam HI and Xho I digested pcDNA3.1/Zeo vector. Restriction digest of one of the positive clones, clone 3, was performed using Bam HI and Xho I, in order to confirm the presence of the insert. As a control, pcDNA3.1/Zeo vector was digested with Bam HI and Xho I (Fig 4.7c). Using the double cesium chloride gradient protocol (section 2.7.2), plasmid DNA from the positive clone 3 was prepared for stable transfections (chapter 7).

4.4 Discussion

The DWNN-13 gene was successfully amplified from 21C4 clone (accession number T25012) using the PCR technique. Sequence analysis showed a 100 % identity of the amplified product with the 21c4 cDNA (accession number T25012). Subcloning of the DWNN-13 gene into pEGFP-C1 and pcDNA3.1/Zeo vectors was performed successfully. The pEGFC1-DWNN-13 fusion protein was used for expression in mammalian cells for protein localisation studies and the pcDNA3.1/Zeo-DWNN-13

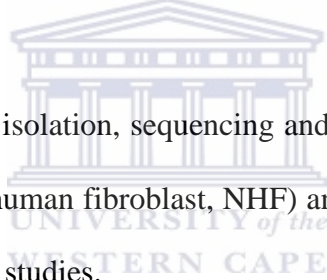
construct was stably transfected into mammalian cells for CTL killing experiments, as will be discussed in subsequent chapters.



CHAPTER 5: CONSTRUCTION OF THE HUMAN DWNN-200 cDNA.

5.1 Introduction

The human DWNN gene is located on chromosome 16. Human DWNN gene encodes two transcripts of 1.1 kb and 6.1 kb encoding 13 kD and 200 kD proteins respectively. The two proteins were named DWNN-13 and DWNN-200. The consensus human DWNN-200 sequence was assembled from various EST data sequences and partial cDNA clones and sequence analysis of the gene showed that it consists of two promoters and 19 exons (Rees, unpublished).



This chapter describes the isolation, sequencing and assembly of DWNN-200 cDNA from non-cancer (normal human fibroblast, NHF) and cancer human cell lines (HeLa and MG-63) for functional studies.

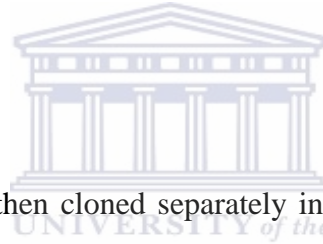
5.2 Generation of DWNN-200 cDNA by RT-PCR

5.2.1 Designing of primers

The coding sequence of DWNN-200 is 5.3 kb long and it has proven to be difficult to amplify the whole fragment using PCR techniques. Therefore, four sets of primers were designed from the assembled DWNN-200 cDNA, so that they were overlapping and had restriction sites in the overlapping regions, in order to facilitate the cloning of the different fragments obtained from PCR (Table 5.1 and Fig 5.1a).

5.2.2 Amplification of DWNN-200 cDNA

Messenger RNA was isolated from normal and cancer human cell lines, purified with oligo dT and cDNA was synthesised with AMV Reverse transcriptase (Chapter 2.15). The cDNA was then amplified using the four sets of primers (Table 5.1) in separate PCR reactions. Fragments of expected sizes were obtained (Fig 5.1a and 5.1b) from both the NHF and the human cancer cell lines. Table 5.2 lists the cell lines from which the four fragments were amplified and the amount which was sequenced from each fragment.



Each PCR fragment was then cloned separately into the pGEM T Easy vector (Fig 5.1b) and restriction digests were performed in order to screen for the positive clones. Fragment 1 was digested with Bam HI and Pvu II to release a 1.5 kb fragment (Fig 5.2a); fragment 2 was digested with Pvu II and Hind III, releasing a 1.3 kb fragment (Fig 5.2b); fragment 3 with Hind III and Pvu II and fragment 4 digested with Pvu II and Eco RI producing fragment sizes of 1.3 kb and 1.7 kb respectively (Fig 5.3a, b). All the clones from the four fragments contained the expected sized- fragments upon restriction digestion, suggesting that the clones were correct.

FRAGMENT	CELL LINE	SEQUENCE
1	HeLa NHF	100 % 100 %
2	MEL-2 NHF	100 % 100 %
3	HeLa	100 %

	Hep G	60 %
	NHF	100 %
4	HeLa	100 %
	MG-63	50 %
	NHF	100 %

Table 5.2 Cell lines used for the amplification and sequencing of DWNN-200 cDNA.

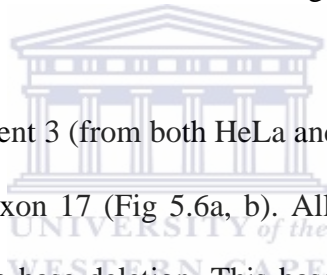
5.3 Sequencing of DWNN-200 cDNA

5.3.1 Sequencing of DWNN-200 clones from cancer cell lines

The different clones isolated from the human cancer cell lines were sequenced in both strands, using M13 forward and reverse primers as well as with PCR primers (Table 5.1) and internal sequencing primers, designed along the entire region of the assembled DWNN-200 cDNA (Table 5.3). However, clones derived from Hep G and MG-63 cell lines were not sequenced fully, only 50-60 % was sequenced (see table 5.3). All the sequences obtained showed a 100 % identity with the assembled DWNN-200 cDNA, except for the sequences from fragment 1 (from HeLa) and fragment 3 (from HeLa and Hep G). Also, the sequence from fragment 2 showed that exon 16, which corresponds to 102 bp, of this cell line was missing.

Sequences from fragment 1 showed two base changes at residues 1275 and 1496, which are situated within the RING finger domain of the DWNN-200 gene. At residue 1275, there was a change from base A to T (Fig 5.4a, b). This base change resulted in the change in the amino acid sequence at position 289 from Leucine to

Glutamine (Fig 5.4c). Residue 1496 showed a base change from base C to T and this resulted in a change in amino acid at position 363 from Serine to Proline (Fig 5.5a, b, c). All the three clones isolated from this fragment were sequenced and they all showed the same changes. Analysis of all the sequences in the Genebank and NCBI SNP databases showed no variations within these regions. It can therefore be concluded that these two base changes may be functionally significant and are due to mutations and are not variations. The Leucine to Glutamine mutation was designated L289Q and the Serine to Proline mutation was designated S363P.



The sequences from fragment 3 (from both HeLa and Hep G) showed a base deletion, base **A**, at base 4034 in exon 17 (Fig 5.6a, b). All seven clones isolated from this fragment showed the same base deletion. This base deletion caused a frameshift of the sequences downstream and this resulted in the introduction of several stop codons (Fig 5.6c). Fragments 1 and 3 were amplified with primers RBBP6 1F and RBBP6 2R and RBBP6 4F and RBBP6 3R respectively (Fig 5.1) and were isolated from HeLa and Hep G cells.

5.3.2 Sequencing of DWNN-200 clones from NHF cell line

The NHF cell line were also sequenced with the same primers used for sequencing the clones isolated from cancer cell lines. All the clones were sequenced in both directions to ensure that the sequences obtained were correct. The sequence analysis

of all the clones showed 100 % identity with the assembled DWNN-200 sequence. Figures 5.7 and 5.8 show the sequences from the RING finger region of fragment 1, which were shown to be mutated in HeLa cells. The sequences from this cell line showed a 100 % identity with the assembled DWNN-200 sequence. Figure 5.9 shows the presence of **A** in fragment 3, which was missing in HeLa and Hep G cells.

Furthermore, RT-PCR and sequence analysis of HeLa and NHF cells have revealed that these cell lines are missing the 244 bp fragment in exon 16. Amplification using primers situated outside exon 16 was performed. The forward primer (RBBP 1F) is situated in exon 11, while the reverse primer (16R) is found in exon 17 (Fig 5.10). Amplification using these primers produced a 856 bp fragment, if exon 16 is missing and if exon 16 is present fragments of 958 bp and 856 bp will be produced, meaning that exon 16 is alternatively spliced (Fig 5.10). It was concluded therefore that in HeLa and NHF cells, exon 16 was spliced out, while in MG-63 cell line it was alternatively spliced.

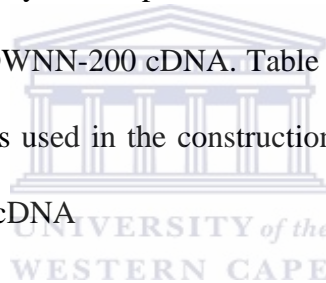
5.4 Assembly of the full-length DWNN-200 cDNA

In order to generate the full length DWNN-200 cDNA, the digested fragments (Fig 5.2 and Fig 5.3) would have to be cloned together into pBC KS cloning vector. However, it was impossible to clone all four fragments in a single reaction. It was therefore decided to first clone two fragments in a single reaction, that is clone Bam

HI/ Pvu II digested fragment 1 and Pvu II/ Hind III digested fragment 2 into Bam HI/ Hind III digested pBC SK vector in a single reaction to generate fragment A (Fig 5.11a) and clone Hind III/ Pvu II digested fragment 3 and Pvu II/ Eco RI digested fragment 4 into Hind III/ Eco RI digested pBC SK vector in a separate reaction, generating fragment B (Fig 5.11b). Ultimately, Bam HI/ Hind III digested fragment A and Hind II/ Eco RI digested fragment B would then be cloned into Bam HI/Eco RI digested pBS SK to generate the full length DWNN-200 cDNA (Fig 5.11c).

However, attempts to clone the Bam HI/ Pvu II digested fragment 1 and Pvu II/Hind III digested fragment 2 into pBC SK⁺ digested with Bam HI and Hind III were unsuccessful. Meanwhile, the Hind III/Pvu II digested fragment 3 and Pvu II/Eco RI digested fragment 4 were cloned successfully between the Hind III and Eco RI sites of pBC SK⁺ and restriction digests of the positive clones with Hind III and Eco RI gave an expected 3.2 kb sized fragment B (Fig 5.12b). This fragment was then excised and eluted using the GeneClean kit (section 2.9.2). Fragments 1 and 2, as well as the 3.2 kb fragment 5 (Fig 5.12b) were cloned between Bam HI and Eco RI sites of pBS KS⁺ sites (Fig 5.13a). The positive clones were digested with Bam HI and Xho I to release fragments of 2.0 kb, 3.0 kb and 3.8 kb (Fig 5.13b). In order to release the 5.8 kb full length DWNN cDNA from pBS vector, the positive clones were first digested with Xho I to completion, and then partially digested with Bam HI (Fig 5.13b). A partial Bam HI digest was performed due to the second internal Bam HI site within the DWNN cDNA (Fig 5.13a). The 5.8 kb full-length DWNN cDNA was then cloned into other vector systems for subsequent experiments.

Ultimately two forms of DWNN-200 cDNA were cloned: the wild type DWNN-200 cDNA and the L289Q and S363P mutated DWNN-200 cDNA, designated L289Q:S363P DWNN-200 cDNA. The wild type DWNN-200 cDNA was constructed from the NHF cell line, while the L289Q:S363P DWNN-200 cDNA was constructed from the various human cancer cell lines, as well as the NHF cell line. Both these cDNAs were cloned into in pDsRed1-C1 vector for localisation studies (Chapter 6). No further analysis was performed on the truncated DWNN-200, which was designated Δ A4034 DWNN-200 cDNA. Table 5.4 summarizes the cell lines and the four DWNN fragments used in the construction of the wild type, L289Q:S363P and Δ A4034 DWNN-200 cDNA.



DWNN-200 cDNA	FRAGMENT	CELL LINE
Wld type	1	NHF
	2	NHF
	3	NHF
	4	NHF
L289Q:S363P	1	HeLa
	2	MEL-2
	3	HeLa
	4	NHF
Δ A4034	1	NHF
	2	MEL-2
	3	NHF
	4	Hep G

Table 5.4 Summary of the cell lines used in the construction of the DWNN-200 cDNA.

5.5 Discussion

This chapter describes the cloning and sequencing of the full length 5.8 kb human DWNN-200 cDNA, which encodes a 200 kD protein. Three forms of DWNN-200 cDNA were isolated in this study: the wild type, the L289Q and S363P mutated and the C-terminal truncated DWNN-200. However, only the wild type and the L289Q:S363P DWNN-200 cDNA were cloned for further characterisation. No further analysis was performed on the Δ A4034 DWNN-200 cDNA. The DWNN-200 cDNA isolated from a various non-cancerous human cell lines was sequenced and showed a 100 % identity with the assembled DWNN-200 sequence, except in three positions. The sequence of DWNN-200 cDNA isolated from HeLa and Hep G cell lines showed two base changes within the RING finger domain and a base deletion at position 4034 in exon 17. The two base changes within the RING finger domain resulted in the amino acid changes, which might alter the protein structure and consequently the protein function. Studies have shown that the RING finger domain may function in direct protein binding of several proteins (Houvras *et al.*, 2000) and functions as ubiquitin-protein ligase (E3) (Hashizume *et al.*, 2001). Mutations within this domain might therefore alter this function.

The base deletion at residue 4034 resulted in a frameshift on the downstream sequences, which therefore introduced stop codons downstream, leading to a truncation of the predicted protein. However, the RING finger mutations and deletion were not present in other human cancer lines tested, such as MG-63 and CaSki. The rest of the DWNN-200 sequence was shown to have 100 % sequence identity with the assembled DWNN-200 sequence.

It has been described previously that a region of 34 amino acid of the PACT protein is alternatively spliced (Simons *et al*, 1997). It was also discovered in this study that the 34 amino acid alternatively spliced region is present in MG-63 cell line and not in HeLa and NHF cells. This region has been mapped to exon 16 of the DWNN gene. The DWNN-200 cDNA cloned in this study is missing the alternatively spliced region. It therefore still remains under investigation as to whether the presence or absence of this region plays a vital role in the functioning of the DWNN gene.

The 'wild type' DWNN-200 cDNA was cloned into pcDNA 3.1/Zeo vector for transfection into mammalian cells, for functional studies (described in chapter 7), while both forms of the DWNN-200 cDNA were cloned into pEGFP C1 for localisation studies (Chapter 6).



CHAPTER 6: LOCALISATION OF DWNN PROTEIN.

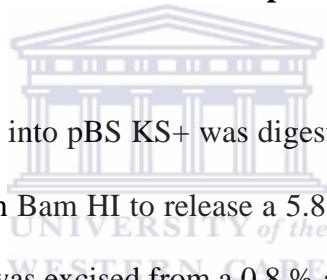
6.1 Introduction

Clontech has developed several optimised GFP variants, such as enhanced green fluorescent protein (EGFP) (section 2.4.3), red fluorescent protein (DsRed) (section 2.4.4) and enhanced yellow fluorescent protein (EYFP), with which they have constructed mammalian expression vectors. This chapter describes the use of EGFP and DsRed for monitoring DWNN localisation in CHO cells.

6.2 Subcloning of DWNN-13 cDNA into pEGFP-C1 vector

The pEGFP-C1-DWNN-13 fusion protein was assembled as described in section 4.3.1. The double cesium chloride gradient protocol (section 2.7.2) was used for the preparation of plasmid DNA for transfection into mammalian cells (Fig 6.1).

6.3 Subcloning of DWNN-200 cDNA into pDsRed1-C1 vector



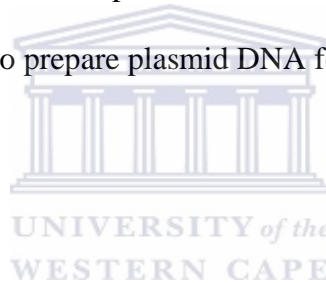
DWNN-200 cDNA cloned into pBS KS+ was digested with Xho I to completion and then partially digested with Bam HI to release a 5.8 kb full length DWNN-200 clone (Fig 6.2b). This fragment was excised from a 0.8 % agarose gel and purified using the GeneClean kit (section 2.9.2) and was cloned between Bgl II and Sal I sites of pDsRed1-C1 (Fig 6.3a). Bam HI and Bgl II have the same overhang, as well as Xho I and Sal, therefore it was possible to clone the Bam HI/ Xho I digested DWNN cDNA between the Bgl II and Sal sites of pDsRed1-C1. However, all the four sites were destroyed during cloning and therefore they will not cut when digested with the respective restriction enzymes. The positive clones were then screened by restriction digestion of the plasmid DNA with Bam HI and Xho I to yield two fragments of 7.8 kb and 2.0 kb (Fig 6.4b).

The same procedure was employed to clone the L289Q and S363P mutated DWNN-200 cDNA (Fig 6.4a) Positive clones were also identified by restriction digestion of

the plasmid DNA with Bam HI and Xho I and fragments of correct sizes were visualized on a 0.8 % agarose gel electrophoresis (Fig 6.4b).

In comparison, the pDsRed1-C1 vector digested with Bam HI and Xho I produced a 4.1 kb fragment (Fig 6.4c).

Both the wild type and the L289Q and S363P mutated DWNN-200 constructs express pDsRed1-C1-DWNN-200 fusion proteins. The double cesium chloride gradient protocol (2.7.2) was used to prepare plasmid DNA for both constructs for transfection into mammalian cells.



6.4 Transient expression of fusion proteins in cultured cells

6.4.1 Transient expression of pEGFPC1-DWNN-13 construct

CHO-Y10, CHO-Mut16 (3x8)^{3.5} and CHO-Mut8 (3x8)^{3.5} cells were used for the transient transfections and were grown to 70 % confluency on coverslips in six well plates (Chapter 2.17.3.1). All the plasmid DNA used for transfections were purified using double caesium chloride gradient protocol (section 2.7.2) to ensure that the DNA was highly pure and good quality for transfections. Cells were transfected with 1 µg of plasmid DNA using the Lipofectamine 2000 Reagent (Invitrogen) according to the manufacturers instructions (section 2.13.3.1). Cells were transfected with DNA

constructs encoding EGFP alone, DsRed1-C1 alone, EGFP- tagged DWNN-13 (section 6.2) and DsRed1-C1-tagged wild type DWNN-200 and DsRed1-C1- tagged L289Q and S363P mutated DWNN-200 (section 6.3). After 24-48 hours, cells were fixed in 4 % paraformaldehyde and stained with DAPI to localise the DNA. The coverslips were mounted onto slides using the Vectorshield Hard Set Mounting medium (Vectorshield) and were analysed using fluorescent microscopy (section 2.14.2).

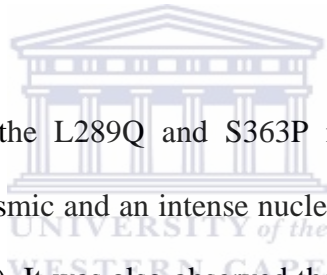
Analysis of the control slides (i.e. cells transfected with EGFP and DsRed1-C1 alone) showed that the transfection efficiency varied from 30-60 % in different experiments. Figure 6.5 showed that cells transfected with EGFP-C1 and DsRed1-C1 only demonstrated no specific localisation, with a distribution of the GFP and the red fluorescent protein (DsRed1-C1) in the cytoplasm and the nucleus. However, all cells transiently transfected with EGFP-tagged with DWNN-13 showed cytoplasmic and an intense nuclear localisation (Fig 6.6).

6.4.2 Transient expression of pDsRed1-C1-DWNN-200 fusion proteins

CHO-Y10, CHO-Mut 8 (3x8)^{3.5} and CHO-Mut 16 (3x8)^{3.5} cells were transiently transfected with both the wild type and L289Q and S363P mutated pDsRed1-C1- and pEGFP-C1-DWNN-200 constructs (section 2.13.3.1).

Cells transfected with pDsRed1-C1 alone and pDsRed1-C1 tagged with DWNN-200 cDNAs were transfected for up to 72 hours. The transfection efficiency was very low and no photographs were taken.

Due to the low transfection efficiency of the pDsRed1-C1-DWNN-200 constructs, the same constructs were rebuilt in pEGFP-C1 vector (data not shown). The same procedure was followed for transient transfections of cultured cells (see section 2.13.3.1).



Both the wild type and the L289Q and S363P mutated DWNN-200-pEGFP-C1 constructs showed cytoplasmic and an intense nuclear localisation in all the cell lines examined (Fig 6.7 and 6.8). It was also observed that some cells were expressing the GFP-DWNN protein more intensely than the others.

6.5 Discussion

In an attempt to determine the localisation of DWNN protein in CHO cells, GFP was employed as a reporter for DWNN localisation *in vivo*. Both EGFP-C1-DWNN-13 and pDsRed1-C1-DWNN-200 constructs were generated. These constructs were transiently transfected in CHO-Y10, CHO-Mut8 (3x8)3.5, CHO-Mut16 (3x8)3.5 and HeLa cells. pDsRed1-C1-DWNN-200 constructs, however RFP constructs showed very low transfection efficiency in all the cell lines. The DWNN-200 cDNA of both forms were then cloned into EGFP-C1 vector. The results showed that both forms of

the protein (DWNN-13 and DWNN-200), when fused to GFP, are expressed in both the nucleus and cytoplasm of the cells.



CHAPTER 7: GENERATION OF STABLE DWNN-COMPLEMENTED MUTANT CELL LINES.

7.1 Introduction

In order to evaluate the outcome of complementing the DWNN-mutant cell lines with DWNN expression, pZeo-DWNN constructs encoding the full-length wild type DWNN-200 and DWNN-13 were developed. These were stably transfected into DWNN-mutant CHO-Mut 8(3x8)3.5 and CHO-Mut 16(3x8)3.5.

This chapter describes the development of DWNN-13 and DWNN-200 constructs in a mammalian pcDNA3.1/Zeo vector, which are stably transfected into mammalian CHO cell lines. pcDNA3.1/Zeo vector has been used for this study because it is

suitable for transfecting into mammalian cells and confers resistance to Zeocin, which is a unique antibiotic for these cell lines, meaning that the cell lines should be susceptible to the antibiotic unless they are expressing the pcDNA3.1/Zeo-DWNN constructs.

7.2 Subcloning of DWNN-13 cDNA into pcDNA3.1/Zeo vector

The cloning of the DWNN-13 cDNA into pcDNA3.1/Zeo vector was described in section 4.3.2 of this thesis. Using the double cesium chloride gradient protocol (section 2.7.2), plasmid DNA was prepared for the stable transfections.

7.3 Subcloning of DWNN-200 cDNA into pcDNA3.1/Zeo vector

The wild type DWNN-200 cDNA constructed as described in section 5.4 was digested with Xho I to completion and partially digested with Bam HI in order to release the 5.8 kb fragment (Fig 7.1a). This fragment was cloned between Bam HI and Xho I sites of pcDNA3.1/Zeo (Fig 7.1a). On digestion with Bam HI and Xho I restriction enzymes, pcDNA3.1/Zeo vector produced a 5.0 kb fragment (Fig 7.1b). Correct constructs were identified by digesting the plasmid DNA with Bam HI and Hind III. Clones containing the DWNN-200 insert produced four fragments of sizes 1.01 kb, 2 kb, 3.8 kb and 5 kb (Fig 7.2a). Figure 7.2b shows the restriction digest of the positive clones, digested with Bam HI and Hind III. Using the double cesium chloride gradient protocol, plasmid DNA was prepared for transfections into

mammalian cells.

7.4 Determination of the optimal concentration of Zeocin for selection of CHO-Y10 cells

In order to establish the minimum concentration of Zeocin required for the selection of stable transfected clones, CHO-Y10 cells were seeded into 6 wells and grown until confluent. They were then exposed to various Zeocin concentrations, replacing the selective media every 3-4 days. CHO-Y10 cells were exposed to concentrations of 50 $\mu\text{g/ml}$, 100 $\mu\text{g/ml}$, 200 $\mu\text{g/ml}$, 300 $\mu\text{g/ml}$, 500 $\mu\text{g/ml}$, 800 $\mu\text{g/ml}$ and 1000 $\mu\text{g/ml}$. The effects of Zeocin on CHO-Y10 were monitored over 7 days of exposure. In cells treated with 50 $\mu\text{g/ml}$ and 100 $\mu\text{g/ml}$ of Zeocin there was an increase in size of the cells compared to the untreated cells (Fig 7.3a-d). While cells exposed to Zeocin concentrations between 200 $\mu\text{g/ml}$ and 400 $\mu\text{g/ml}$ started to enlarge and showed an abnormal cell shape (Fig 7.3e-f). At concentrations above 400 $\mu\text{g/ml}$ the morphology of the cells was abnormal and were enlarged. There was a clear breakdown of the plasma and nuclear membranes (Fig 7.3g-h). After 14 days of exposure cells treated with Zeocin at concentrations between 50 $\mu\text{g/ml}$ and 100 $\mu\text{g/ml}$ cells were still enlarged and abnormal in shape; while those cells treated with concentrations between 200 $\mu\text{g/ml}$ and 1000 $\mu\text{g/ml}$ were completely broken down and only cell debris remained. It was therefore concluded that at concentrations between 200 $\mu\text{g/ml}$ and 400 $\mu\text{g/ml}$, Zeocin kills all the cells within two weeks and these concentrations

corresponded to the manufacturer's protocol and the documented literature (Graham *et al.*, 1977 and Mulsant *et al.*, 1988). Therefore 300 µg/ml Zeocin was chosen to be the optimal concentration for the selection of stable transfected cells.

7.5 Stable transfection of pcDNA3.1/Zeo-DWNN-13 and pcDNA3.1/Zeo-DWNN-200 constructs into mammalian cells

The stable transfection of CHO-Mut8 (3x8)3.5 and CHO-Mut16 (3x8)3.5 was performed using the lipofectamine method (section 2.13.3.2) with DNA constructs containing pcDNA3.1/Zeo-DWNN-13, pcDNA3.1/Zeo-DWNN-200 and CIT BAC clone, accession number AC010321 (obtained from Los Alamos National Laboratory for the US Dept of Energy in New Mexico) in six well culture plates. CIT BAC clone is a 20 kb genomic DNA containing the full length DWNN cDNA, which is situated in the middle the clone. Table 7.1 summarizes the DNA constructs used for the transfections of the mammalian cells.

CELL LINE	DNA TRANSFECTED
CHO-Mut 8 (3x8)3.5	pcDNA3.1/Zeo-DWNN-200
CHO-Mut 8 (3x8)3.5	pcDNA3.1/Zeo-DWNN-13 and pcDNA3.1/Zeo-DWNN-200
CHO-Mut 16 (3x8)3.5	pcDNA3.1/Zeo-DWNN-13
CHO-Mut 16 (3x8)3.5	BAC clone and pcDNA3.1/Zeo-DWNN-200
CHO-Mut 16 (3x8)3.5	BAC clone and pcDNA3.1/Zeo vector

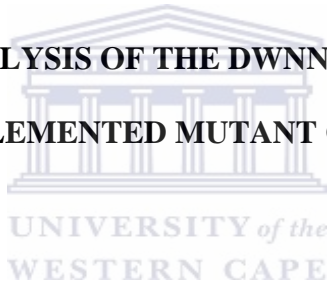
Table 7.1 Summary of DNA constructs used for transfecting CHO-Mut 8 (3x8)3.5 and CHO-Mut 16 (3x8)3.5 cells.

Thereafter, the stable clones were selected and continuously cultured in 300 µg/ml Zeocin. This concentration has been determined to kill CHO-Y10 optimally (section 7.4). After 3 to 4 weeks single isolated colonies, the number of colonies obtained varied from 5 to 15 colonies from each plate, and these were cloned using cloning rings (section 2.13.3.2) and were continuously propagated in media containing 300 µg/ml Zeocin. Figure 7.4 shows a representation of the colonies obtained from each transfected plate.

7.6 Discussion



Plasmids containing DWNN DNA cloned into pcDNA3.1/Zeo vector encoding both the DWNN-13 and DWNN-200 protein were developed. These were stably transfected into CHO-Mut 8(3x8)3.5 and CHO-Mut 16(3x8)3.5 successfully. The cells were either transfected with constructs encoding DWNN-13, DWNN-200 or both. The DWNN BAC clone was also used for the transfection of the cells. The concentration of 300 µg/ml of Zeocin was determined to be the optimal concentration for the selection of the stably transfected clones. Stable Zeocin resistant clones were observed after 3 weeks of selection and 5- 15 clones were isolated from the various plates. Fig 6.4 shows an example of clones that were selected after 4 weeks. These clones were analysed further and compared to the DWNN-mutant cell lines (Chapter 8).



CHAPTER 8: ANALYSIS OF THE DWNN-MUTANT AND DWNN-COMPLEMENTED MUTANT CELL LINES.

8.1 Introduction

In order to characterise a novel gene, it is important to determine its function. There are various ways of determining the role of a gene. This chapter employs a number of techniques in order to elucidate the function of the DWNN gene. These techniques are carried out in both the DWNN-mutant cell lines (chapter 3) and in DWNN-complemented mutant cell lines (chapter 7).

Generation of anti-DWNN antibodies (Lutya, 2002) has assisted in determining the subcellular localisation of the endogenous DWNN *in vivo*, by making use of immunostaining and Western blot analysis, and hence providing more insight into the functioning of the DWNN gene.

This chapter also investigates the effect of exposure to CTLs and staurosporine-induced apoptosis on the cell lines in order to explore the role of DWNN in CTL resistance, and to relate CTL resistance to chemically induced cell death.

8.2 Analysis of the DWNN expression

8.2.1 Immunofluorescent microscopy

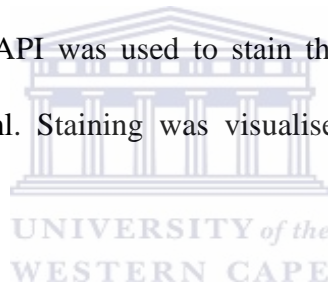
In order to determine the subcellular localisation of the endogenous DWNN protein in cultured mammalian cells, polyclonal antibodies specific for the DWNN-13 protein have been generated in rabbits (Lutya, 2002). Antibody staining experiments were performed in DWNN-mutant and DWNN-complemented mutant cell lines, as well as in CHO-Y10, HeLa and MG-63 cells. Table 8.1 lists all the cell lines used in for antibody staining, a detailed description of these cell lines is presented in table 2.6.

CELL LINE	DESCRIPTION
CHO-Y10	Chinese Hamster, parental cell line
CHO-Mut8 (3x8)3.5	Chinese Hamster, DWNN-mutant cell line
CHO-Mut16 (3x8)3.5	Chinese Hamster, DWNN-mutant cell line
CHO-Mut8 (3x8)3.5/ DWNN-200 & DWNN-13	Chinese Hamster, DWNN-complemented mutant cell line
CHO-Mut8 (3x8)3.5/ DWNN-200	Chinese Hamster, DWNN-complemented mutant cell line

CHO-Mut16 (3x8)3.5/ DWNN-13	Chinese Hamster, DWNN-complemented mutant cell line
CHO-Mut16 (3x8)3.5/ BAC clone & DWNN-13	Chinese Hamster, DWNN-complemented mutant cell line
HeLa	Human, cervical cancer cell line
MG-63	Human, bone cancer cell line

Table 8.1 Description of the cell lines used for Immunostaining.

The cell lines were grown on coverslips until confluent. Cells were fixed as described in section 2.14.1. The anti-DWNN antibody was used at a 1:100 000 dilution, while the Alexa Fluor 594 (red dye) or Alexa 499 (green dye) anti-rabbit antibody was used at a dilution of 1:500. DAPI was used to stain the DNA and was used at a final concentration of 15 µg/ml. Staining was visualised using fluorescent microscopy (section 2.14.2).

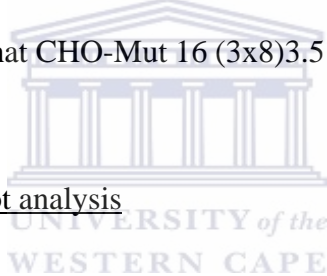


All cells stained with DAPI showed nuclear staining as expected because DAPI stains the DNA. Controls included cells stained with preimmune serum and cells stained with the Alexa Fluor 594 anti-rabbit IgG antibody only. Cells stained with the Alexa Fluor 594 anti-rabbit IgG antibody were negative (Fig 8.1a). This proved that the results obtained from cells stained with the polyclonal anti-DWNN antibody were due to the effect of this antibody and not the Alexa Fluor 594 anti-rabbit IgG antibody. Cells stained with the preimmune serum were also labelled with the secondary Alexa Fluor 594 goat anti-rabbit IgG antibody and no staining was seen (Fig 8.1b). In HeLa, MG-63 and CHO-Y10 cell lines, the endogenous DWNN localised predominantly in the nucleus, but small amounts were also present in the

cytoplasm (Fig 8.1c, d, e). DWNN-complemented mutant cell lines stained with the anti-DWNN antibodies also showed a significantly nuclear staining (Fig 8.1h, i, j, k).

However, in CHO-Mut 8 (3x8)3.5 cells, DWNN preferentially localised in the cytoplasm and it was completely excluded from the nucleus in all cells (Fig 8.1f).

Localisation of DWNN in CHO-Mut 16 (3x8)3.5 cells showed two types of distribution. There were some cells in which DWNN was distributed in both the cytoplasm and the nucleus, while other cells DWNN localised in the cytoplasm only (Fig 8.1g). This suggests that CHO-Mut 16 (3x8)3.5 cell line might be polyclonal.



8.2.2 Western blot analysis

In order to determine the DWNN protein levels and the size of the expressed protein in CHO-Mut8 (3x8)3.5 and CHO-Mut16(3x8)3.5 cells, as well as in the DWNN-complemented mutant cell lines, Western blots analysis was employed, using the polyclonal anti-DWNN antibody as a probe (section 2.18). Table 8.2 lists the cell lines used for Western blot analysis. Total protein extracts were isolated from the DWNN-mutant and DWNN-complemented mutant cell lines (section 2.18.1) and were resolved on a 10 % SDS-PAGE (section 2.18.2). The results showed three fragments of approximately 160 kD, 105 kD and 13 kD, which were present in all the CHO cell lines (Fig 8.2). The 13 kD fragment might represent the DWNN-13 protein. It is unclear what the other two fragments might be, but they might represent the DWNN-200 protein, although their sizes are smaller than the predicted 200 kD of the

DWNN-200 protein. This might suggest that the DWNN-200 protein is modified *in vivo* or that the DWNN-200 gene is expressing the truncated protein form or there is antibody cross reactivity. Several attempts of the Western blotting experiments, probing with anti-PACT (M56) mouse monoclonal IgG1 antibodies (Santa Cruz Biotechnology) failed to produce results.

CELL LINE	DESCRIPTION
CHO-Y10	Chinese Hamster, parental cell line
CHO-Mut8 (3x8)3.5	Chinese Hamster, DWNN-mutant cell line
CHO-Mut16 (3x8)3.5	Chinese Hamster, DWNN-mutant cell line
CHO-Mut8 (3x8)3.5/ DWNN-200 & DWNN-13	Chinese Hamster, DWNN-complemented mutant cell line
CHO-Mut8 (3x8)3.5/ DWNN-200	Chinese Hamster, DWNN-complemented mutant cell line
CHO-Mut16 (3x8)3.5/ DWNN-13	Chinese Hamster, DWNN-complemented mutant cell line
CHO-Mut16 (3x8)3.5/ BAC clone & DWNN-13	Chinese Hamster, DWNN-complemented mutant cell line

Table 8.2 Cell lines used for Western blot analysis.

8.3 CTL killing analysis

8.3.1 Target cell lines used

The following cell lines were used for the CTL killing studies: CHO 22, CHO-Y10, CHO-Mut8 (3x8)3.5, CHO-Mut16 (3x8)3.5, CHO-J363 and the DWNN-complemented mutant cell lines (Table 8.3). The target cells were grown in 75 cm² flasks until confluency and were harvested for labelling with ⁵¹Cr as described in section 2.16.3.

CELL LINE	DESCRIPTION
CHO-Y10	Chinese Hamster, parental cell line
CHO-Mut8 (3x8)3.5	Chinese Hamster, DWNN-mutant cell line
CHO-Mut16 (3x8)3.5	Chinese Hamster, DWNN-mutant cell line
CHO-J363	Chinese Hamster cell line, promoter-trapped
CHO 22	Chinese Hamster cell line, non promoter-trapped
CHO-Mut8 (3x8)3.5/ DWNN-200 & DWNN-13	Chinese Hamster, DWNN-complemented mutant cell line
CHO-Mut8 (3x8)3.5/ DWNN-200	Chinese Hamster, DWNN-complemented mutant cell line
CHO-Mut16 (3x8)3.5/ DWNN-13	Chinese Hamster, DWNN-complemented mutant cell line
CHO-Mut16 (3x8)3.5/ BAC clone & DWNN-13	Chinese Hamster, DWNN-complemented mutant cell line

Table 8.3 Cell lines used for the CTL killing assay.

8.3.2 CTL killing assay

The HA8 CTL clone was used for the killing assays and was harvested as described in section 2.16.1 and 2.20.2. Target cells were exposed to different dilutions of CTL for 6 hrs. Lysis of the target cells was quantitated by measuring the amount of ⁵¹Cr released from the target cells. Table 8.3 lists the target cell lines used for the CTL killing assay. CHO-Y10 and CHO-J363 were shown to be sensitive to lysis by HA8-

specific CTL, (Fig 8.3a). However, CHO-Mut8 (3x8)3.5, CHO-Mut16 (3x8)3.5 and the DWNN-complemented mutant cells lines were found to be completely resistant to lysis on exposure to HA8-specific CTL (Fig 8.3a, b, c).

8.4 Analysis of the expression of the transfected MHC class I H-2K^K and Haemagglutinin transgenes

In the earlier study, all the promoter-trapped cell lines, including the parental cell line, CHO-Y10, were transfected with A/PR8/34 Haemagglutinin (HA) and MHC class I H-2K^K in order to be recognized by HA specific K^K restricted CTL clones, HA8 and HA11 (George, 1994). Loss of expression of either of the two transgenes in the target cell lines would result in the HA specific K^K restricted CTL clones not recognizing the target cell lines. It was therefore crucial to ensure that the failure of the HA8 specific CTL clone to recognize the DWNN-mutant and DWNN-complemented mutant cell lines (section 8.3.2) was not due to the loss of expression of the transfected transgenes in these cell lines. Therefore, analysis of the expression of both the transgenes was undertaken.

8.4.1 FACS analysis for the expression of the MHC class I H-2K^K

The cell surface expression of MHC class I K^K was investigated by antibody staining and FACS analysis as described in section 2.15. This experiment was carried out in CHO-Y10, CHO-Mut 8 (3x8)3.5 and CHO-Mut 16 (3x8)3.5 and the DWNN-

complemented mutant cell lines (see Table 8.4). CHO 22 cells were also used as a negative control because they were not transfected with MHC class I K^K.

CELL LINE	DESCRIPTION
CHO-Y10	Chinese Hamster, parental cell line
CHO-Mut8 (3x8)3.5	Chinese Hamster, DWNN-mutant cell line
CHO-Mut16 (3x8)3.5	Chinese Hamster, DWNN-mutant cell line
CHO 22	Chinese Hamster cell line, non promoter-trapped
CHO-Mut8 (3x8)3.5/ DWNN-200 & DWNN-13	Chinese Hamster, DWNN-complemented mutant cell line
CHO-Mut8 (3x8)3.5/ DWNN-200	Chinese Hamster, DWNN-complemented mutant cell line
CHO-Mut16 (3x8)3.5/ DWNN-13	Chinese Hamster, DWNN-complemented mutant cell line

Table 8.4 Cell lines used for the analysis of MHC class I H-2K^K expression.

The results showed that all the cell lines analysed were expressing MHC class I H-2K^K glycoprotein at the same levels as the parental CHO-Y10 cell line, except for the CHO 22 cells, which the stained negative for MHC class I K^K. This was as expected because the CHO 22 cells were not transfected with MHC class I H-2K^K (Fig 8.4). CHO 22 cells were also stained with the secondary FITC conjugated anti-mouse IgG monoclonal antibody (Molecular Probes) to test for any background staining. These cells stained negative (green peak, Fig 8.4), indicating that the secondary antibody does not give any background staining.

Immunofluorescence microscopy also confirmed these results. The cells were stained with a mouse monoclonal anti-H-2K^K antibody (Molecular Probes) as described in section 2.14.1. Table 8.5 shows the list of cell lines used for this experiment. Figure

8.5 shows the expression of MHC class I H-2K^K on the cell surface of CHO-Y10, CHO-Mut 8 (3x8)3.5, CHO-Mut 16 (3x8)3.5 and CHO-Mut 8 (3x8)3/DWNN-200.

CELL LINE	DESCRIPTION
CHO-Y10	Chinese Hamster, parental cell line
CHO-Mut8 (3x8)3.5	Chinese Hamster, DWNN-mutant cell line
CHO-Mut16 (3x8)3.5	Chinese Hamster, DWNN-mutant cell line
CHO-Mut8 (3x8)3.5/ DWNN-200	Chinese Hamster, DWNN-complemented mutant cell line

Table 8.5 Cell lines used in the staining of the endogenous MHC class I H-2K^K.

FACS analysis and immunofluorescence staining showed that MHC class I H-2K^K was expressed at satisfactory levels in all the cell lines. This shows that there was no loss of MHC class I H-2K^K expression of through the cloning process and subsequent expansion of these clones.

8.4.2 Analysis of the influenza haemagglutinin (HA) expression

As stated in section 8.4.1, the promoter-trapped target cell lines were double transfected with the LHA, LHA-puro and MHC class I H-2K^K transgenes in order to be recognised by HA specific K^K restricted CTL clones, HA8 and HA11.

Subsequently the levels of the HA protein in these cells were determined. The cells lines were originally transfected with two forms of HA transcripts, the full length HA transcript, encoding a 1.7 kb fragment and a truncated 1.2 kb HA linked to a

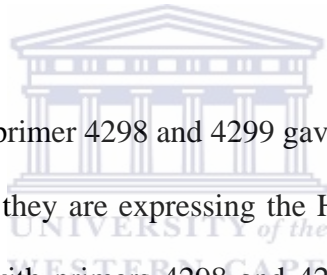
puromycin (HA-Puro) transcript (George, 1995). The full length HA nucleotide sequence is represented in figure 8.6 and the sequence of the HA8 and HA11 epitopes is underlined. However, antibodies against the HA protein were not available in the laboratory, for performing FACS of western blots. However, in the early study (George, 1994) the HA protein could not be detected on western blots. It was therefore chosen to analyse the sequence and the levels of HA mRNA in these cell lines in order to show that the sequence is correct and that the mRNA is expressed. This was achieved by firstly amplifying suitably size fragments from both the full length HA and HA-Puro transcripts and analysing the sequence of these fragments, and secondly by making use of Real-Time Quantitative PCR to compare the levels of expression of the HA mRNA amongst the DWNN-mutant lines and the DWNN-complemented mutant cell lines. Table 8.6 lists all the primer sequences used for the amplification of the HA fragment.

PRIMER NAME	PRIMER SEQUENCE	POSITION
4298	5' CTTGCTAAAACCCGGAGACA 3'	726-756
4299	5' AACTCAAAACATCCATTTCCG 3'	1459-1480
4300	5' CTTGCAGCTCGGTGACC 3'	388-404
3819	5' TCCAGAAGTAGTGAGGAGGC 3'	296-324
HAF	5' TTCGCACTGAGTAGAGG 3'	802-818
HAR	5' GTAATCCCGTTAATGGCATT 3'	1148-1167

Table 8.6 Sequence of the primers used for the amplification of HA.

8.4.3 PCR amplification and sequencing of HA mRNA

Total RNA was isolated from CHO-Y10, DWNN-mutant and DWNN-complemented mutant cell lines as described in section 2.19 and was shown to contain intact 18S and 28S rRNA (Fig 8.7). cDNA was reverse transcribed from RNA preparations using primers 4299 and 4300 (Fig 8.8a, c), complementary to the 3' end of the full length HA or to the 3' end of the HA-Puro cDNA respectively. PCR amplification was performed using primer 4299 or primer 4300 and a forward primer 4298 (Fig 8.8a, c). The resulting PCR products contained sequences encoding the antigenic epitopes for HA11 and HA8 (Fig 8.8b).



All cell lines analysed for primer 4298 and 4299 gave PCR products of expected sizes (Fig 8.8b), indicating that they are expressing the HA transcript. The PCR products were sequenced directly with primers 4298 and 4299. Sequencing analysis showed that both the HA11 and HA8 epitopes were still intact (data not shown). In order to determine whether the epitopes are in frame, the 5' end of the HA transcript had to be sequenced as well. Primer 3819, which is complementary to the SV40 early promoter of pKG16AG vector, which expresses HA, was used together with primer HAR to amplify a fragment of 1.281 kb (Fig 8.9a). The expected fragment was amplified in all three cell lines (Fig 8.9b) and was sequenced directly using primers 3819 and HAR and the sequencing results showed that the epitopes are in the correct reading frame.

However, it was impossible to amplify the HA-Puro fragment from the cell lines (data not shown), this could have been due to the primer 4300 not amplifying well.

However the cell lines were cultured in the presence of puromycin and were resistant to the antibiotic, indicating that these cells were expressing the puromycin resistance gene.

Therefore, both HA constructs (L⁺HA and L⁺HA-puro) are expressed in the cells and should be available to be processed and presented to MHC class I H-2K^K.

8.4.5 Real-Time Quantitative PCR analysis of the HA mRNA amplification

In order to analyse the levels of HA mRNA in the CHO cell lines, Real-Time quantitative PCR was utilised (section 2.22). Table 8.7 lists the cell lines used in the Real-Time Quantitative PCR. The HA mRNA levels were determined relative to the housekeeping gene, hypoxanthine phosphoribosyltransferase (HPRT), which was used as a standard. Primers were designed using the Real-Time Quantitative PCR probe design software (Roche Diagnostics). The primers used for the amplification of the HA/HA-puro fragments were HAF and HAR (Table 8.6), which amplify a fragment of 365 bp as shown in figure 8.10a. The HA fragment was amplified in all the cell lines analysed non-quantitatively (Fig 8.10b).

CELL LINE	DESCRIPTION
CHO-Y10	Chinese Hamster, parental cell line
CHO-Mut8 (3x8)3.5	Chinese Hamster, DWNN-mutant cell line
CHO-Mut16 (3x8)3.5	Chinese Hamster, DWNN-mutant cell line

Table 8.7 Cell lines used for the analysis of HA expression.

Reactions for determining the relative HPRT and HA gene expression in samples was set up as described in section 2.21. The relative standard curve was prepared with 10 fold serial dilutions (undiluted, 1:10 and 1:100) of cDNA from CHO-Y10, CHO-Mut8 (3x8)3.5 and CHO-Mut16 (3x8)3.5 cell lines. The template concentrations were given arbitrary values of 1 (for undiluted), 0.1 (for 1:10 dilution) and 0.01 (for 1:100 dilution).

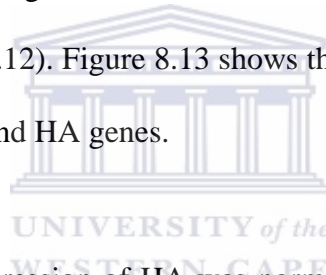
The default (fit point/arithmetic) method of Real-Time Quantitative Software version 3 was used to determine the relative starting copy numbers of target in each reaction. The Real-Time Quantitative Software generates a standard curve by plotting the logarithm of fluorescence versus the cycle number for each serial dilution of the standard template and then identifies the crossing point (cycle number) where the fluorescent signal emerges from background and enters the log-linear phase. Each crossing point is then plotted against the user-defined concentration of that standard to produce a standard curve. The relative gene expression is expressed as a ratio of the target gene (HA) concentration to the housekeeping gene (HPRT) concentration.

Figures 8.11 and 8.12 show the representative Real-Time Quantitative PCR amplification curves and the respective standard curves for both HPRT and HA respectively, using the 10 fold serial dilutions of cDNA from all three cell lines (Table 8.7). The linear regression analysis of the standard curves (CP plotted against log cDNA input) showed high linearity, with regression coefficients (r) greater than

0.90. The Real-Time Quantitative PCR efficiencies (E) were calculated from the resulting slopes provided by the Real-Time Quantitative PCR software and was calculated according to the equation:

$$E = 10^{[-1/\text{slope}]} \text{ (Rasmussen, 2001)}$$

The Real-Time Quantitative PCR efficiencies were calculated in all three cell lines for both the HPRT and HA genes and were shown to be almost equal (ranging from 1.9 to 2.2) (Fig 8.11 and 8.12). Figure 8.13 shows the standard curve of the combined cell lines for both HPRT and HA genes.



For each cell line, the expression of HA was normalized with the HPRT expression from the respective cell line. The results were then expressed as the ratio of the normalized HA expression of the sample (CHO-Mut8 (3x8)3.5 or CHO-Mut16 (3x8)3.5) versus the control (CHO-Y10). In order to determine this ration, the following equation was used:

$$R = \frac{(E_{\text{target}})^{\Delta CP_{\text{target}} \text{ (control-sample)}}}{(E_{\text{ref}})^{\Delta CP_{\text{ref}} \text{ (control-reference)}}} \text{ (Pfaffl, 2001)}$$

where the E_{target} and E_{ref} are the efficiencies of the target (CHO-Mut8 (3x8)3.5 or CHO-Mut16 (3x8)3.5) and reference genes (HPRT) respectively; $\Delta CP_{\text{target}}$ is the crossing point (CP) deviation of control-sample of the target gene transcript and ΔCP_{ref} is the CP deviation of control-sample of reference gene transcript. Table 8.8 lists the ΔCP

values between control and investigated samples, as well as the calculated ratios of the target gene (HA) and in comparison to the reference gene (HPRT).

The ratio of the normalized HA expression of CHO-Mut8 (3x8)3.5 and CHO-Mut16 (3x8)3.5 versus CHO-Y10 was calculated for each of the serial dilutions. It was determined that CHO-Y10 and CHO-Mut16 (3x8)3.5 are expressing comparable levels of the HA gene, as the ratio of HA expression in CHO-Mut16 (3x8)3.5 ranges from 0.3 to 1.6 between the serial diluted sample. However, CHO-Mut8 (3x8)3.5 seems to have substantially reduced HA levels. The calculated ratios show that there is between 100 to 500-fold reduction in HA levels in CHO-Mut8 (3x8)3.5, as compared to CHO-Y10.

It can therefore be concluded that CHO-Mut8 (3x8)3.5 (and consequently DWNN-complemented CHO-Mut8 (3x8)3.5 cells) are resistant to HA8-specific CTL killing due to the reduced HA levels, and hence could not be recognised by the CTLs. It is however, unclear why CHO-Mut16 (3x8)3.5 are resistant to HA8-specific CTL killing because they are expressing similar levels of HA as CHO-Y10.

SAMPLES	HPRT CP VALUES	HA CP VALUES	Δ CP HA	Δ CP HPRT	RATIO OF HA EXPRESSION
Y10 undiluted	28.78	21.13			
Y10 1:10	33.54	25.16			
Y10 1:100	34.59	28.45			
CHO-Mut8 (3x8)3.5 undiluted	25.68	22.78	-1.65	3.09	0.04
CHO-Mut8 (3x8)3.5 1:10	28.63	26.99	-1.83	4.91	0.01
CHO-Mut8 (3x8)3.5 1:100	31.97	30.01	-1.56	2.62	0.05
CHO-Mut16 (3x8)3.5 undiluted	27.56	18.98	2.15	1.22	1.46
CHO-Mut16 (3x8)3.5 1:10	30.76	23.77	1.39	2.78	0.27
CHO-Mut16 (3x8)3.5 1:100	33.85	26.76	1.69	0.74	1.58

Table 8.8 CP values, Δ CP and the calculated ratios of the relative HA expression of CHO-Mut8 (3x8)3.5 or CHO-Mut16 (3x8)3.5 versus CHO-Y10.

UNIVERSITY of the
WESTERN CAPE

8.5 Apoptosis killing assay

Since the DWNN-mutant and DWNN-complemented mutant cell lines did not show any specific lysis with HA8 specific CTL, as compared to CHO-Y10 and CHO-J363 cell lines (section 8.5.2), it was therefore decided to evaluate the induction of apoptosis in these cell lines with the classic apoptosis inducer, staurosporine. Staurosporine was used as a method of inducing apoptosis in these cell lines. Staurosporine (*Streptomyces staurospores*) is a relatively non-selective protein kinase inhibitor, which blocks many kinases to different degrees. Staurosporine is often used as a general method for inducing apoptosis (Kabir *et al.*, 2002) and has been shown to

induce apoptosis in a wide variety of cell types (Bertrand *et al.*, 1994) Table 8.9 lists the cell lines used in the staurosporine-induced apoptosis assay.

CELL LINE	DESCRIPTION
CHO-Y10	Chinese Hamster, parental cell line
CHO-Mut8 (3x8)3.5	Chinese Hamster, DWNN-mutant cell line
CHO-Mut16 (3x8)3.5	Chinese Hamster, DWNN-mutant cell line
CHO-Mut8 (3x8)3.5/ DWNN-200 & DWNN-13	Chinese Hamster, DWNN-complemented mutant cell line
CHO-Mut8 (3x8)3.5/ DWNN-200	Chinese Hamster, DWNN-complemented mutant cell line
CHO-Mut16 (3x8)3.5/ DWNN-13	Chinese Hamster, DWNN-complemented mutant cell line
CHO-Mut16 (3x8)3.5/ BAC clone & DWNN-13	Chinese Hamster, DWNN-complemented mutant cell line

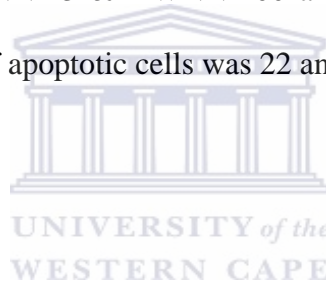
Table 8.9 Cell used in the APOPercentage™ apoptosis assay.

UNIVERSITY of the
WESTERN CAPE

Cells were propagated in six well plates and were treated with 1 μ M staurosporine for 3 hours. In order to measure the occurrence apoptosis the APOPercentage™ apoptosis assay was used (section 2.17). This assay works by the accumulation of the APOPercentage™ dye within all cells that are at the mid-phase stage of apoptosis. This stage corresponds with the translocation of phosphatidylserine to the outer surface of the cell membrane (Fadok *et al.*, 1992). In other words, all cells undergoing ‘mid-phase apoptosis’ will be stained fluorescent pink with the APOPercentage™ dye and the actual percentage of apoptotic cells is measured by FACS.

Flow cytometric analysis showed that 44 % of CHO-Y10 and 45 % of CHO-Mut16 (3x8)3.5 treated with 1 μ M Staurosporine, compared to the 8 and 16 % of cells that underwent spontaneous apoptosis in the untreated samples (Fig 8.15). However, in DWNN-complemented mutant CHO cell lines there seemed to be more cells resistant to staurosporine induction, compared to CHO-Y10 and CHO-Mut16 (3x8)3.5 cells. For instance, in CHO-Mut16 (3x8)3/DWNN-13 and CHO-Mut16 (3x8)3.5 /BAC & DWNN-13 cells only 26 % and 28 % of the cells were apoptotic respectively and in CHO-Mut8 (3x8)3.5/DWNN-13 & DWNN-200 and CHO-Mut8 (3x8)3.5/ DWNN-200 cells the percentage of apoptotic cells was 22 and 24 respectively.

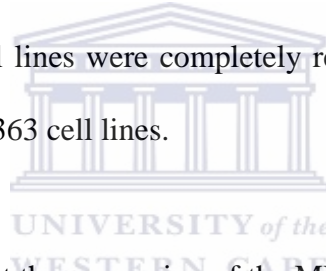
8.6 Discussion



In an attempt to understand the role played by DWNN in mammalian cells, an investigation has been carried out in DWNN-mutant CHO cells complemented with the DWNN cDNA versus the DWNN-mutant cell lines. Antibody staining of human cancer cell lines, CHO-Y10, CHO-J363 and DWNN-complemented mutant cell lines using anti-DWNN antibody showed that the endogenous DWNN is localised predominantly in the nucleus and also to a much lower level in the cytoplasm. However, CHO-Mut 8(3x8)3.5 and CHO-Mut 16(3x8)3.5 cells showed nuclear exclusion of the DWNN protein but there was cytoplasmic staining.

Western blot analysis detected a 13 kD protein (corresponding to DWNN-13), and two other proteins of about 160 kD and 105 kD in size in all the cell lines derived from CHO. These proteins might correspond to the degradation products of the DWNN-200 protein or might be truncated forms of the DWNN-200 protein, or they represent antibody cross reactivity.

The cell lines were exposed to CTLs in order to elucidate the role played by DWNN in CTL killing. The results showed that the DWNN mutant and DWNN-complemented mutant cell lines were completely resistant to CTL killing compared the CHO-Y10 and CHO-J363 cell lines.

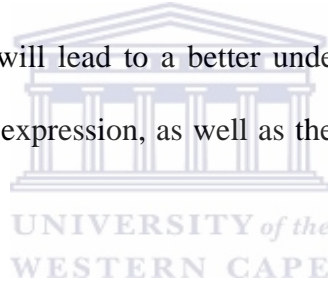


FACS analysis showed that the expression of the MHC class I K^K glycoprotein on the cell surface of the DWNN mutant and DWNN-complemented mutant cell lines was comparable to the parental cell line, CHO-Y10.

PCR and sequencing analysis, coupled with the resistance of the cell lines to puromycin, confirmed the reading frame and the expression of both copies the L^{HA} mRNA and L^{HA}-puro transgenes.

However, Real-Time Quantitative PCR showed that the expression of HA is comparable in CHO-Y10 and CHO-Mut16 (3x8)_{3.5} cells and substantially reduced in CHO-Mut8 (3x8)_{3.5} cells. The results imply that there was insufficient HA levels in CHO-Mut8 (3x8)_{3.5} and consequently in DWNN-complemented CHO-Mut8 (3x8)_{3.5},

hence the cell lines were resistant to CTL killing. However, CHO-Mut16 (3x8)3.5 have been shown to be expressing similar HA levels as CH-Y10, but yet are resistant to CTL killing. However, immunofluorescence data (Fig 8.1) suggested that CHO-Mut16 (3x8)3.5 cell line is polyclonal. . It is therefore, postulated that some of the clones which are DWNN negative might contain reduced levels of HA and those clones staining positive for DWNN have similar HA levels as CHO-Y10. This however, still does not explain why CHO-Mut16 (3x8)3.5 cell line is totally resistant to CTL killing, similarly as CHO-Mut8 (3x8)3.5 (Fig 8.3). Re-cloning of the CHO-Mut16 (3x8)3.5 cell line will lead to a better understanding of the presence of the levels of HA and DWNN expression, as well as the extent of CTL resistance of this cell line



It is hypothesised that the knocking-out of DWNN by promoter-trap mutagenesis might have resulted in the disruption of polyadenylation signal of the plasmid vector containing the L-HA and L-HA-Puro constructs (George, 1995), resulting in the instability of the HA mRNA. This therefore, resulted in reduced levels of HA in CHO-Mut8 (3x8)3.5 cells and consequently, resistance to CTL killing. It is therefore proposed that DWNN plays a role in the 3' polyadenylation process and this proposal corresponds with the previous study of the DWNN yeast homologue, Mpe1, which was shown to be essential in the cleavage and polyadenylation of mRNA (Vo *et al*, 2001).

The effect of apoptosis induction in DWNN-mutant and DWNN-complemented mutant cell lines was also investigated. This was carried out by exposing the cells to

staurosporine and the apoptosis was measured by APOPercentage™ assay. The results suggest that the cells complemented with DWNN are resistant to Staurosporine-induced apoptosis compared to CHO-Y10 and the DWNN mutant cell lines.



UNIVERSITY *of the*
WESTERN CAPE

CHAPTER 9: GENERAL DISCUSSION.

9.1 Identification of the DWNN gene in promoter-trapped cell lines (Chapter 3)

Four Chinese Hamster ovary cell lines which were generated from a previous study (George, 1994) to identify novel genes involved in the processing and presentation of antigens to CTL killing by promoter trap mutagenesis have been used in this study.

Inverse PCR was utilised in order to identify the genes mutated in these cell lines. A gene, named DWNN, has been identified by this method in CHO-Mut8 (3x8)3.5, CHO-Mut 16 (3x8)3.5 cell lines, and also in an earlier study by RACE PCR in CHO-Mut7 (3x8)3.5 (George, 1994). This gene was previously shown to have no significant matches to any entries in the database and was not yet characterised (George, 1994). Analysis of the DWNN sequence in all these cell lines showed the same site of retrovirus integration. This suggested that either this particular site was a hot spot for the retrovirus integration site or that all these cell lines originated from the same clone during the selection of these cell lines in the promoter-trap mutagenesis study (George, 1994).

The human DWNN gene was shown to encode two proteins of 13 kD and 200 kD, named DWNN-13 and DWNN-200 respectively.

9.2 Generation of the human DWNN-13 construct (Chapter 4)

This section reports the isolation of DWNN-13 cDNA using PCR. DWNN-13 cDNA was amplified from 21C4 clone (obtained from ATCC, Rockville, USA). Sequence analysis of DWNN-13 showed that the PCR product amplified was correct and had 100 % identity with the DWNN sequence in the database (accession number T25012). DWNN-13 cDNA was successfully cloned into pEGFPC1 vector for localisation studies (chapter 6) and also cloned into pcDNA3.1/Zeo vector for stable expression into cells (chapter 7).

9.3 Construction of the human DWNN-200 cDNA (Chapter 5)

DWNN-200 cDNA was constructed from mRNA isolated human cell lines. After several unsuccessful attempts of amplifying the entire 5.8 kb region, it was decided to amplify smaller fragments of ~1 kb along the entire gene. The fragments were then assembled together to generate the full length construct.

The 5.8 kb DWNN cDNA was sequenced in both strands. Three different constructs were generated: a wild type DWNN-200, a L289Q:S363P DWNN-200 and a Δ A4034 DWNN-200. The wild type DWNN-200 cDNA was shown to have a 100 % sequence identity to the assembled DWNN-200 sequence. The L289Q:S363P DWNN-200 cDNA contained two mutations within the RING finger of the DWNN gene. These mutations were identified from an epithelial cancer cell line, HeLa, and were not found in the other human cancer lines analysed, MG-63 and CaSki. The third

construct generated, the $\Delta A4034$ DWNN-200, contained a deletion of an adenosine at residue 4034 and therefore resulted in the truncation of the DWNN protein at the C-terminus. The base deletion was only observed in HeLa cell line and not in any other human cancer lines analysed. Further investigations are needed to explore the possibility of these mutations contributing to the phenotype of this cell line.

It is however not surprising to find mutations in this gene isolated from a cancer cell line because in a previous study, two nucleotide deletions were also found in the RBQ1 gene, a truncated human DWNN homologue (Sakai *et al.*, 1995). RBQ1 was isolated from a human small cell lung carcinoma cell line. The two nucleotide deletions present in RBQ1 are however, absent from the HeLa cells and the mutations that were found in this study were absent from all the DWNN sequences present in the database.

The wild type DWNN-200 cDNA was successfully cloned into pEGFP C1 and pcDNA 3.1/Zeo vectors for localisation studies and stable transfections. The L289Q:S363P DWNN-200 cDNA was also cloned into pEGFP C1 vector to determine whether the mutations would have any effect on the expression of the DWNN protein in mammalian cells. No further analysis was performed on the truncated DWNN-200 cDNA.

9.4 Localisation of DWNN protein (Chapter 6)

Both the DWNN-13 and DWNN-200 proteins were successfully cloned into pEGFP C1 vector, which serves as a fluorescent tag for monitoring the expression and localisation of the DWNN protein in CHO cells. In addition, the L289Q:S363P mutated DWNN-200 construct (generated in Chapter 5) was also used in these experiments.

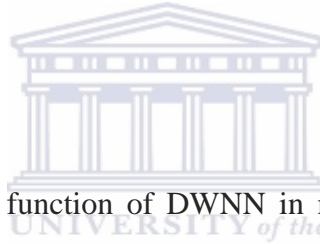
All three forms of the DWNN constructs (DWNN-13 wild type DWNN-200 and L289Q:S363P DWNN-200) were efficiently transfected into CHO cells and they were shown to localise identically inside the cells. They showed an intense nuclear staining and slight staining in the cytoplasm, compared to the GFP alone, which stained the entire cell. It was therefore concluded that the localisation signal of this protein is within the DWNN-13 domain due to the same pattern of localisation of the protein within the cell. It was also shown that the mutations within the RING finger did not affect the localisation of the protein.

9.5 Generation of stable DWNN-complemented mutant cell lines (Chapter 7)

pcDNA 3.1/Zeo vector was used in the cloning of both DWNN-13 and DWNN-200 cDNA. These constructs were then stably transfected into CHO-Mut8 (3x8)^{3.5} and CHO-Mut16 (3x8)^{3.5}. 300 µg/ml Zeocin was found to be the optimal concentration for the selection of stably transfected cell clones. The Zeocin resistant clones were cloned singly using cloning rings and in total about 50 resistant clones were isolated.

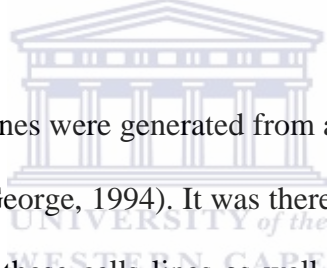
The various clones contained CHO-Mut8 (3x8)3.5 cells expressing either DWNN-200 or both DWNN-13 and DWNN-200 and CHO-Mut16 (3x8)3.5 cells expressing DWNN-13, DWNN BAC clone (CIT-254DM10 accession number AC010321) or both DWNN BAC clone and DWNN-13. These clones were used for further analysis (in comparison with the DWNN-mutant cell lines) in order to elucidate the function of the DWNN gene (Chapter 8).

9.6 Analysis of the DWNN-mutant and DWNN-complemented mutant cell lines (Chapter 8)



In order to determine the function of DWNN in mammalian cells, analysis of the DWNN-mutant and DWNN-complemented mutant cell lines was undertaken. Firstly, the analysis of the DWNN expression in these cell lines was evaluated. The subcellular localisation of the endogenous DWNN protein in these cells was investigated using immunostaining with polyclonal anti-DWNN antibodies. The results demonstrated that the parental CHO-Y10 cells, the DWNN-complemented mutant cell lines, CHO-J363, HeLa and MG-63 cell lines showed an intense DWNN staining in the nucleus. These findings are consistent with the previously reported nuclear staining of the mouse homologue partial cDNA, P2PR (Witte and Scott, 1997). However, in CHO-Mut8 (3x8)3.5 and CHO-Mut 16(3x8)3.5 cells anti-DWNN antibodies did not stain the nucleus and only stained the cytoplasm. It can therefore be concluded that the endogenous DWNN protein is localised mainly within the nucleus.

Western blots were carried out in order to determine the size of the DWNN protein expressed in DWNN-mutant and DWNN-complemented mutant cell lines. The results showed three bands of sizes, 13 kD 105 kD and 160 kD. The 13 kD protein corresponds to the DWNN-13 transcript. However, it still remains unclear what the other two large-sized proteins are but it is speculated that they may be degradation products of the DWNN-200 protein or cross reaction of antibodies or even the truncation of the DWNN protein on the other allele.



The DWNN-mutant cell lines were generated from a previous study to identify genes involved in CTL killing (George, 1994). It was therefore interesting to investigate the effects of CTL killing on these cell lines as well as in the DWNN-complemented mutant cells. Analysis of these cell lines for susceptibility to lysis by HA8 CTL clone by ⁵¹Cr-release assay showed that these cell lines were totally resistant to killing with the HA8 CTL compared to CHO-Y10 and CHO-J363 cell lines. In order to ensure that the resistance of these cell lines to CTL killing was not due to the loss of expression of the previously transfected MHC class I H-2K^K and HA genes, expression levels of both these genes was analysed in these cell lines. All the cell lines were expressing comparable levels of MHC class I H-2K^K using the FACScan. Real-Time Quantitative PCR showed that the levels of the HA mRNA were reduced by 100-fold in CHO-Mut8 (3x8)3.5 compared to CHO-Y10. However, CHO-Mut16 (3x8)3.5 expressed comparable HA levels with CHO-Y10. This data explains why the CHO-Mut8 (3x8)3.5 cells were resistant to CTL killing because they are not

expressing enough HA levels and therefore cannot be recognised by the HA8-specific CTL clone. On the contrary, CHO-Mut16 (3x8)3.5 are expressing similar levels of HA as CHO-Y10 but yet are resistant to CTL killing. It is unclear what is causing these cells to be resistant, but from immunofluorescence microscopy (section 8.2.1) it was discovered that CHO-Mut16 (3x8)3.5 cells are polyclonal. Re-cloning of this cell lines might provide additional information about the levels of CTL resistance in this cell line.

It is therefore hypothesized that by knocking-out DWNN using promoter-trap mutagenesis, might have led to the disruption of polyadenylation processing of the transfected L-HA and L-HA-puro, resulting in insufficient HA mRNA.

In an attempt to discover the role of the DWNN gene, the effects of apoptosis were also investigated in the cell lines. Cell lines were treated with staurosporine and apoptosis was measured using the APOPercentage™ assay. It was discovered that the DWNN-complemented mutant cell lines were less susceptible to staurosporine-induced apoptosis measured by the APOPercentage assay, as compared to CHO-Y10 and DWNN-mutant lines. This finding was analogous to the observations made in experiments where CHO cells transduced with DWNN-13 protein were less susceptible to apoptosis induced by serum-deprivation, compared to non-transduced CHO cells (Seameco, personal communication).

9.7 Conclusion

This study has shown that inverse PCR can be employed in order to identify promoter-trapped genes. A novel gene, DWNN, has been identified in promoter-trapped cell lines using the inverse PCR.

Sequence analysis showed that DWNN is a conserved protein, found in all eukaryotes. It encodes two proteins of 13 kD and 200 kD. The 13 kD protein contains the DWNN domain only, while the 200 kD protein is attached to several domains, including the CCHC domain, the C3HC4 domain, the Rb- and p53- binding domains. The Rb- and p53-binding domains have been previously shown to bind to tumour suppressor genes, Rb and p53 respectively.

In an attempt to investigate the role played by the DWNN gene, several experiments have been undertaken and the following conclusions were drawn:

- (a) Immunostaining experiments, together with GFP transient expression studies, confirmed that DWNN is localised in the nucleus.
- (b) Strong evidence has been presented in this study on the involvement of this gene in human cancers. Identification of several mutations in the human cervical cancer cell line (HeLa) has led to the question of whether the mutations within the DWNN gene contribute to the phenotype in this cell line. Analysis of more cancer cell lines needs to be undertaken in order to understand the role played by DWNN in human cancer

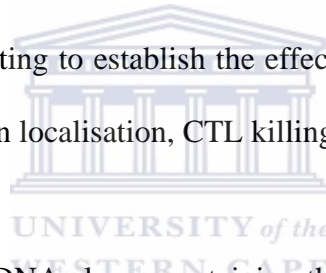
- (c) There seems to be some correlation between this gene and apoptosis. Further studies need to be undertaken in order to investigate the exact role played by this gene in apoptosis.
- (d) The presence of the Rb- and p53-binding domains on the human DWNN-200 gene might suggest that this gene interacts with the Rb and p53 tumour suppressors.
- (e) The ubiquitin-like structure of the DWNN domain, which has been recently solved (Faro, 2004), coupled with the presence of the RING finger domain within the DWNN-200 gene, suggests the possibility that DWNN operates as an E3 ubiquitin ligase, tagging probably p53, Rb or even itself for degradation.
- (f) Finally, this study proposes the involvement of DWNN in the 3' polyadenylation process.

9.8 Future Work

Several mutations have been identified within the RING finger domain of the DWNN-200 gene in this study. GFP fused to DWNN-200 containing these RING finger mutations did not seem to affect the localisation of DWNN in mammalian cells (chapter 6). The effect of these mutations on p53 and Rb interactions will have to be characterised through *in vitro* studies using protein expression and BIAcore analysis.

The characterisation of DWNN interactions with p53 and Rb with this system will provide a detailed understanding of the effects of mutations on these interactions. These experiments will strengthen our understanding of the involvement of DWNN in tumours and the role of DWNN mutations in disrupting the p53 and Rb systems of tumour suppression.

It is unclear what role is played by the alternatively spliced region (in exon 16) of the DWNN-200 gene. All the constructs built in this study were missing exon 16, it would therefore be interesting to establish the effects of overexpressing DWNN-200 containing exon 16 have on localisation, CTL killing and apoptosis.



Full-length DWNN-200 cDNA clones containing the RING finger mutations need to be expressed in mammalian cells in order to evaluate their function in CTL killing and apoptosis induction assays. This study showed that mutant cell lines complemented with the wild type DWNN-200 cDNA showed slight resistance to staurosporine-induced apoptosis measured by the APOPercentageTM assay. Additional tests need be undertaken in DWNN-mutant and DWNN-complemented mutant CHO lines to investigate their resistance to apoptosis induced by several known apoptotic inducers such as staurosporine, camptothecin, ceramide, as well recombinant perforin and granzymes. Apoptosis will then be measured using various assays, such as determination of caspase 3 activity, PARP cleavage and Annexin V staining. This will determine whether the apoptotic pathway has been blocked or not in these cell lines, and if it has been blocked, where in the pathway.

This study proposes the involvement DWNN in the polyadenylation process. This proposal will be confirmed by analysis of the 3' end of the HA mRNA of both CHO-Mut8 (3x8)3.5 and re-selected CHO-Mut16 (3x8)3.5 cells. This study will determine if the 3' HA mRNA has been properly processed.



REFERENCES.

Abbas, AK, Lichtman, AH and Pober, JS. (1997) Cellular and Molecular Immunology. **third edition**. WB Saunders Company.

Adams JM and Cory S. (1998) The Bcl-2 protein family: arbiters of cell survival. Science. **281**: 1322-1326.

Alnemri ES, Livingston DJ, Nicholson DW, Salvesen G, Thornberry NA, Wong WW, Yuan J. (1996) Human ICE/CED-3 protease nomenclature. *Cell*. **87**: 171.

Altschul SF, Gish W, Miller W, Myers EW, Lipman DJ. (1990) Basic local alignment search tool. *J Mol Biol*. **215**: 403-410.

An WG, Kanekal M, Simon MC, Maltepe E, Blagosklonny MV, Neckers LM. (1998) Stabilization of wild-type p53 by hypoxia-inducible factor 1 α . *Nature*. **39**: 405-408.

Ashcroft M and Vousden KH. (1999). Regulation of p53 stability. *Oncogene*. **18**: 7637-7643.



Barak Y, Juven T, Haffner R, Oren M. (1993) Mdm2 expression is induced by wild type p53 activity. *EMBO J*. **12**: 461-468.

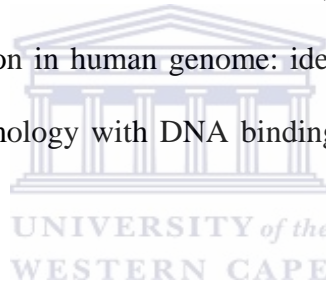
Barry M, Heibein JA, Pinkoski MJ, Lee SF, Moyer RW, Green DR, Bleackley RC. (2000) Granzyme B short-circuits the need for caspase 8 activity during granule-mediated cytotoxic T-lymphocyte killing by directly cleaving Bid. *Mol Cell Biol*. **20**: 3781-3794.

Bennett M, Macdonald K, Chan SW, Luzio JP, Simari R, Weissberg P. (1998) Cell surface trafficking of Fas: a rapid mechanism of p53-mediated apoptosis. *Science*. **282**: 290-293.

Benoist C and Mathis D. (1999) T-cell development: a new marker of differentiation state. *Curr Biol.* **9**: R59-61.

Benoist and Mathis D. (1998) T cell differentiation and biology. *Fundamental Immunology* 4th edition W. Paul, ed. Lippincott-Raven, publ. pp 367-409.

Berdichevskii FB, Chumakov IM, Kiselev LL. (1988) Decoding of the primary structure of the son3 region in human genome: identification of a new protein with unusual structure and homology with DNA binding proteins. *Mol Biol (Mosk).* **22**: 794-801.



Berke G. (1995) The CTL's kiss of death. *Cell.* **81**: 9-12.

Bertrand R, Solary E, O'Connor P, Kohn KW, Pommier Y. (1994) Induction of a common pathway of apoptosis by staurosporine. *Exp Cell Res.* **211**: 314-321.

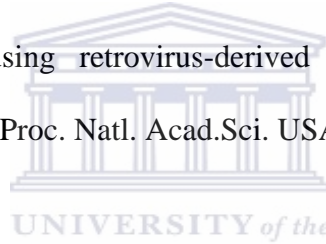
Boehringer Mannheim manual. (1998) Apoptosis and Cell proliferation. **2nd edition**: 2-3.

Boldin MP, Goncharov TM, Goltsev YV, Wallach D. (1996) Involvement of MACH, a novel MORT1/FADD-interacting protease, in Fas/APO-1- and TNF receptor-induced cell death. *Cell.* **85**: 803-815.

Bowen ID, Bowen SM and Jones AH. (1998) Mitosis and Apoptosis-Matters of life and death. Chapman and Hall, London and New York.

Breitschopf K, Bengal E, Ziv T, Admon A, Ciechanover A. (1998) A novel site for ubiquitination: the N-terminal residue, and not internal lysines of MyoD, is essential for conjugation and degradation of the protein. EMBO J. **17**: 5964-5973.

Brenner DG, Lin-Chao S and Cohen SN. (1989) Analysis of mammalian cell genetic regulation *in situ* by using retrovirus-derived “portable exons” carrying the *Escherichia coli* lacZ gene. Proc. Natl. Acad.Sci. USA. **86**: 5517-5521.



Casadaban MJ and Cohen SN. (1980) Analysis of gene control signals by DNA fusion and cloning in *Escherichia coli*. J Mol Biol. **138**: 179-207.

Carr AM. (2000) Cell cycle. Piecing together the p53 puzzle. Science. **287**: 1765-1766.

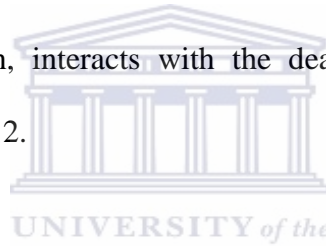
Chalfie M, Tu Y, Euskirchen G, Ward WW, Prasher DC. (1994) Green fluorescent protein as a marker for gene expression. Science. **263**: 802-805.

Chau BN, Cheng EH, Kerr DA, Hardwick JM. (2000) Aven, a novel inhibitor of caspase activation, binds Bcl-xL and Apaf-1. Mol Cell. **6**: 31-40.

Chen PL, Riley DJ, Chen Y, Lee WH. (1996) Retinoblastoma protein positively regulates terminal adipocyte differentiation through direct interaction with C/EBPs. *Genes Dev.* **10**: 2794-2804.

Chinnaiyan AM, O'Rourke K, Lane BR, Dixit VM. (1997) Interaction of CED-4 with CED-3 and CED-9: a molecular framework for cell death. *Science.* **275**: 1122-1126.

Chinnaiyan AM, O'Rourke K, Tewari M, Dixit VM. (1995) FADD, a novel death domain-containing protein, interacts with the death domain of Fas and initiates apoptosis. *Cell.* **81**: 505-512.



Cikala M, Wilm B, Hobmayer E, Bottger A, David CN. (1999) Identification of caspases and apoptosis in the simple metazoan Hydra. *Curr Biol.* **9**: 959-962.

Clancy, J. (1998) *Basic concepts in Immunology.* McGraw-Hill Companies. pp 1-11.

Clontech Living Colors User Manual: Introduction.
<http://www.clontech.com/clontech/Manuals/GFP/Intro.html> Accessed 1999 Feb 13.

Cohen GM. (1997) Caspases: the executioners of apoptosis. *Biochem J.* **326**: 1-16.

Collins FS and Weissman SM. (1984) Directional cloning of DNA fragments at a large distance from an initial probe: a circularization method. *Proc Natl Acad Sci USA*. **81**: 6812-6816.

Darmon AJ, Nicholson DW, Bleackley RC. (1995) Activation of the apoptotic protease CPP32 by cytotoxic T-cell-derived granzyme B. *Nature*. **377**: 446-448.

Davis MM and Bjorkman PJ. (1988) T-cell antigen receptor genes and T-cell recognition. *Nature*. **334**: 395-402.

del Peso L, Gonzalez VM, Nunez G. 1998 *Caenorhabditis elegans* EGL-1 disrupts the interaction of CED-9 with CED-4 and promotes CED-3 activation. *J Biol Chem*. **273**: 33495-33500.

Desagher S and Martinou JC. 2000 Mitochondria as the central control point of apoptosis. *Trends Cell Biol*. **10**: 369-377.

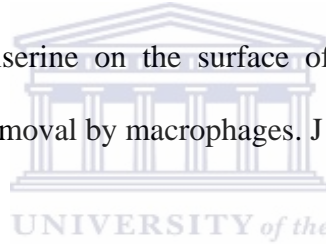
Desterro JM, Rodriguez MS, Hay RT. (1998) SUMO-1 modification of I κ B α inhibits NF- κ B activation. *Mol Cell*. **2**: 233-239.

Eastman A. (1985) Interstrand cross-links and sequence specificity in the reaction of cis-dichloro(ethylenediamine)platinum(II) with DNA. *Biochemistry*. **24**: 5027-5032.

el-Deiry WS, Kern SE, Pietenpol JA, Kinzler KW, Vogelstein B. (1992) Definition of a consensus binding site for p53. *Nat Genet.* **1**: 45-49.

Elgert, KD. (1996) *Immunology: Understanding the Immune system.* Wiley-Liss Inc, pp 1-22.

Fadok VA, Voelker DR, Campbell PA, Cohen JJ, Bratton DL, Henson PM. (1992) Exposure of phosphatidylserine on the surface of apoptotic lymphocytes triggers specific recognition and removal by macrophages. *J Immunol.* **148**: 2207-2216.



Faleiro L, Kobayashi R, Fearnhead H, Lazebnik Y. (1997) Multiple species of CPP32 and Mch2 are the major active caspases present in apoptotic cells. *EMBO J.* **16**: 2271-2281.

Faro A. (2004). Recombinant expression and full backbone assignment of the human DWNN domain using heteronuclear NMR. (MSc thesis). University of the Western Cape.

Freemont PS. (2000) RING for destruction? *Curr Biol.* **10**: R84-87.

Friend SH, Bernards R, Rogelj S, Weinberg RA, Rapaport JM, Albert DM, Dryja TP. (1986) A human DNA segment with properties of the gene that predisposes to retinoblastoma and osteosarcoma. *Nature.* **323**: 643-646.

Gao S and Scott RE. (2002) P2P-R protein overexpression restricts mitotic progression at prometaphase and promotes mitotic apoptosis. *J Cell Physiol.* **193**: 199-207.

Gao S, Witte MM, Scott RE. (2002) P2P-R protein localises to the nucleolus of interphase cells and the periphery of chromosomes in mitotic cells that show maximum P2P-R immunoreactivity. *J Cell Physiol.* **191**: 145-154. Erratum in: *J Cell Physiol* (2002) **192**: 359-360.

George AE. (1995) A new method for isolating genes involved in the processing and presentation of antigens to cytotoxic T cells. (D.Phil. Thesis). University of Oxford.

Glickman MH and Ciechanover A. (2002) The ubiquitin-proteasome proteolytic pathway: destruction for the sake of construction. *Physiol Rev.* **82**: 373-428.

Goff SP. (1987) Insertional mutagenesis to isolate genes. *Methods in Enzymology.* **151**: 489-502.

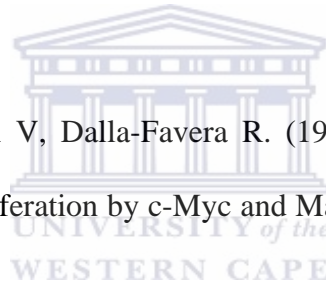
Graham FL, Smiley J, Russell WC, Nairn R. (1977) Characteristics of a human cell line transformed by DNA from human adenovirus type 5. *J Gen Virol.* **36**: 59-74.

Green DR and Reed JC. (1998) Mitochondria and apoptosis. *Science*. **281**: 1309-1312.

Gui JF, Lane WS, Fu XD. (1994) A serine kinase regulates intracellular localisation of splicing factors in the cell cycle. *Nature*. **369**: 678-682.

Gu W and Roeder RG. (1997) Activation of p53 sequence-specific DNA binding by acetylation of the p53 C-terminal domain. *Cell*. **90**: 595-606.

Gu W, Cechova K, Tassi V, Dalla-Favera R. (1993) Opposite regulation of gene transcription and cell proliferation by c-Myc and Max. *Proc Natl Acad Sci U S A*. **90**: 2935-2939.



Gu L, Ying H, Zheng H, Murray SA, Xiao ZX. (2003) The MDM2 RING finger is required for cell cycle-dependent regulation of its protein expression. *FEBS Lett*. **544**: 218-222.

Haas AL. (1997) Introduction: evolving roles for ubiquitin in cellular regulation. *FASEB J*. **11**: 1053-1054.

Haas AL and Siepmann TJ. (1997) Pathways of ubiquitin conjugation. *FASEB J*. **11**: 1257-1268.

Hansen S, Midgley CA, Lane DP, Freeman BC, Morimoto RI, Hupp TR. (1996) Modification of two distinct COOH-terminal domains is required for murine p53 activation by bacterial Hsp70. *J Biol Chem.* **271**: 30922-30928.

Harbour JW and Dean DC. (2000) Rb function in cell-cycle regulation and apoptosis. *Nat Cell Biol.* **2**: E65-67.

Harbour JW, Luo RX, Dei Santi A, Postigo AA, Dean DC. (1999) Cdk phosphorylation triggers sequential intramolecular interactions that progressively block Rb functions as cells move through G1. *Cell.* **98**: 859-869.

Hashizume R, Fukuda M, Maeda I, Nishikawa H, Oyake D, Yabuki Y, Ogata H, Ohta T. (2001) The RING heterodimer BRCA1-BARD1 is a ubiquitin ligase inactivated by a breast cancer-derived mutation. *J Biol Chem.* **276**: 14537-14540.

Haupt Y, Maya R, Kazanietz A, Oren M. (1997) Mdm2 promotes the rapid degradation of p53. *Nature.* **387**: 296-299.

Hengartner MO. (2000) The biochemistry of apoptosis. *Nature.* **407**: 770-776.

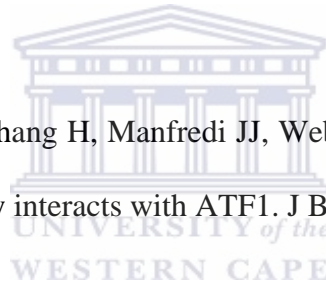
Hermeking H and Eick D. (1994) Mediation of c-Myc-induced apoptosis by p53. *Science.* **265**: 2091-2093.

Hershko A and Ciechanover A. (1998) The ubiquitin system. *Annu Rev Biochem.* **67**: 425-479.

Hollstein M, Sidransky D, Vogelstein B, Harris CC. (1991) p53 mutations in human cancers. *Science.* **253**: 49-53.

Honda R, Tanaka H, Yasuda H. (1997) Oncoprotein MDM2 is a ubiquitin ligase E3 for tumor suppressor p53. *FEBS Lett.* **420**: 25-27.

Houvras Y, Benezra M, Zhang H, Manfredi JJ, Weber BL, Licht JD. (2000) BRCA1 physically and functionally interacts with ATF1. *J Biol Chem.* **275**: 36230-36237.



Hsieh J-K, Chan FSG, O'Connor DJ, Mittnacht S, Zhong S and Lu X (1999) RB regulates the stability and the apoptotic function of p53 via MDM2. *Molecular Cell.* **3**:181-193.

Hsu H, Xiong J, Goeddel DV. (1995) The TNF receptor 1-associated protein TRADD signals cell death and NF- κ B activation. *Cell.* **81**: 495-504.

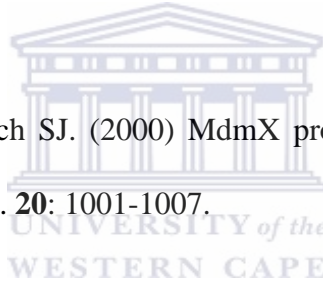
Hubbard SC, Walls L, Ruley HE, Muchmore EA. (1994) Generation of Chinese hamster ovary cell glycosylation mutants by retroviral insertional mutagenesis.

Integration into a discrete locus generates mutants expressing high levels of N-glycolylneuraminic acid. *J Biol Chem.* **269**: 3717-3724.

Hupp TR and Lane DP. (1994) Allosteric activation of latent p53 tetramers. *Curr Biol.* **4**: 865-875.

Hupp TR, Lane DP, Ball KL. (2000) Strategies for manipulating the p53 pathway in the treatment of human cancer. *Biochem J.* **352**:1-17.

Jackson MW and Berberich SJ. (2000) MdmX protects p53 from Mdm2-mediated degradation. *Mol Cell Biol.* **20**: 1001-1007.



Janeway CA and Travers P. (1996) *Immunobiology: The immune system in health and disease*. Current Biology/Garland Publishing, London. **3rd edition**: 155-187.

Jeffrey PD, Gorina S, Pavletich NP. (1995) Crystal structure of the tetramerization domain of the p53 tumor suppressor at 1.7 angstroms. *Science.* **267**: 1498-1502.

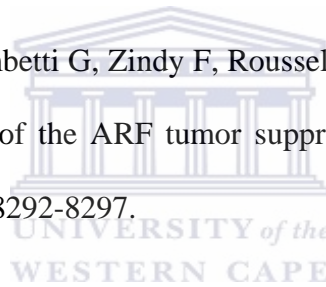
Jentsch S and Pyrowolakis G. (2000) Ubiquitin and its kin: how close are the family ties? *Trends Cell Biol.* **10**: 335-342.

Johnson PR and Hochstrasser M. (1997) SUMO-1 ubiquitination gains weight. *Trends Cell Biol.* **7**: 408-413.

Jones SN, Roe AE, Donehower LA, Bradley A. (1995) Rescue of embryonic lethality in Mdm2-deficient mice by absence of p53. *Nature*. **378**: 206-208.

Kabir J, Lobo M, Zachary I. (2002) Staurosporine induces endothelial cell apoptosis via focal adhesion kinase dephosphorylation and focal adhesion disassembly independent of focal adhesion kinase proteolysis. *Biochem J*. **367**: 145-155.

Kamijo T, Weber JD, Zambetti G, Zindy F, Roussel MF, Sherr CJ. (1998) Functional and physical interactions of the ARF tumor suppressor with p53 and Mdm2. *Proc Natl Acad Sci U S A*. **95**: 8292-8297.



Kerr, JFR, Wyllie, AH and Currie, AR. (1972) A basic biological phenomenon with wide ranging implications in tissue kinetics. *Br. J. Cancer*. **26**: 239-257.

Koopmann JO, Hammerling GJ, Momburg F. (1997) Generation, intracellular transport and loading of peptides associated with MHC class I molecules. *Curr Opin Immunol*. **9**: 80-88.

Krahenbuhl O and Tschopp J. (1991) Debate: the mechanism of lymphocyte-mediated killing. Perforin-induced pore formation. *Immunol Today*. **12**: 399-402.

Krammer PH. (2000) CD95's deadly mission in the immune system. *Nature*. **407**: 789-795.

Krippner A, Matsuno-Yagi A, Gottlieb RA, Babior BM. (1996) Loss of function of cytochrome c in Jurkat cells undergoing Fas-mediated apoptosis. *J Biol Chem*. **271**: 21629-21636.

Kroemer G, Petit P, Zamzami N, Vayssiere JL, Mignotte B. (1995) The biochemistry of programmed cell death. *FASEB J*. **9**: 1277-1287.

Kubbutat MH, Jones SN, Vousden K. (1997) Regulation of p53 stability by Mdm2. *Nature*. **387**: 299-303.

Laemmli UK. (1970) Cleavage of structural proteins during the assembly of the head of bacteriophage T4. *Nature*. **227**: 680-685.

Lanier LL and Bakker AB. (2000) The ITAM-bearing transmembrane adaptor DAP12 in lymphoid and myeloid cell function. *Immunol Today*. **21**: 611-614.

Lee WH, Bookstein R, Hong F, Young LJ, Shew JY, Lee EY. (1987) Human retinoblastoma susceptibility gene: cloning, identification, and sequence. *Science*. **235**: 1394-1399.

Lehner PJ, Hewitt EW, Romisch K. (2000) Antigen presentation: peptides and proteins scramble for the exit. *Curr Biol.* **10**: R839-842.

Liakopoulos D, Doenges G, Matuschewski K, Jentsch S. (1998) A novel protein modification pathway related to the ubiquitin system. *EMBO J.* **17**: 2208-2214.

Li H, Zhu H, Xu CJ, Yuan J. (1998) Cleavage of BID by caspase 8 mediates the mitochondrial damage in the Fas pathway of apoptosis. *Cell.* **94**: 491-501.

Lincz LF. (1998) Deciphering the apoptotic pathway: all roads lead to death. *Immunol Cell Biol.* **76**: 1-19.

Linzer DI and Levine AJ. (1979) Characterisation of a 54K dalton cellular SV40 tumor antigen present in SV40-transformed cells and uninfected embryonal carcinoma cells. *Cell.* **17**: 43-52.

Living Colors Enhanced GFP Vectors. (1996) *CLONTECHniques.* **XI**: 2-3.

Lohrum MA and Vousden KH. (2000) Regulation and function of the p53-related proteins: same family, different rules. *Trends Cell Biol.* **10**: 197-202.

Long EO. (1999) Regulation of immune responses through inhibitory receptors. *Annu Rev Immunol.* **17**: 875-904.

Lowe SW and Lin AW. (2000) Apoptosis in cancer. *Carcinogenesis.* **21**: 485-495.

Luciani MG, Hutchins JR, Zheleva D, Hupp TR. (2000) The C-terminal regulatory domain of p53 contains a functional docking site for cyclin A. *J Mol Biol.* **300**: 503-518.

Lundberg AS and Weinberg RA. (1998) Functional inactivation of the retinoblastoma protein requires sequential modification by at least two distinct cyclin-cdk complexes. *Mol Cell Biol.* **18**: 753-761.

Lutya PT. (2002) Expression and purification of the novel protein domain DWNN. (MSc Thesis) University of the Western Cape.

Macleod K. (2000) Tumor suppressor genes. *Curr Opin Genet Dev.* **10**: 81-93.

Marchenko ND, Zaika A, Moll UM. (2000) Death signal-induced localisation of p53 protein to mitochondria. A potential role in apoptotic signalling. *J Biol Chem.* **275**: 16202-16212.

Masson D and Tschopp J. (1987) A family of serine esterases in lytic granules of cytolytic T lymphocytes. *Cell*. **49**: 679-685.

Matz MV, Fradkov AF, Labas YA, Savitsky AP, Zaraisky AG, Markelov ML, Lukyanov SA. (1999) Fluorescent proteins from nonbioluminescent Anthozoa species. *Nat Biotechnol*. **17**: 969-973.

Meek DW. (1999) Mechanisms of switching on p53: a role for covalent modification? *Oncogene*. **18**: 7666-7675.

Meyer M. (2003) Characterisation and identification of the role of endozepine in apoptosis induced by ceramide.. (PhD thesis) University of the Western Cape.

Montes de Oca Luna R, Wagner DS, Lozano G. (1995) Rescue of early embryonic lethality in Mdm2-deficient mice by deletion of p53. *Nature*. **378**: 203-206.

Morgenbesser SD, Williams BO, Jacks T, DePinho RA. (1994) p53-dependent apoptosis produced by Rb-deficiency in the developing mouse lens. *Nature*. **371**: 72-74.

Morris EJ and Dyson NJ. (2001) Retinoblastoma protein partners. *Adv Cancer Res*. **82**: 1-54.

Mulsant P, Gatignol A, Dalens M, Tiraby G. (1988) Phleomycin resistance as a dominant selectable marker in CHO cells. *Somat Cell Mol Genet.* **14**: 243-252.

Murray NE. (1991) Special uses of lambda phage for molecular cloning. *Methods Enzymol.* **204**:280-301.

Newton J. (1995) Use of a novel gene trap retrovirus to generate and characterise cell lines resistant to lysis by MHC class I restricted Cytotoxic T-Lymphocytes. (PhD thesis). University of Oxford.

Ng FW, Nguyen M, Kwan T, Branton PE, Nicholson DW, Cromlish JA, Shore GC. (1997) p28 Bap31, a Bcl-2/Bcl-XL- and procaspase-8-associated protein in the endoplasmic reticulum. *J Cell Biol.* **139**: 327-338.

Niwa H, Araki K, Taniguchi A, Wakasugi S and Yamamura K. (1993) An efficient gene trap method using poly A trap vectors and characterisation of gene-trap events. *J Biochem* **113**: 343-349.

Ochman H, Gerber AS, Hartl DL. (1988) Genetic applications of an inverse polymerase chain reaction. *Genetics.* **120**: 621-623.

Oda E, Ohki R, Murasawa H, Nemoto J, Shibue T, Yamashita T, Tokino T, Taniguchi T, Tanaka N. (2000) Noxa, a BH3-only member of the Bcl-2 family and candidate mediator of p53-induced apoptosis. *Science.* **288**: 1053-1058.

Oliner JD, Kinzler KW, Meltzer PS, George DL, Vogelstein B. (1992) Amplification of a gene encoding a p53-associated protein in human sarcomas. *Nature*. **358**: 80-83.

Oren M. (1999) Regulation of the p53 tumor suppressor protein. *J Biol Chem*. **274**: 36031-36034.

Pan G, O'Rourke K, Chinnaiyan AM, Gentz R, Ebner R, Ni J, Dixit VM. (1997) The receptor for the cytotoxic ligand TRAIL. *Science*. **276**: 111-113.

Pfaffl MW. (2001) A new mathematical model for relative quantification in real-time RT-PCR. *Nucleic Acid Research*. **29**: 1-16.

Pickart CM. (2001) Ubiquitin enters the new millennium. *Mol Cell*. **8**: 499-504.

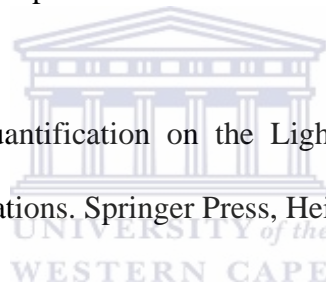
Pieters J. (1997) MHC class II restricted antigen presentation. *Curr Opin Immunol*. **9**: 89-96.

Polyak K, Xia Y, Zweier JL, Kinzler KW, Vogelstein B. (1997) A model for p53-induced apoptosis. *Nature*. **389**: 300-305.

Pomerantz J, Schreiber-Agus N, Liegeois NJ, Silverman A, Alland L, Chin L, Potes J, Chen K, Orlow I, Lee HW, Cordon-Cardo C, DePinho RA. (1998) The Ink4a tumor suppressor gene product, p19Arf, interacts with MDM2 and neutralizes MDM2's inhibition of p53. *Cell*. **92**: 713-723.

Pretorius A. (2000) Identification and isolation of novel components of the antigen presentation and processing pathway via the MHC class I molecule. (MSc thesis). University of the Western Cape.

Rasmussen R. (2001) Quantification on the LightCycler. Rapid Cycle Real-time PCR, methods and Applications. Springer Press, Heidelberg, 21-34.



Reed JC. (1997) Bcl-2 family proteins: regulators of apoptosis and chemoresistance in hematologic malignancies. *Semin Hematol*. **34**: 9-19.

Rees DJ, Jones IM, Handford PA, Walter SJ, Esnouf MP, Smith KJ, Brownlee GG. (1988) The role of beta-hydroxyaspartate and adjacent carboxylate residues in the first EGF domain of human factor IX. *EMBO J*. **7**: 2053-2061.

Rodrigues NR, Rowan A, Smith ME, Kerr IB, Bodmer WF, Gannon JV, Lane DP. (1990) p53 mutations in colorectal cancer. *Proc Natl Acad Sci U S A*. **87**: 7555-7559.

Roy S and Nicholson DW. (2000) Programmed cell-death regulation: basic mechanisms and therapeutic opportunities. *Mol Med Today*. 6: 264-266.

Sadasivan B, Lehner PJ, Ortmann B, Spies T, Cresswell P. (1996) Roles for calreticulin and a novel glycoprotein, tapasin, in the interaction of MHC class I molecules with TAP Immunity. *5*: 103-114.

Sakai Y, Saijo M, Coelho K, Kishino T, Niikawa N, Taya Y. (1995) cDNA sequence and chromosomal localisation of a novel human protein, RBQ-1 (RBBP6), that binds to the retinoblastoma gene product. *Genomics*. **30**: 98-101.

Saijo M, Sakai Y, Kishino T, Niikawa N, Matsuura Y, Morino K, Tamai K, Taya Y. (1995) Molecular cloning of a human protein that binds to the retinoblastoma protein and chromosomal mapping. *Genomics*. **27**: 511-519.

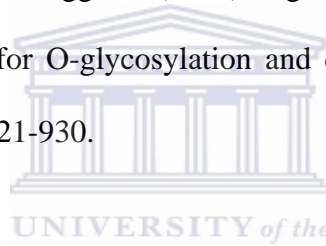
Sattler M, Liang H, Nettlesheim D, Meadows RP, Harlan JE, Eberstadt M, Yoon HS, Shuker SB, Chang BS, Minn AJ, Thompson CB, Fesik SW. (1997) Structure of Bcl-xL-Bak peptide complex: recognition between regulators of apoptosis. *Science*. **275**: 983-986.

Scheffner M, Nuber U, Huibregtse JM. (1995) Protein ubiquitination involving an E1-E2-E3 enzyme ubiquitin thioester cascade. *Nature*. **373**: 81-83.

Scheffner M. (1998) Ubiquitin, E6-AP, and their role in p53 inactivation. *Pharmacol Ther.* **78**: 129-139.

Scott RE, Giannakouros T, Gao S, Peidis P. (2003) Functional potential of P2P-R: a role in the cell cycle and cell differentiation related to its interactions with proteins that bind to matrix associated regions of DNA? *J Cell Biochem.* **90**: 6-12.

Shaw P, Freeman J, Bovey R, Iggo R. (1996) Regulation of specific DNA binding by p53: evidence for a role for O-glycosylation and charged residues at the carboxy-terminus. *Oncogene.* **12**: 921-930.



Shieh SY, Ikeda M, Taya Y, Prives C. (1997) DNA damage-induced phosphorylation of p53 alleviates inhibition by MDM2. *Cell.* **91**: 325-334.

Shih CC, Stoye JP, Coffin JM. (1988) Highly preferred targets for retrovirus integration. *Cell.* **53**: 531-537.

Silver J and Keerikatte V. (1989) Novel use of polymerase chain reaction to amplify cellular DNA adjacent to an integrated provirus. *J Virol.* **63**: 1924-1928.

Siminovitch L. (1985) Mechanisms of genetic variation in Chinese hamster ovary cells. In 'Molecular Cell Genetics' (MM Gottesman, Ed), pp 869-879. Wiley, New York.

Simons A, Melamed-Bessudo C, Wolkowicz R, Sperling J, Sperling R, Eisenbach L, Rotter V. (1997) PACT: cloning and characterisation of a cellular p53 binding protein that interacts with Rb. *Oncogene*. **14**: 145-155.

Smith CA, Farrah T, Goodwin RG. (1994) The TNF receptor superfamily of cellular and viral proteins: activation, costimulation, and death. *Cell*. **76**: 959-962.

Spector DL (1993) Nuclear organization of pre-mRNA processing. *Curr Opin Cell Biol*. **5**: 442-447.



Stambolic V, Suzuki A, de la Pompa JL, Brothers GM, Mirtsos C, Sasaki T, Ruland J, Penninger JM, Siderovski DP, Mak TW. (1998) Negative regulation of PKB/Akt-dependent cell survival by the tumor suppressor PTEN. *Cell*. **95**: 29-39.

Sternsdorf T, Jensen K, Will H. (1997) Evidence for covalent modification of the nuclear dot-associated proteins PML and Sp100 by PIC1/SUMO-1. *J Cell Biol*. **139**: 1621-1634.

Stone JD, Conroy LA, Byth KF, Hederer RA, Howlett S, Takemoto Y, Holmes N, Alexander DR. (1997) Aberrant TCR-mediated signalling in CD45-null thymocytes involves dysfunctional regulation of Lck, Fyn, TCR-zeta, and ZAP-70. *J Immunol*. **158**: 5773-5782.

Symonds H, Krall L, Remington L, Saenz-Robles M, Lowe S, Jacks T, Van Dyke T. (1994) p53-dependent apoptosis suppresses tumor growth and progression in vivo. *Cell*. **78**: 703-711.

Talanian RV, Brady KD, Cryns VL. (2000) Caspases as targets for anti-inflammatory and anti-apoptotic drug discovery. *J Med Chem*. **43**: 3351-3371.

Tao W and Levine AJ. (1999) p19(ARF) stabilizes p53 by blocking nucleocytoplasmic shuttling of Mdm2. *Proc Natl Acad Sci U S A*. **96**: 6937-6941.

Tartaglia LA, Ayres TM, Wong GH, Goeddel DV. (1993) A novel domain within the 55 kD TNF receptor signals cell death. *Cell*. **74**: 845-853.

Thompson CB. (1995) Apoptosis in the pathogenesis and treatment of disease. *Science*. **267**: 1456-1462.

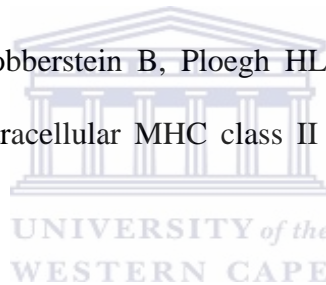
Thome M, Schneider P, Hofmann K, Fickenscher H, Meinel E, Neipel F, Mattmann C, Burns K, Bodmer JL, Schroter M, Scaffidi C, Krammer PH, Peter ME, Tschopp J. (1997) Viral FLICE-inhibitory proteins (FLIPs) prevent apoptosis induced by death receptors. *Nature*. **386**: 517-521.

Tokino T and Nakamura Y. (2000) The role of p53-target genes in human cancer. *Crit Rev Oncol Hematol.* **33**: 1-6.

Trinchieri G. (1989) Biology of natural killer cells. *Adv Immunol.* **47**: 187-376.

Tsujimoto Y, Cossman J, Jaffe E, Croce CM. (1985) Involvement of the bcl-2 gene in human follicular lymphoma. *Science.* **228**: 1440-1443.

Tulp A, Verwoerd D, Dobberstein B, Ploegh HL, Pieters J. (1994) Isolation and characterisation of the intracellular MHC class II compartment. *Nature.* **369**: 120-126.



Varmus HE, Quintrell N and Ortty S. (1981) Retroviruses as mutagens: insertion and excision of a non-transforming provirus alters expression of a resident transforming provirus. *Cell.* **25**:23-36.

van Endert PM. (1999) Genes regulating MHC class I processing of antigen. *Curr Opin Immunol.* **11**: 82-88.

Vo LT, Minet M, Schmitter JM, Lacroute F, Wyers F. (2001) Mpe1, a zinc knuckle protein, is an essential component of yeast cleavage and polyadenylation factor required for the cleavage and polyadenylation of mRNA. *Mol Cell Biol.* **21**: 8346-8356.

Vogelstein B, Lane D, Levine AJ. (2000) Surfing the p53 network. *Nature*. **408**: 307-310.

von Melchner H, Reddy S and Ruley HE. (1990) Isolation of cellular promoters by using a retrovirus promoter trap. *Proc. Natl. Sci. USA* **87**: 3733-3737.

von Melchner H and Ruley HE. (1989) Identification of cellular promoters by using a retrovirus promoter trap. *J Virol*. **63**: 3227-3233.

Vousden KH. (2000) p53: death star. *Cell*. **103**: 691-694.

Welch PJ and Wang JY. (1993) A C-terminal protein-binding domain in the retinoblastoma protein regulates nuclear c-Abl tyrosine kinase in the cell cycle. *Cell*. **75**: 779-790.

Weinberg RA. (1995) The molecular basis of oncogenes and tumor suppressor genes. *Ann N Y Acad Sci*. **758**: 331-338.

White K, Grether ME, Abrams JM, Young L, Farrell K, Steller H. (1994) Genetic control of programmed cell death in *Drosophila*. *Science*. **264**: 677-683.

Williams L and Grafi G. (2000) The retinoblastoma protein- a bridge to heterochromatin. *Trends Plant Sci*. **5**: 239-240.

Wilson KP, Black JA, Thomson JA, Kim EE, Griffith JP, Navia MA, Murcko MA, Chambers SP, Aldape RA, Raybuck SA, *et al.* (1994) Structure and mechanism of interleukin-1 beta converting enzyme. *Nature*. **370**: 270-275.

Witte MM and Scott RE. (1997) The proliferation potential protein-related (P2P-R) gene with domains encoding heterogeneous nuclear ribonucleoprotein association and Rb1 binding shows repressed expression during terminal differentiation. *Proc Natl Acad Sci U S A*. **94**: 1212-1217.

Wolf BB and Green DR. (1999) Suicidal tendencies: apoptotic cell death by caspase family proteinases. *J Biol Chem*. **274**: 20049-20052.

Xiao B, Shi YQ, Zhao YQ, You H, Wang ZY, Liu XL, Yin F, Qiao TD, Fan DM. (1998) Transduction of Fas gene or Bcl-2 antisense RNA sensitizes cultured drug resistant gastric cancer cells to chemotherapeutic drugs. *World J Gastroenterol*. **4**: 421-425.

Xiao ZX, Chen J, Levine AJ, Modjtahedi N, Xing J, Sellers WR, Livingston DM. (1995) Interaction between the retinoblastoma protein and the oncoprotein MDM2. *Nature*. **375**: 694-698.

Yang X, Khosravi-Far R, Chang HY, Baltimore D. (1997) Daxx, a novel Fas-binding protein that activates JNK and apoptosis. *Cell*. **89**: 1067-1076.

Yin C, Knudson CM, Korsmeyer SJ, Van Dyke T. (1997) Bax suppresses tumorigenesis and stimulates apoptosis in vivo. *Nature*. **385**: 637-640.

Zhang Y, Xiong Y, Yarbrough WG. (1998) ARF promotes MDM2 degradation and stabilizes p53: ARF-INK4a locus deletion impairs both the Rb and p53 tumor suppression pathways. *Cell*. **92**: 725-734.

Zhang H, Xu Q, Krajewski S, Krajewska M, Xie Z, Fuess S, Kitada S, Pawlowski K, Godzik A, Reed JC. (2000) BAR: An apoptosis regulator at the intersection of caspases and Bcl-2 family proteins. *Proc Natl Acad Sci U S A*. **97**: 2597-2602.

Zhou L, Song Z, Tittel J, Steller H. (1999) HAC-1, a *Drosophila* homolog of APAF-1 and CED-4 functions in developmental and radiation-induced apoptosis. *Mol Cell*. **4**: 745-755.